THE TEMPORAL RELATIONSHIP BETWEEN SYNUCLEINOPATHY, NIGROSTRIATAL DEGENERATION, AND NEUROINFLAMMATION IN THE ALPHA-SYNUCLEIN PREFORMED FIBRIL MODEL OF PARKINSON'S DISEASE

By

Megan Frances Duffy

A DISSERTATION

Submitted to
Michigan State University
in partial fulfillment of the requirements
for the degree of

Neuroscience—Doctor of Philosophy

2018

ABSTRACT

THE TEMPORAL RELATIONSHIP BETWEEN SYNUCLEINOPATHY, NIGROSTRIATAL DEGENERATION, AND NEUROINFLAMMATION IN THE ALPHA-SYNUCLEIN PREFORMED FIBRIL MODEL OF PARKINSON'S DISEASE

By

Megan Frances Duffy

Numerous studies have documented risk variants in immune genes and increased microglial inflammatory markers in the parenchyma and biofluids of Parkinson's disease (PD) patients. Recently our lab has characterized a new rat model of PD induced by injection of α-syn preformed fibrils (α-syn PFFs). The PFF model more faithfully recapitulates key features of idiopathic PD: namely early development of Lewy body-like pathology in widespread, PD-relevant brain regions under the context of normal levels of endogenous α-syn and protracted nigrostriatal degeneration over the course of 6 months. The distinct stages afforded by this model allow for investigation of neuroinflammation at different stages of synucleinopathy without the confound of α-syn pathology and degeneration occurring concurrently.

First, I histologically examined the time course of synucleinopathy, microgliosis and nigral degeneration at monthly intervals. Microglia in the vicinity of Lewy body-like inclusions display significantly increased cell body area and observable differences in extent and thickness of branching at 2 months post-injection, months prior to degeneration. Interestingly, major-histocompatibility complex-II (MHC-II; present on antigen-presenting microglia) was significantly increased in PFF-injected animals compared to controls 3 months prior to degeneration and relatively absent during the interval of degeneration. Moreover, the number of microglia expressing MHC-II at 2

months was positively correlated with the number of Lewy body-like inclusions in the substantia nigra, similar to observations documented in human PD tissue.

I next investigated the temporal profile of inflammatory cytokine expression in cerebrospinal fluid and plasma in the context of naïve aging animals and in PFF-injected animals. In the context of normal aging, tumor necrosis factor (TNF) and keratinocyte chemoattractant (KC/GRO) were significantly increased in aged animals compared to young and young-adult animals. In the synucleinopathy cohort when α-syn burden in the SN is greatest, I observed significant correlations between number of nigral α-syn inclusions and CSF levels of interferon-gamma (IFN-γ) were observed. At 4 months I continued to observe correlations between α-syn burden and CSF IFN-γ and TNF, and significantly elevated interleukin-6 in PFF animals compared to controls. During the interval of degeneration, significantly increased levels of interleukin-5 (IL-5), keratinocyte chemoattractant (KC/GRO), and TNF were observed, though cytokines did not correlate with magnitude of degeneration at this time point. These results suggest that a certain threshold of α-syn burden must be present in order for deviations in cytokine levels to be detected in early stages of disease and that overt differences in cytokines between PD patients and controls require the effect of pathology *and* time. Collectively, our results suggest that inflammatory mechanisms, specifically antigen presentation by microglia, in the substantia nigra have the potential to contribute to degeneration. Moreover, deviations in pro-inflammatory cytokines that occur in early disease stages are closely associated with α-syn burden within the SN. Importantly the combination of biofluid sampling and measurement of α-syn within the brain may represent a biomarker for early disease detection.

To Rosemary

ACKNOWLEDGEMENTS

My adviser has often said that it takes a village to raise a graduate student. With that said, there are many people who helped me navigate this journey. First, my adviser Caryl Sortwell for her unwavering support and guidance, and for being the archetype superwoman adviser who does it all, and does it all *well.* My co-adviser Tim Collier, for reminding me that often, the opposite of the expected result is the more interesting story and that if things don't go as planned, it's **not** the end of the world. My committee members Nick Kanaan, Brian Gulbransen, Kelvin Luk, and Malu Tansey for their guidance and feedback, but most importantly for forcing me to think critically about results from multiple angles. My lab colleagues Chris Kemp, Joe Patterson, Luke Fischer and Nicole Polinski for their friendship and help with various experiments, new techniques and troubleshooting, and rereading many iterations of manuscript drafts. While I initially aimed to travel outside the Midwest for graduate school, I was lucky to end up only 2 hours away from my family (Baileydog included!) who provided moral support (JLC: PMA) and reminded me of the bigger picture when things got hard and imposter syndrome became a norm. My fiancé Jens, who has loved and supported me in more ways than I can count through the last rollercoaster ride of this journey.

Last but not least, a special thank you to Christian Banda, Tim Brandt, Jimmy Choi, John Humphreys, Christopher Maycock, Sara Riggare, Israel Robledo, Allyson Sheltrown, Kristin Barr-Smith, Benjamin Stecher, Jasmine Sturr and Martin Taylor. Your willingness to openly discuss the daily ups and downs of living with PD, desire to

[friendlily!] debate about all things science, and fierce determination to make a difference through advocacy have taught me things that no textbook or experiment ever could. As Oliver Sacks said, “Our patients are our teachers.” Thank you for not only being my teachers and friends, but for giving me purpose.

PREFACE

At the time of submitting this dissertation, one chapter has been published, one chapter is currently under review and one chapter is in preparation for submission in August 2018. Chapter 2 is a perspective under review for inclusion in *Frontiers in Neuroscience | Neurodegeneration* under the research topic “The Protein Alpha-Synuclein: Its Normal Role (in Neurons) and its Role in Disease.” Chapter 3 was published in *Journal of Neuroinflammation* in May 2018. Chapter 4 is being edited for submission in August 2018.

TABLE OF CONTENTS

LIST OF TABLES

LIST OF FIGURES

KEY TO ABBREVIATIONS

6-OHDA	6-hydroxydopamine
AAV	Adenoassociated virus
ADAM	Absolute Deviation Around the Median
ANOVA	Analysis of Variance
APC	Antigen-presenting cell
α-syn	Alpha-synuclein
BBB	Blood-brain barrier
BCB	Blood-CSF barrier
CD4	Cluster of differentiation 4
CD68	Cluster of differentiation 68
CD8	Cluster of differentiation 8
CLIP	Class II-associated invariant chain peptide
CNS	Central nervous system
CSF	Cerebrospinal fluid
CXCL1	chemokine ligand 1
D1	Dopamine receptor 1
D2	Dopamine receptor 2
DA	Dopamine
DAergic	Dopaminergic
DAMP	Damage associated molecular pattern
DAT	Dopamine transporter

DJ-1	Protein deglycase
DMS	Dorsomedial striatum
DOPA	Dihydroxyphenylalanine
DOPAC	3,4-Dihydroxyphenylacetic acid
DPBS	Dulbecco's phosphate buffered saline
ER	Endoplasmic reticulum
GAPDH	Glyceraldehyde 3-phosphate dehydrogenase
GPe	Globus pallidus externa
GPi	Globus pallidus interna
GWAS	Genome-wide association study
HLA-DR	Human Leukocyte antigen - antigen D related
Iba-1	Ionized calcium binding adaptor-1
IF	Immunofluorescence
IFN-γ	Interferon gamma
IHC	Immunohistochemistry
IL-10	Interleukin-10
IL-13	interleukin-13
IL-1β	Interleukin-1 beta
IL-4	Interleukin-4
IL-5	Interleukin-5
IL-6	Interleukin-6
JAK	Janus kinase
KC/GRO	Keratinocyte chemoattractant

L-DOPA	Levadopa
LB	Lewy body
LN	Lewy neurite
LRRK2	Leucine rich repeat kinase 2
LV	Lentivirus
MAO-B	Monoamine oxidase B
MHC-I	Major histocompatibility complex-1
MHC-II	Major histocompatibility complex-2
ml	Milliliter
MPTP	1-methyl-4-phenyl-1,2,3,6-tetrahydropyridine
mRNA	Messenger ribonucleic acid
MyD88	Myeloid differentiation primary response 88
NADPH	Nicotinamide adenine dinucleotide phosphate
NeuN	Neuronal Nuclei
NFκB	Nuclear factor kappa-b
p.i.	Post-injection
p62	Nucleoporin p62
PAMP	Pathogen associated molecular pattern
PARK2	Gene encoding for Parkin
PARK7	Gene encoding for DJ-1
PBS	Dulbecco's phosphate buffered saline
PD	Parkinson's disease

PET	Positron emission tomography
PFFs	Alpha-synuclein preformed fibrils
pg	Picogram
PINK 1	PTEN-induced putative kinase 1
Pro-k	Proteinase-K
pSyn	Alpha-synuclein phosphorylated at Serine 129
RNA	Ribonucleic acid
ROS	Reactive oxygen species
RSA	Rat serum albumin
SEM	Standard error of the mean
SN	Substantia nigra
SNc	Substantia nigra pars compacta
SNCA	Alpha-synuclein (gene)
SNr	Substantia nigra pars reticulata
STAT	Signal Transducer and Activator of Transcription
TAP	Transporter associated with antigen processing
TBS	Tris-buffered saline
TH	Tyrosine Hydroxylase
TLR	Toll-like receptor
TNF	Tumor necrosis factor
TNFR1	Tumor necrosis factor receptor 1

TNFR2	Tumor necrosis factor receptor 2
TSPO	Translocator protein
UPDRS	Unified Parkinson's Disease Rating Scale
VLS	Ventrolateral striatum
VMAT	Vesicular monoamine transporter
WT	Wildtype
µg	Microgram
µl	Microliter

Chapter 1: Parkinson's Disease General Introduction

History

Parkinson's disease (PD) was first described as *paralysis agitans* by Dr. James Parkinson in his 1817 publication *Essay on the Shaking Palsy.* His landmark publication was based on his clinical assessment of three patients, as well as three individuals which he observed on the street. He defined the symptoms he observed with descriptions much like those used today: "*involuntary tremulous motion, with lessened muscular power, in parts not in action and even when supported; with a propensity to bend the trunk forward, and to pass from a walking to a running pace: the senses and intellect being uninjured*" [1]. These original observations were expanded upon and refined by Jean Martin Charcot, who aided in distinguishing parkinsonian resting tremor from tremor induced by other diseases including multiple sclerosis and alcoholism, described the four primary motor symptoms used for clinical diagnosis, and described in detail the heterogeneous symptomology and progressive, insidious nature of the disease [2].

Parkinson commented on the potential for disease modification, stating "*it is very probably that the remedial means might be employed with success: and even, if unfortunately deferred to a later period, they might then arrest the farther progress of the disease, although the removing of the effects already produced might be hardly to be expected* [1]." Although these initial observations were recorded over 200 years ago, no therapy currently exists to slow, halt, or reverse the progression of PD. With increasing life-expectancy and the rapidly growing elderly population, it is estimated that prevalence of PD will double in the next 20-30 years [3, 4].

Clinical Presentation

Motor Symptoms

PD is clinically diagnosed on the basis of core motor symptoms: bradykinesia, resting tremor, rigidity, postural instability, and gait disturbance [5, 6]. While bradykinesia is required, any one or more of the latter 4 symptoms may be present. As these symptoms are common to other disorders (essential tremor, drug-induced parkinsonism, psychogenic parkinsonism) patients will often undergo a DaTScan and their responsiveness to dopaminergic (DAergic) medication may be assessed to aid in reaching a conclusive diagnosis [7]. However, no single metric is conclusive, and accurate diagnosis of PD may take several months to a year to complete. Progression of symptoms is monitored by longitudinal examination of criteria known as the Unified Parkinson's Disease Rating Scale (UPDRS). UPDRS includes patient reported changes in mood and memory, changes in activities of daily living, and motor examination [8]. It should be noted that while Parkinson's disease represents a singular diagnosis, it has become increasingly recognized that symptomology is heterogeneous among patients, thus representing a difficulty in making a diagnosis and prescribing effective treatment. Despite the depth and battery of clinical testing, diagnosis cannot be completely confirmed until post-mortem examination.

Non-motor symptoms

In addition to motor symptoms, the prevalence of non-motor symptoms in PD disease is being increasingly recognized [9]. Many patients experience loss of smell and constipation, predating motor symptoms [10, 11]. Anxiety and depression, apathy, REM

sleep disorder, and orthostatic hypotension are also common [12-17]. In later stages, it is estimated that cognitive decline affects up to 80% of patients 15-20 years post-diagnosis [18]. Many patients report these symptoms as having a strong impact on quality of daily life, though currently few therapies are targeted toward these issues.

Neuropathology

Neuroanatomy

While PD is a multi-circuit, multi-system disease, the primary affected CNS circuit underlying PD motor symptoms is the basal ganglia [19]. In healthy individuals, the striatum (putamen) receives dopaminergic input from the substantia nigra pars compacta (SNc). SNc neurons release dopamine which binds to either D1 or D2 receptors on medium spiny neurons within the putamen which are responsible for facilitating movement (D1 direct pathway) or inhibiting movement (D2 indirect pathway). In the direct pathway, excitatory dopaminergic input to D1 receptors in the putamen project inhibitory input to the globus pallidus interna (GPi) and substantia nigra pars reticulata (SNr) resulting in disinhibition of the thalamus and excitation of the motor cortex, thereby facilitating movement. The indirect pathway balances out this facilitation via inhibitory action of dopamine on D2 receptors, further sending inhibitory signals to the globus pallidus externa (GPe), and from the GPe to subthalamic nucleus (STN), GPi, and SNr. Inhibitory input to the STN induces excitation of the GPI, which sends inhibitory signals to thalamocortical projections, resulting in inhibition of movement. In the parkinsonian brain, loss of nigral dopamine input from the SNc results in overactivity

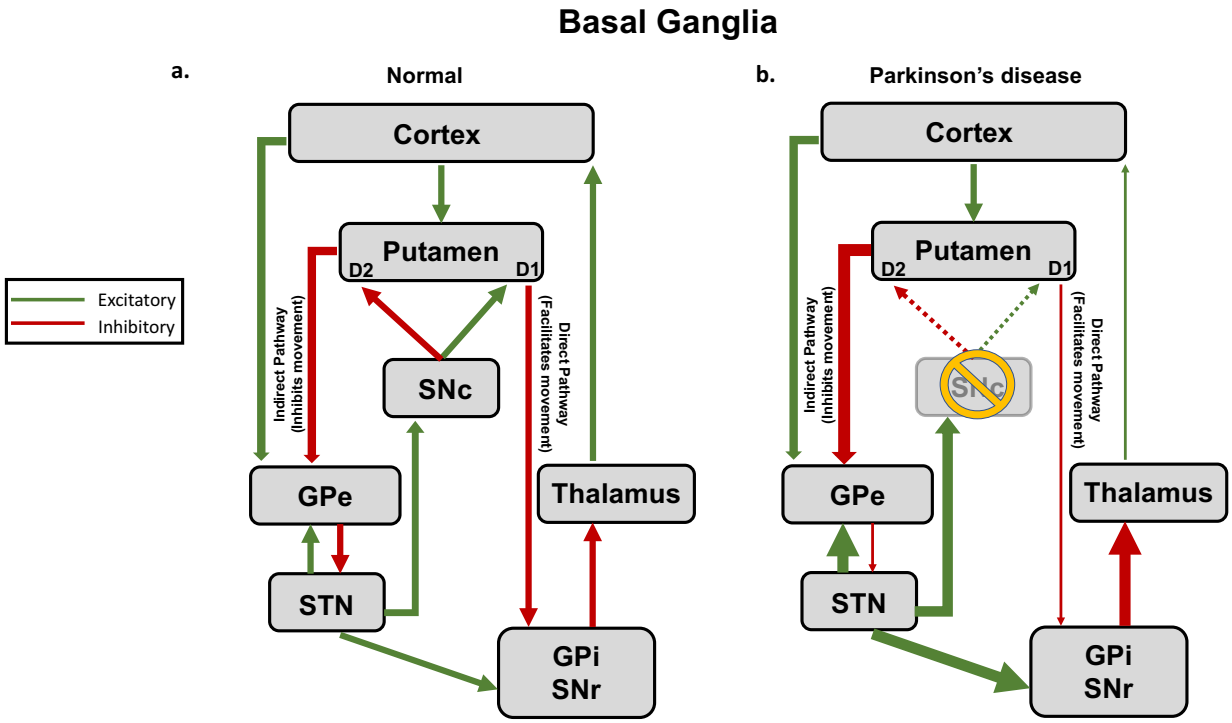

Figure 1.1: Normal and Parkinsonian basal ganglia circuit
a) Balance of excitatory and inhibitory basal ganglia pathways in healthy brain. b) Loss of DAergic innervation to the striatum from the SN results in increased inhibition of thalamocortical projections, responsible for bradykinetic symptoms of PD. Thickness of arrows denotes increased or decreased strength of output.

of the indirect pathway and decreased activity of the direct pathway, with the net effect of loss of goal directed movement **(Figure 1.1)**.

Lewy Pathology

The first of two major pathological hallmarks required to confirm diagnosis of PD *post mortem* is intracellular proteinaceous inclusions termed Lewy bodies, found both in axons (Lewy neurites) and cell bodies of surviving neurons. Lewy bodies were first described in 1912 by Friedrich Heinrich Lewy, when he noted eosinophilic inclusions in the dorsal motor nucleus of the vagus nerve and nucleus basalis of Meynert [20, 21]. However, the composition of these inclusions largely remained a mystery until 1998. Lewy bodies possess several dozen components including lipids, components of the ubiquitin-proteasome system, structural proteins, and most notably, alpha-synuclein (α-syn) [22-24]. The normal function of α-syn and its contribution to idiopathic and genetic cases of PD is discussed in Chapter 2.

Patterns and staging of Lewy pathology

The temporal and regional distribution of Lewy pathology described by Heiko Braak in 2003 has remained the gold-standard for staging of PD. He noted a spatiotemporal pattern of Lewy pathology: first observed in the vagus nerve and olfactory nucleus, progressing in an ascending manner to the brainstem and midbrain, and eventually in limbic and neocortical regions in end-stage cases [25, 26]. Although some variability between cases was noted, the ascending pattern of Lewy pathology described by Braak has in part led to the idea of an ascending, prion-like spread from the gut to the brain [27]. While Braak staging remains the primary pathological staging scheme for PD, it

has been met with criticism recently due to two major caveats: 1) its failure to classify and confirm up to 50% of PD cases, and 2) its exclusion of cases which do not present with pathology in the dorsal motor nucleus [28-31]. While new staging schemes which take into account the spatiotemporal heterogeneity in synucleinopathies have been proposed, Braak staging remains the framework under which post-mortem staging is conducted.

Nigrostriatal degeneration

The second major hallmark for confirmed diagnosis of PD is degeneration of the melanized DAergic neurons of the SNc which can be readily observed macroscopically. Characteristics of SN DA neurons which may render this cellular population more susceptible to degeneration may include: high metabolic demand and oxidative stress production, iron and neuromelanin content, and proximity to the dense microglial population of the SNr [32-35]. Loss of dopamine (DA) from nigrostriatal neurons results in increased activity of the indirect pathway (movement inhibiting) and decreased activity of the direct (movement facilitating) basal ganglia pathways (**Figure 1.1**) resulting in the classic bradykinetic and akinetic symptoms. At the time of clinical diagnosis, it is estimated that there is a >60% reduction in striatal dopamine resulting from the initial dying back of axons [36], followed by >50% loss of nigrostriatal dopamine neuron cell bodies [37]. Cell replacement therapy to replace striatal dopamine via grafts has been attempted, though symptomatic benefit is short-lived and in most cases, produces no long-term benefit [38]. Moreover, it is unlikely that grafted cells form the appropriate connections in a degenerated environment.

Current Treatment Strategies

Pharmacotherapies

Current Parkinson's therapies focus on symptomatic relief and thus have remained dopamine-centric. For over five decades, the gold standard pharmacotherapy for PD has been administration of levodopa (L-DOPA; [39, 40]), which is taken up by amino acid transporters in the intestine, crosses the blood-brain-barrier (BBB) and is converted to dopamine by the enzyme DOPA decarboxylase (Figure 1.2). L-DOPA acts to replenish depleted dopamine and increase the efficacy of DA production by remaining dopamine neurons. When administered orally, the majority of L-DOPA is metabolized before it crosses the BBB. Thus, L-DOPA is often administered in conjunction with carbidopa (combination L-DOPA/carbidopa; Sinemet), which acts to limit L-DOPA conversion to DA before reaching the BBB. While L-DOPA is initially effective in alleviating motor symptoms of PD, it is not without adverse side effects. With continued use, many patients experienced increased variability and intervals of on-off periods, that is, a decrease in motor symptoms while taking medication and reemergence of motor symptoms as one dose wears off prior to taking the next dose [41]. Many patients additionally experience debilitating uncontrolled movements (dyskinesias) after prolonged use [42, 43], which poses a significant problem to early-onset PD patients who will typically require treatment for longer periods of time than those diagnosed with sporadic, late-onset PD [44].

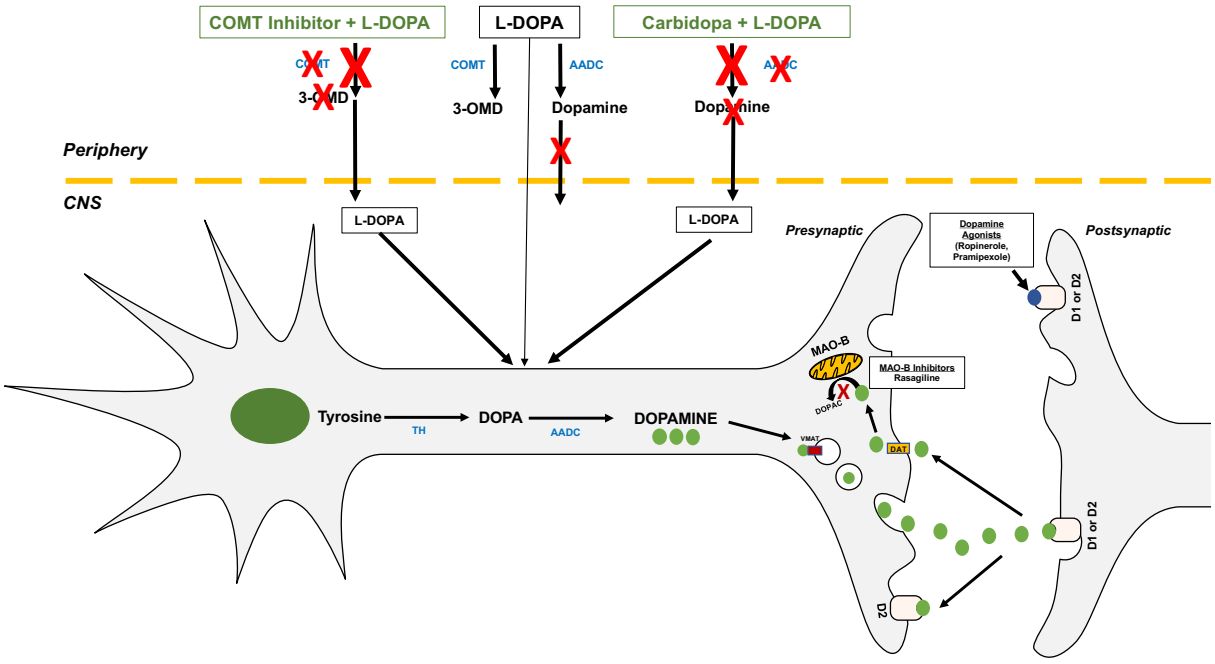

Figure 1.2: Dopamine synthesis and pharmacotherapies
Tyrosine hydroxylase adds a hydroxyl group to tyrosine converting it to DOPA. DOPA decarboxylase removes a carboxyl group from DOPA, converting it to dopamine, which is then packaged into synaptic vesicles by VMAT and released where it can interact with either D1 or D2 receptors on the postsynaptic neuron. Synaptic dopamine may be taken up into the presynaptic cell through DAT. Dopamine remaining in the neuron can be deaminated back into DOPA by MAO-B. Boxes indicate dopaminergic pharmacotherapies and their mechanism of action.

Dopamine agonists are sometimes used to delay the need for L-DOPA, so as to stave off L-DOPA induced dyskinesias. DA agonists such as Ropinerole act by binding to either D1 or D2 receptors on postsynaptic neurons (Figure 1.2), and often result in fewer on-off periods than L-DOPA [45, 46]. Thus, DA agonists are usually the first treatment option explored, particularly for younger patients. However, problematic side effects such as insomnia, hallucinations and decreased impulse control are common [47, 48].

Two classes of drugs are often used in conjunction with L-DOPA: Monoamine oxidase inhibitors (MAO's) and catechol-o methyl transferase (COMT) inhibitors. MAO's work to prevent deamination of dopamine by monoamine oxidase-B (Figure 1.2), thereby prolonging existing dopamine levels while decreasing the need for increasing doses of L-DOPA. Similarly to dopamine agonists, MAO inhibitors can be attempted as a first treatment option to delay need for L-DOPA, but are often prescribed in conjunction with L-DOPA to increase its efficacy and decrease the number of on/off periods [49]. COMT inhibitors are often prescribed in conjunction with L-DOPA to prevent its breakdown into 3-methoxytyramine prior to reaching the BBB ([50, 51]; Figure 1.2). Given the relatively short half-life of L-DOPA, increasing its efficacy in an effort to decrease dose and thus prolong the appearance of LIDs is of importance.

Deep Brain Stimulation

Deep brain stimulation (DBS) is the most commonly used surgical treatment of

PD. DBS acts as a pacemaker: an electrode is implanted into one of several regions in the brain (thalamus, internal globus pallidus, subthalamic nucleus) [52], to modulate an imbalance in excitation and inhibition that results from nigrostriatal degeneration (**Figure 1.1**), although the exact mechanism by which patients receive symptomatic alleviation is currently under debate. Recent studies suggest that certain subpopulations of PD patients will benefit more than others from DBS [53]. Given the risky nature of this procedure, especially in the elderly, this treatment is often used as a last resort when pharmacotherapies are no longer effective. This is less of a concern in younger patients.

Etiology: A Combination of Genetic, Environmental, and Aging factors

Genetic Factors

While the majority of PD cases are likely the culmination of multiple genetic risk factors and environmental insults (**Figure 1.3**), 10% of total Parkinson's cases are estimated to be monogenic, or attributed to a single gene. The first genetic link to PD was identified as a point mutation in *SNCA* (the gene for α-syn, [54]), resulting in young-onset PD. Additional point mutations in addition to duplication or triplication of *SNCA* were identified soon after, as discussed in chapter 2. Additional monogenic associations with autosomal dominant or recessive inheritance patterns have been identified including but not limited to *LRRK2*, *PINK*1, *PARK7* and *PARK2*, which have implications in immune, mitochondrial, ubiquitin-proteasome and oxidative stress activity [55]. For the 90-95% of idiopathic PD cases, a number of risk loci have been identified, however, these risk

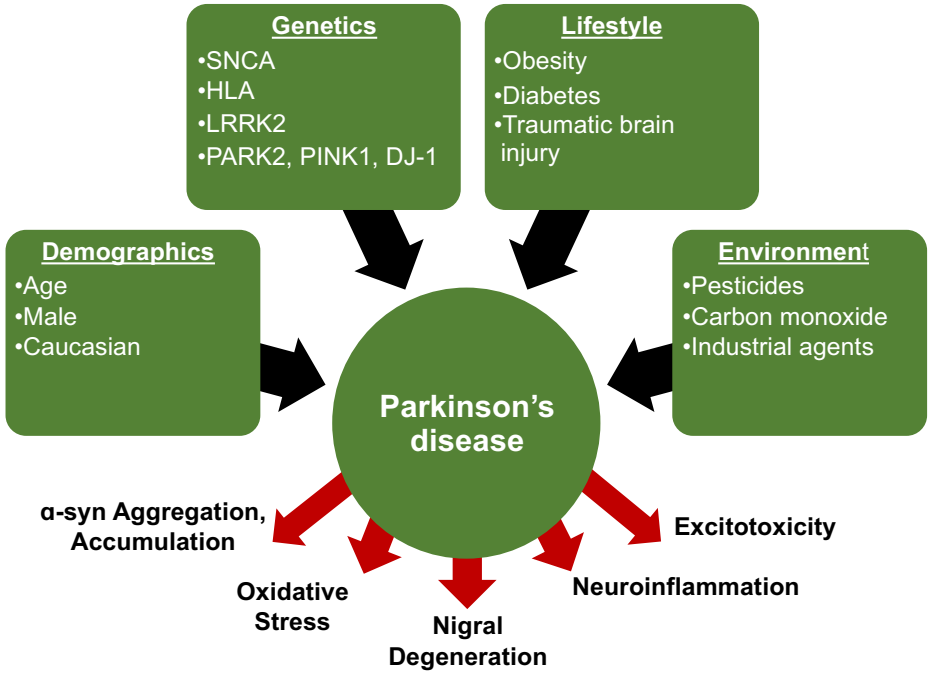

Figure 1.3 Stochastic nature of PD etiology
PD is multi-faceted: a culmination of aging related changes in brain environment, genetic predispositions, and environmental insults that result in 1) accumulation of proteinaceous Lewy-body inclusions composed, in part, of alpha-synuclein (α-syn) and 2) degeneration of the nigrostriatal system associated with the motor symptoms of PD. In addition to aberrant protein accumulation, excitotoxicity, oxidative stress, and neuroinflammation has been proposed to be involved in PD.

factors likely act in concert with each other and/or environmental insults and lifestyle factors.

Environmental Factors

Epidemiological studies suggest that lose-dose occupational exposure to pesticides herbicides such as rotenone, paraquat, and dieldrin and may contribute to the development of PD [56-60]. Rotenone and paraquat in particular have been used in both *in vitro* and *in vivo* models to induce selective loss of dopaminergic neurons. Studies from cell culture and animal models suggest that insecticides can induce loss of dopaminergic neurons through several mechanisms: mitochondrial complex-I inhibition, enhanced microglial phagocytosis and NAPDH oxidase production, and release of α-syn from enteric neurons [61-64]. Interestingly, the olfactory bulb and the gut constitute two sites which develop abundant Lewy pathology and have the greatest exposure to toxins in the environment via inhalation and digestion. Therefore, it is likely that environmental toxins contribute to early development of pathology in these regions.

Aging

Aging represents the largest risk factor for developing PD, as the majority of affected PD patients are over the age of 65. Evidence from rodent and non-human primates suggests that as a byproduct of normal aging, processes within nigral DA neurons including mitochondrial turnover, and ubiquitin-proteasome mediated degradation simultaneously become less efficient [34, 65-69]. Senescence of these mechanisms renders nigral DA neurons more susceptible to degeneration when multiple-hits such as genetic or environmental factors come in to play (i.e. “stochastic acceleration” [70, 71]).

Inflammation

As dopamine-centric pharmacotherapy only addresses motor symptoms long after the damage has been done, efforts are currently being made to investigate other abnormal processes that occur during disease progression. Ideally, identifying dysfunctional processes that occur prior to- and act as contributors to neurodegeneration would aid in the discovery of disease modifying therapies. One of the most consistent findings among post-mortem PD tissue and sampling of biofluids from living patients is the emergence of a disturbed inflammatory environment. Evidence from positron emission tomography (PET) imaging studies of microglial activation via radiolabeled mitochondrial translocator protein (TSPO, microglial) ligand [^{11}C)-(*R*)-PK11195 in both *de novo* [72] and early-to-advanced PD patients [73] has suggested inflammation occurs early and is sustained at increased levels compared to age matched controls. Therefore, honing in on specific inflammatory mechanisms and their temporal role in PD may be a promising target for disease modification.

Microglia

Microglia are derived from yolk sac progenitors in the mesoderm and in their immature state migrate into the parenchyma where they account for ~10% of the total cell population, although density varies by region [74, 75]. Microglia are crucial for synaptic pruning and cortical structure formation during development [76, 77]. However, microglia are proposed to be more senescent (i.e., less efficient at mounting an appropriate response) with age, which may constitute a contributing risk factor for developing age-related neurodegenerative diseases [78]. Although microglia are often

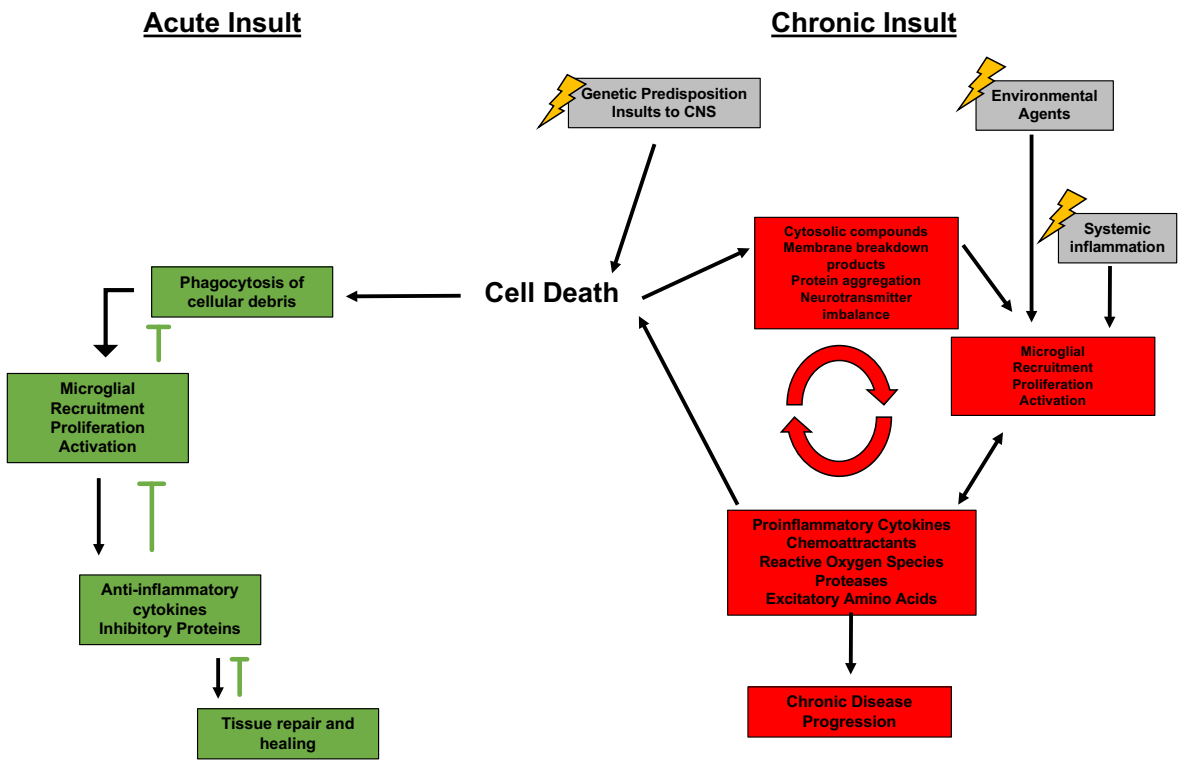

Figure 1.4: Neuroinflammation can be protective or harmful, depending on the type and duration of insult

During the acute presence of cellular debris or proteins or acute neuronal injury, microglia proliferate and migrate to the site of injury to phagocytose cell debris products and secrete anti-inflammatory cytokines such as interleukin-10 in a self-limiting manner. However, in the case of PD where environmental and genetic insults in combination with misfolding and chronic accumulation of proteins inside cells which are unable to be broken down by other methods such as the ubiquitin-proteasome system, microglia proliferate, migrate, and secrete pro-inflammatory cytokines, chemoattractants to peripheral immune cells, and reactive oxygen species. When this occurs over an extended period of time, attempts at tissue repair which are possible during acute injury fail, and an unregulated vicious cycle of protein accumulation, cell death, and inflammation ensues.

referred to as “resting” or “activated,” activity state is much more dynamic, as microglia constantly extend and retract processes to survey the environment [79, 80].

As the brain’s resident antigen-presenting cells (APCs) and phagocytes, microglia represent the first line of defense and are the CNS effectors of inflammation induced by infection, cell death, neurotransmitter imbalances, or other stressors. In response to insult, microglia secrete cytokines and chemoattractants which act on nearby microglia, astrocytes, and neurons to promote tissue healing and recovery. However in the presence of chronic insults, microglia initiate a feed forward cycle of inflammatory cytokine secretion which can further exacerbate protein aggregation, ROS production, cell death, and cytokine secretion. Studies in humans have implicated several different innate (local; toll-like receptors, cytokines) and adaptive (peripheral; MHC expression, T-cell infiltration) immune response components as being differentially regulated in PD. Three of the most consistent observations indicating an altered inflammatory milieu in PD are upregulation of toll-like receptors, major-histocompatibility complex-II (MHC-II) on microglia and differential expression of proinflammatory cytokines.

Toll-Like Receptors: Innate Response

Toll-like receptors (TLRs) are critical in initiation and execution of the innate immune response. TLRs fall into the class of pattern recognition receptors (PRRs), which recognize both pattern associated molecular patterns (PAMPS; exogenous structures such as bacteria or viruses) and damage associated molecular patterns (DAMPS; molecules released following cellular damage [81]). Of particular relevance to PD are TLR2 and TLR4, although TLR2 has been more extensively studied in PD [82].

Activation of TLR2 induces heterodimerization with TLR1 or TLR6, leading to MyD88 dependent translocation of nuclear factor kappa light chain enhancer of activated B-cells, ultimately resulting in increased production of proinflammatory cytokines TNF and IL-1β. In PD, observations in human tissue an animal models have implicated that TLR2 is closely associated to Lewy pathology and α-syn [82]. TLR2 is increased on microglia in early Braak stages (I-III) compared to later stage PD (IV-VI; [83]). Interestingly, a recent study identified TLR2 expression on Lewy body-containing neurons which significantly correlated with disease stage [84]. *In vitro*, oligomeric α-syn released from cells acts as an endogenous agonist for TLR2, resulting in downstream secretion of proinflammatory cytokines tumor necrosis factor (TNF) and interleukin-6 (IL-6; [85]). Furthermore, genetic ablation of TLR2 abolished proinflammatory cytokine production and MHC-II expression induced by overexpression of α-syn. Currently, several studies have been funded to investigate the disease-modifying potential of TLR2 antagonists in preclinical PD models.

Major-Histocompatibility complexes: bridging the gap between innate and adaptive responses

MHC-II is one of two classes of MHC surface proteins on antigen presenting cells encoded by the human leukocyte antigen complex (HLA) in humans and RT1 complex in rats [86]. MHC molecules are crucial regulators of the inflammatory response, as they present antigens on the surface of APCs for interaction with T-cells. MHC-I presents intracellular peptides derived from the cytosol and presents them on the surface for interaction with CD8+ cytotoxic T-cells which can induce cell death directly through induction of caspases by release of granzymes and perforin ([87, 88], Figure

1.5). MHC-II presents endocytosed peptides derived from the extracellular space for presentation to CD4+ helper T-cells which can secrete inflammatory cytokines or induce B cells to produce antibodies against the specific antigen (Figure 1.5). Alterations in T-cell subsets have been reported in blood from PD patients [89-92], but the presence of T-cells within the parenchyma in PD is still unclear. Nonetheless, imbalance of T-cell subpopulations suggest that immune system in PD becomes unable to ascertain self from non-self, mounting a response that ultimately becomes detrimental.

The HLA complex is highly polymorphic, and genome-wide association (GWAS) studies have suggested several variants in the HLA region encoding for class II (HLA-DR, -DQ) increase risk for developing PD [93-96]. These variants have also been implicated in several classical autoimmune disorders including rheumatoid arthritis, celiac disease, and type 1 diabetes. In regards to PD, differential risk association varies depending on ethnic population and region [97-99], suggesting gene-environment interactions are important for conferring risk to develop PD.

MHC-II is present on microglia and is rarely induced on astrocytes, but is largely undetectable in the healthy CNS, thus the observation of HLA-DR immunoreactive microglia in the SN and later putamen, hippocampus, and cortical regions of PD patients [100-102] suggested that either Lewy pathology and/or degeneration induces an inflammatory response. One study in mice has demonstrated that MHC-II is necessary for both α-syn-mediated neurodegeneration and T-cell infiltration [103].

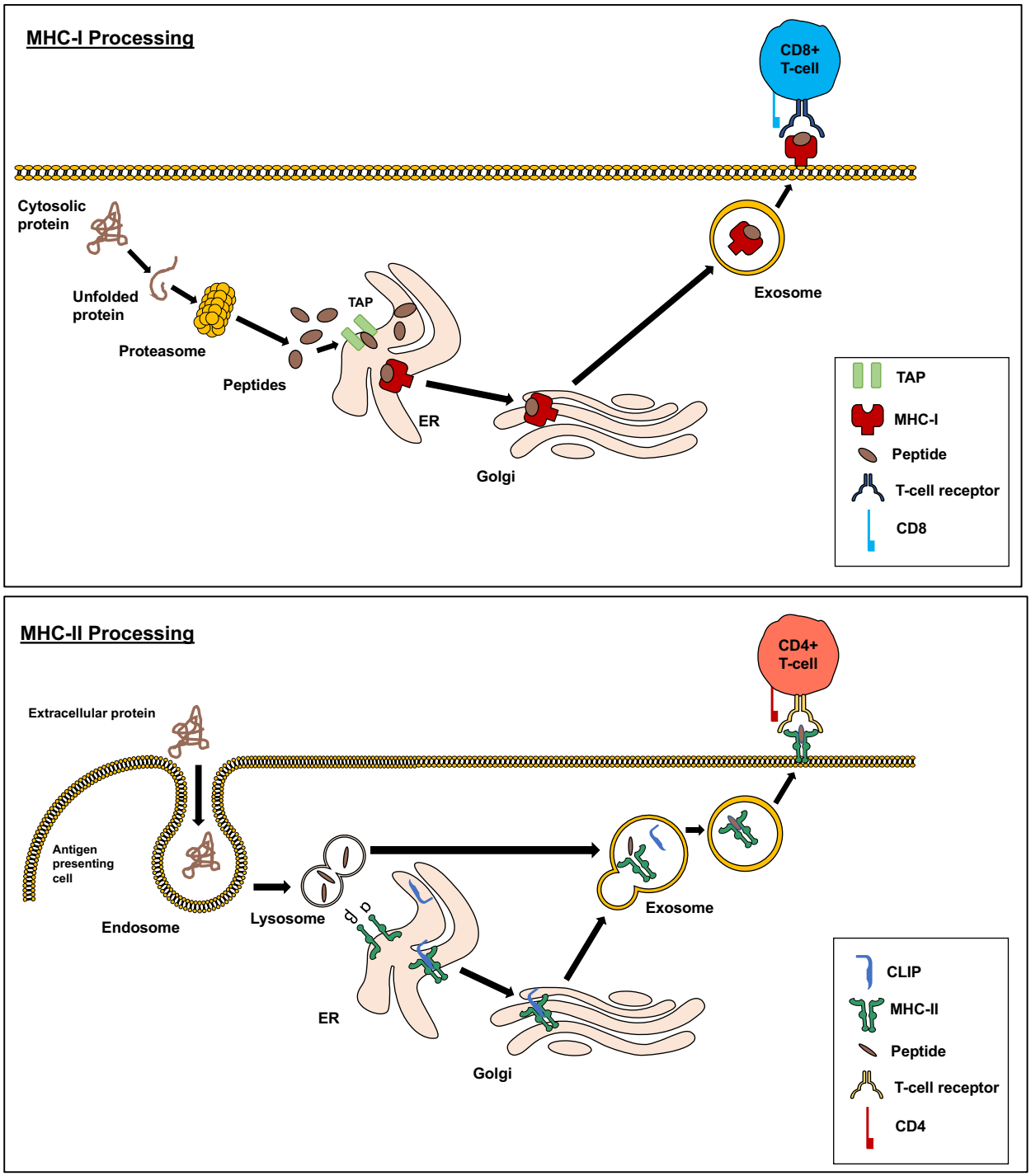

Figure 1.5: MHC-I and MHC-II processing of antigens
(TOP) Intracellular proteins are processed by the proteasome and broken down into smaller peptides, which are transferred to the ER by transporter associated with antigen processing (TAP) and are loaded on to MHC-I. The MHC-I – antigen complex is expressed on the cell surface for interaction with CD8+ cytotoxic T-cells.

Figure 1.5 cont'd
(BOTTOM) Extracellular protein is endocytosed or phagocytosed by an antigen presenting cell. Once in the lysosome, the protein is broken down into small peptides of 11-30 amino acids long. MHC-II is synthesized in the ER and then bound by the CLIP in the binding region until the peptide is loaded. The MHC-II complex is transported via the golgi to the exosome, where the acidic pH of the vesicle releases CLIP and and allows for the processed peptide to be loaded into MHC-II. Expression of the MHC-II – peptide complex is expressed on the cell surface to interact with CD4+ T cells.

However, a recent study reported an acceleration and increased magnitude of degeneration in rats with decreased MHC-II expression [104]. Thus, the association of MHC-II with either a proinflammatory or anti-inflammatory phenotype still remains a grey area. Nonetheless, differences in HLA genes and expression of MHC-II are consistently demonstrated in PD and thus suggest an altered inflammatory environment can influence disease progression. While the focus has been predominantly on MHC-II in PD, MHC-I expression has been observed on SN DA neurons [105], leading to the concept that PD may in part be an autoimmune disease.

Inflammatory Cytokines

Inflammatory cytokines secreted by microglia, astrocytes, and peripheral immune cells are the primary inflammatory contributors to the vicious feed-forward cycle of protein accumulation, inflammation, and cell death in PD. Single nucleotide polymorphisms in proinflammatory cytokine genes including tumor necrosis factor (TNF), interleukin-1 beta (IL-1β), and interleukin-6 (IL-6) are associated in an increased risk for PD [106-108]. Increases in proinflammatory cytokines and decreases in anti-inflammatory cytokines have been documented in PD affected regions including the SN, putamen, and frontal cortex [109]. The most well-studied cytokine in the context of PD is TNF. Levels of TNF and its receptor TNFR1 are consistently found to be increased in post-mortem PD tissue, particularly in the SN [110-112]. TNF can have both pro- and anti-apoptotic effects dependent on which of its two receptors it binds to: TNFR1 or TNFR2, respectively [113]. Interestingly, TNFR1 expression can be increased by interactions with dopamine as demonstrated in vitro [114]. Furthermore, introduction of TNF to DA neuron cultures induced toxicity [115]. Lastly, cytokines in PD have gained attention in

recent years as potential biomarkers to aid in early PD diagnosis, as they are detectable in both cerebrospinal fluid, whole blood, and plasma. Indeed, levels of interferon gamma (IFN-γ), interleukin-10 (IL-10), interleukin-13 (IL-13), interleukin-1 beta (IL-1β), interleukin-4 (IL-4), IL-6, and TNF are differentially expressed in PD patients compared to healthy controls (Chapter 4, Figure 4.1).

Gap In Knowledge: Is Inflammation a contributor to- or a consequence of degeneration?

Data from human studies and preclinical *in vitro* and *in vivo* studies (discussed in subsequent chapters) demonstrate a relationship between α-syn and inflammation or neurodegeneration and inflammation (Figure 1.6). However, the time course of these events has been unable to be investigated from onset of Lewy pathology formation through the interval of degeneration, as by the time of diagnosis, over half of SN DA neurons have already degenerated. As reviewed in chapter 2, animal models have also aided in our understanding between inflammation and α-syn or neurodegeneration, however, previously available models have generally failed to recapitulate key features of human PD which would allow for a clear time course of these events to be delineated. Using a novel rat model with distinct disease stages, the aim of this dissertation was to investigate the time course of α-syn accumulation, inflammation, and nigral degeneration both within the brain and in peripheral fluids.

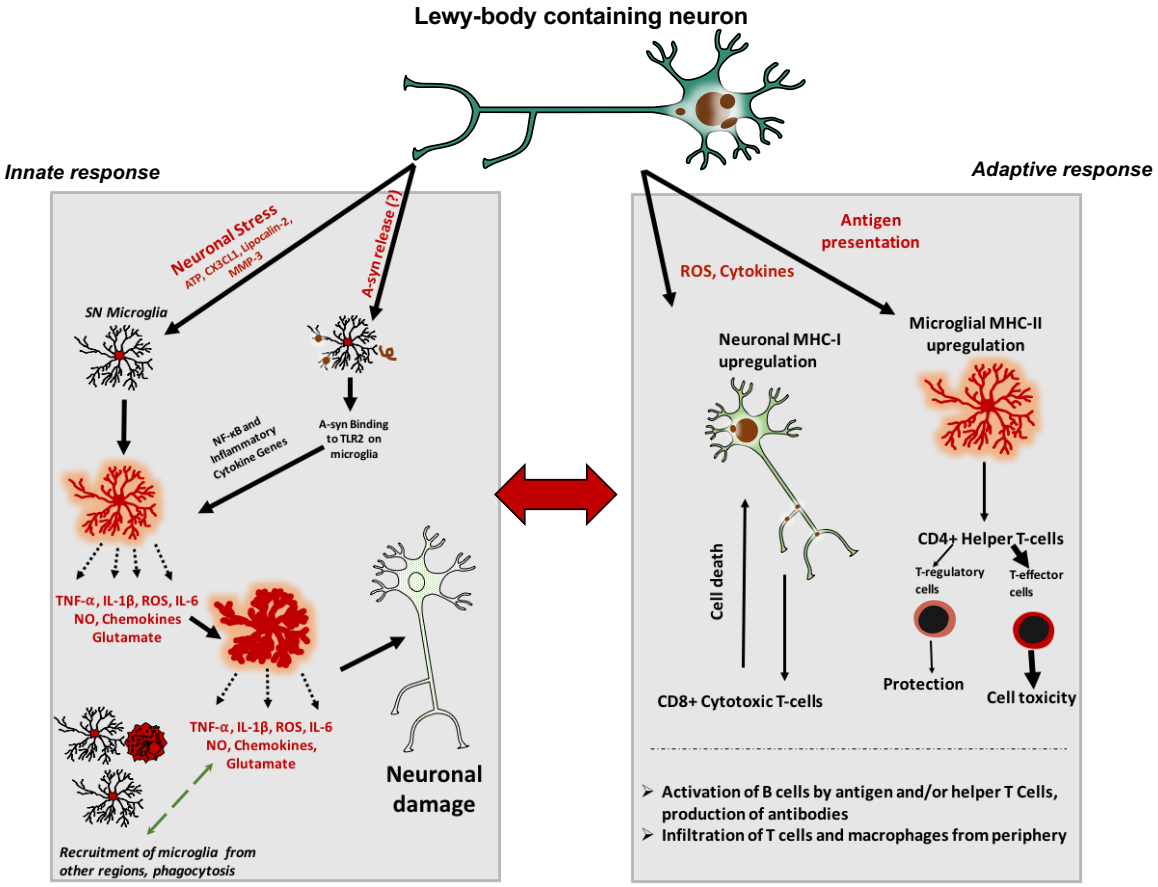

Figure 1.6 Potential innate and adaptive immune responses to accumulation of Lewy bodies in PD

Chronic accumulation of intraneuronal inclusions can cause aberrations in mitochondrial function, protein degradation systems, production of reactive oxygen species. Both neuronal stress signals and presentation of abnormal proteins as antigen can trigger an innate inflammatory response mediated by microglia within the CNS, but also signal to the adaptive immune system peripheral lymphocytes to invade, resulting in production of antibodies against the target “sick” neurons, and cytotoxicity through interactions with CD8+ T cells.

REFERENCES

REFERENCES

1. Parkinson, J., *An essay on the shaking palsy. 1817.* J Neuropsychiatry Clin Neurosci, 2002. **14**(2): p. 223-36; discussion 222.

2. Goetz, C.G., *The history of Parkinson's disease: early clinical descriptions and neurological therapies.* Cold Spring Harb Perspect Med, 2011. **1**(1): p. a008862.

3. Dorsey, E. and B.R. Bloem, *The parkinson pandemic—a call to action.* JAMA Neurology, 2018. **75**(1): p. 9-10.

4. Obeso, J.A., et al., *Past, present, and future of Parkinson's disease: A special essay on the 200th Anniversary of the Shaking Palsy.* Mov Disord, 2017. **32**(9): p. 1264-1310.

5. Fahn, S., *Description of Parkinson's disease as a clinical syndrome.* Ann N Y Acad Sci, 2003. **991**: p. 1-14.

6. Jankovic, J., *Parkinson's disease: clinical features and diagnosis.* J Neurol Neurosurg Psychiatry, 2008. **79**(4): p. 368-76.

7. Seifert, K.D. and J.I. Wiener, *The impact of DaTscan on the diagnosis and management of movement disorders: A retrospective study.* Am J Neurodegener Dis, 2013. **2**(1): p. 29-34.

8. Postuma, R.B., et al., *MDS clinical diagnostic criteria for Parkinson's disease.* Mov Disord, 2015. **30**(12): p. 1591-601.

9. Khoo, T.K., et al., *The spectrum of nonmotor symptoms in early Parkinson disease.* Neurology, 2013. **80**(3): p. 276-81.

10. Savica, R., et al., *Medical records documentation of constipation preceding Parkinson disease: A case-control study.* Neurology, 2009. **73**(21): p. 1752-8.

11. Ponsen, M.M., et al., *Idiopathic hyposmia as a preclinical sign of Parkinson's disease.* Ann Neurol, 2004. **56**(2): p. 173-81.

12. Peralta, C., et al., *Orthostatic hypotension and attention in Parkinson's disease with and without dementia.* J Neural Transm (Vienna), 2007. **114**(5): p. 585-8.

13. Chaudhuri, K.R., et al., *International multicenter pilot study of the first comprehensive self-completed nonmotor symptoms questionnaire for Parkinson's disease: the NMSQuest study.* Mov Disord, 2006. **21**(7): p. 916-23.

14. Bower, J.H., et al., *Anxious personality predicts an increased risk of Parkinson's disease.* Mov Disord, 2010. **25**(13): p. 2105-13.

15. Leentjens, A.F., et al., *Higher incidence of depression preceding the onset of Parkinson's disease: a register study.* Mov Disord, 2003. **18**(4): p. 414-8.

16. Shannon, K.M., et al., *Is alpha-synuclein in the colon a biomarker for premotor Parkinson's disease? Evidence from 3 cases.* Mov Disord, 2012. **27**(6): p. 716-9.

17. Iranzo, A., et al., *Neurodegenerative disease status and post-mortem pathology in idiopathic rapid-eye-movement sleep behaviour disorder: an observational cohort study.* Lancet Neurol, 2013. **12**(5): p. 443-53.

18. Biundo, R., L. Weis, and A. Antonini, *Cognitive decline in Parkinson's disease: the complex picture.* Npj Parkinson'S Disease, 2016. **2**: p. 16018.

19. Redgrave, P., et al., *Goal-directed and habitual control in the basal ganglia: implications for Parkinson's disease.* Nat Rev Neurosci, 2010. **11**(11): p. 760-72.

20. Lewy, F.H., *Paralysis agitans. I. Pathologische Anatomie.* Handbuch der Neurologie, 1912. **3**: p. 920-958.

21. Holdorff, B., *Friedrich Heinrich Lewy (1885-1950) and his work.* J Hist Neurosci, 2002. **11**(1): p. 19-28.

22. Goldman, J.E., et al., *Lewy bodies of Parkinson's disease contain neurofilament antigens.* Science, 1983. **221**(4615): p. 1082-4.

23. Maroteaux, L., J.T. Campanelli, and R.H. Scheller, *Synuclein: a neuron-specific protein localized to the nucleus and presynaptic nerve terminal.* J Neurosci, 1988. **8**(8): p. 2804-15.

24. Spillantini, M.G., et al., *alpha-Synuclein in filamentous inclusions of Lewy bodies from Parkinson's disease and dementia with lewy bodies.* Proc Natl Acad Sci U S A, 1998. **95**(11): p. 6469-73.

25. Braak, H., et al., *Staging of brain pathology related to sporadic Parkinson's disease.* Neurobiol Aging, 2003. **24**(2): p. 197-211.

26. Braak, H., et al., *Stages in the development of Parkinson's disease-related pathology.* Cell Tissue Res, 2004. **318**(1): p. 121-34.

27. Olanow, C.W. and P. Brundin, *Parkinson's disease and alpha synuclein: is Parkinson's disease a prion-like disorder?* Mov Disord, 2013. **28**(1): p. 31-40.

28. Jellinger, K.A., *A critical reappraisal of current staging of Lewy-related pathology in human brain.* Acta Neuropathol, 2008. **116**(1): p. 1-16.

29. Kalaitzakis, M.E., et al., *The dorsal motor nucleus of the vagus is not an obligatory trigger site of Parkinson's disease: a critical analysis of alpha-synuclein staging.* Neuropathol Appl Neurobiol, 2008. **34**(3): p. 284-95.

30. Jellinger, K.A., *Critical evaluation of the Braak staging scheme for Parkinson's disease.* Ann Neurol, 2010. **67**(4): p. 550.

31. Kingsbury, A.E., et al., *Brain stem pathology in Parkinson's disease: an evaluation of the Braak staging model.* Mov Disord, 2010. **25**(15): p. 2508-15.

32. Chan, C.S., T.S. Gertler, and D.J. Surmeier, *A molecular basis for the increased vulnerability of substantia nigra dopamine neurons in aging and Parkinson's disease.* Mov Disord, 2010. **25 Suppl 1**: p. S63-70.

33. Hirsch, E., A.M. Graybiel, and Y.A. Agid, *Melanized dopaminergic neurons are differentially susceptible to degeneration in Parkinson's disease.* Nature, 1988. **334**(6180): p. 345-8.

34. Kanaan, N.M., J.H. Kordower, and T.J. Collier, *Age-related changes in glial cells of dopamine midbrain subregions in rhesus monkeys.* Neurobiol Aging, 2010. **31**(6): p. 937-52.

35. A., K., et al., *Is the Vulnerability of Neurons in the Substantia Nigra of Patients with Parkinson's Disease Related to Their Neuromelanin Content?* Journal of Neurochemistry, 1992. **59**(3): p. 1080-1089.

36. Kurowska, Z., et al., *Is Axonal Degeneration a Key Early Event in Parkinson's Disease?* J Parkinsons Dis, 2016. **6**(4): p. 703-707.

37. Kordower, J.H., et al., *Disease duration and the integrity of the nigrostriatal system in Parkinson's disease.* Brain, 2013. **136**(Pt 8): p. 2419-31.

38. Kordower, J.H., et al., *Robust graft survival and normalized dopaminergic innervation do not obligate recovery in a Parkinson disease patient.* Ann Neurol, 2017. **81**(1): p. 46-57.

39. Cotzias, G.C., P.S. Papavasiliou, and R. Gellene, *Modification of Parkinsonism--chronic treatment with L-dopa.* N Engl J Med, 1969. **280**(7): p. 337-45.

40. Nagatsua, T. and M. Sawadab, *L-dopa therapy for Parkinson's disease: past, present, and future.* Parkinsonism Relat Disord, 2009. **15 Suppl 1**: p. S3-8.

41. LeWitt, P.A., *Levodopa therapy for Parkinson's disease: Pharmacokinetics and pharmacodynamics.* Mov Disord, 2015. **30**(1): p. 64-72.

42. Prashanth, L.K., S. Fox, and W.G. Meissner, *l-Dopa-induced dyskinesia-clinical presentation, genetics, and treatment.* Int Rev Neurobiol, 2011. **98**: p. 31-54.

43. Porras, G., et al., *L-dopa-induced dyskinesia: beyond an excessive dopamine tone in the striatum.* Sci Rep, 2014. **4**: p. 3730.

44. Nissen, T., et al., *Duration of L-dopa and dopamine agonist monotherapy in Parkinson's disease.* Scott Med J, 2012. **57**(4): p. 217-20.

45. Adler, C.H., et al., *Ropinirole for the treatment of early Parkinson's disease. The Ropinirole Study Group.* Neurology, 1997. **49**(2): p. 393-9.

46. Pahwa, R., K.E. Lyons, and R.A. Hauser, *Ropinirole therapy for Parkinson's disease.* Expert Rev Neurother, 2004. **4**(4): p. 581-8.

47. Weintraub, D., et al., *Impulse control disorders in Parkinson disease: a cross-sectional study of 3090 patients.* Arch Neurol, 2010. **67**(5): p. 589-95.

48. Etminan, M., et al., *Risk of Gambling Disorder and Impulse Control Disorder With Aripiprazole, Pramipexole, and Ropinirole: A Pharmacoepidemiologic Study.* J Clin Psychopharmacol, 2017. **37**(1): p. 102-104.

49. Pagonabarraga, J. and M.C. Rodriguez-Oroz, *[Rasagiline in monotherapy in patients with early stages of Parkinson's disease and in combined and adjunct therapy to levodopa with moderate and advanced stages].* Rev Neurol, 2013. **56**(1): p. 25-34.

50. T., M.P. and K. S., *Rationale for Selective COMT Inhibitors as Adjuncts in the Drug Treatment of Parkinson's Disease.* Pharmacology & Toxicology, 1990. **66**(5): p. 317-323.

51. Olanow, C.W. and F. Stocchi, *COMT inhibitors in Parkinson's disease.* Neurology, 2004. **62**: p. S72-S81.

52. Wagle Shukla, A. and M.S. Okun, *Surgical treatment of Parkinson's disease: patients, targets, devices, and approaches.* Neurotherapeutics, 2014. **11**(1): p. 47-59.

53. Angeli, A., et al., *Genotype and phenotype in Parkinson's disease: lessons in heterogeneity from deep brain stimulation.* Mov Disord, 2013. **28**(10): p. 1370-5.

54. Polymeropoulos, M.H., et al., *Mutation in the alpha-synuclein gene identified in families with Parkinson's disease.* Science, 1997. **276**(5321): p. 2045-7.

55. Houlden, H. and A.B. Singleton, *The genetics and neuropathology of Parkinson's disease.* Acta Neuropathol, 2012. **124**(3): p. 325-38.

56. Narayan, S., et al., *Household organophosphorus pesticide use and Parkinson's disease.* Int J Epidemiol, 2013. **42**(5): p. 1476-85.

57. Sanchez-Santed, F., M.T. Colomina, and E. Herrero Hernandez, *Organophosphate pesticide exposure and neurodegeneration.* Cortex, 2016. **74**: p. 417-26.

58. Wan, N. and G. Lin, *Parkinson's Disease and Pesticides Exposure: New Findings From a Comprehensive Study in Nebraska, USA.* J Rural Health, 2016. **32**(3): p. 303-13.

59. Dhillon, A.S., et al., *Pesticide/environmental exposures and Parkinson's disease in East Texas.* J Agromedicine, 2008. **13**(1): p. 37-48.

60. Baltazar, M.T., et al., *Pesticides exposure as etiological factors of Parkinson's disease and other neurodegenerative diseases--a mechanistic approach.* Toxicol Lett, 2014. **230**(2): p. 85-103.

61. Gao, H.M., B. Liu, and J.S. Hong, *Critical role for microglial NADPH oxidase in rotenone-induced degeneration of dopaminergic neurons.* J Neurosci, 2003. **23**(15): p. 6181-7.

62. Wu, F., et al., *Rotenone impairs autophagic flux and lysosomal functions in Parkinson's disease.* Neuroscience, 2015. **284**: p. 900-11.

63. Emmrich, J.V., et al., *Rotenone induces neuronal death by microglial phagocytosis of neurons.* Febs j, 2013. **280**(20): p. 5030-8.

64. Pan-Montojo, F., et al., *Environmental toxins trigger PD-like progression via increased alpha-synuclein release from enteric neurons in mice.* Sci Rep, 2012. **2**: p. 898.

65. Bardou, I., et al., *Age and duration of inflammatory environment differentially affect the neuroimmune response and catecholaminergic neurons in the midbrain and brainstem.* Neurobiol Aging, 2014. **35**(5): p. 1065-73.

66. Collier, T.J., et al., *Aging-related changes in the nigrostriatal dopamine system and the response to MPTP in nonhuman primates: diminished compensatory mechanisms as a prelude to parkinsonism.* Neurobiol Dis, 2007. **26**(1): p. 56-65.

67. Bobela, W., P. Aebischer, and B.L. Schneider, *Alphalpha-Synuclein as a Mediator in the Interplay between Aging and Parkinson's Disease.* Biomolecules, 2015. **5**(4): p. 2675-700.

68. Ross, J.M., L. Olson, and G. Coppotelli, *Mitochondrial and Ubiquitin Proteasome System Dysfunction in Ageing and Disease: Two Sides of the Same Coin?* Int J Mol Sci, 2015. **16**(8): p. 19458-76.

69. Sulzer, D., *Multiple hit hypotheses for dopamine neuron loss in Parkinson's disease.* Trends Neurosci, 2007. **30**(5): p. 244-50.

70. Collier, T.J., N.M. Kanaan, and J.H. Kordower, *Aging and Parkinson's disease: Different sides of the same coin?* Mov Disord, 2017. **32**(7): p. 983-990.

71. Collier, T.J., N.M. Kanaan, and J.H. Kordower, *Ageing as a primary risk factor for Parkinson's disease: evidence from studies of non-human primates.* Nat Rev Neurosci, 2011. **12**(6): p. 359-66.

72. Ouchi, Y., et al., *Microglial activation and dopamine terminal loss in early Parkinson's disease.* Ann Neurol, 2005. **57**(2): p. 168-75.

73. Gerhard, A., et al., *In vivo imaging of microglial activation with [11C](R)-PK11195 PET in idiopathic Parkinson's disease.* Neurobiol Dis, 2006. **21**(2): p. 404-12.

74. Doorn, K.J., et al., *Brain region-specific gene expression profiles in freshly isolated rat microglia.* Frontiers in Cellular Neuroscience, 2015. **9**: p. 84.

75. De Biase, L.M., et al., *Local Cues Establish and Maintain Region-Specific Phenotypes of Basal Ganglia Microglia.* Neuron, 2017. **95**(2): p. 341-356.e6.

76. Frost, J.L. and D.P. Schafer, *Microglia: Architects of the Developing Nervous System.* Trends in cell biology, 2016. **26**(8): p. 587-597.

77. Cunningham, C.L., V. Martínez-Cerdeño, and S.C. Noctor, *Microglia regulate the number of neural precursor cells in the developing cerebral cortex.* The Journal of neuroscience : the official journal of the Society for Neuroscience, 2013. **33**(10): p. 4216-4233.

78. Streit, W.J., et al., *Dystrophic microglia in the aging human brain.* Glia, 2004. **45**(2): p. 208-12.

79. Kettenmann, H., et al., *Physiology of microglia.* Physiol Rev, 2011. **91**(2): p. 461-553.

80. Nimmerjahn, A., *Two-photon imaging of microglia in the mouse cortex in vivo.* Cold Spring Harb Protoc, 2012. **2012**(5).

81. Arroyo, D.S., et al., *Toll-like receptors are key players in neurodegeneration.* Int Immunopharmacol, 2011. **11**(10): p. 1415-21.

82. Drouin-Ouellet, J., et al., *Toll-like receptor expression in the blood and brain of patients and a mouse model of Parkinson's disease.* Int J Neuropsychopharmacol, 2014. **18**(6).

83. Doorn, K.J., et al., *Microglial phenotypes and toll-like receptor 2 in the substantia nigra and hippocampus of incidental Lewy body disease cases and Parkinson's disease patients.* Acta Neuropathol Commun, 2014. **2**: p. 90.

84. Dzamko, N., et al., *Toll-like receptor 2 is increased in neurons in Parkinson's disease brain and may contribute to alpha-synuclein pathology.* Acta Neuropathol, 2017. **133**(2): p. 303-319.

85. Kim, C., et al., *Neuron-released oligomeric alpha-synuclein is an endogenous agonist of TLR2 for paracrine activation of microglia.* Nat Commun, 2013. **4**: p. 1562.

86. Gunther, E. and L. Walter, *The major histocompatibility complex of the rat (Rattus norvegicus).* Immunogenetics, 2001. **53**(7): p. 520-42.

87. Peng, S.P., et al., *Participation of perforin in mediating dopaminergic neuron loss in MPTP-induced Parkinson's disease in mice.* Biochem Biophys Res Commun, 2017. **484**(3): p. 618-622.

88. Murphy Kenneth, T.P., Walport Mark, Janeway Charles, *Janeway's Immunobiology*. 8 ed. 2012: Garland Science.

89. Chen, Y., et al., *Clinical correlation of peripheral CD4+cell subsets, their imbalance and Parkinson's disease.* Mol Med Rep, 2015. **12**(4): p. 6105-11.

90. Stevens, C.H., et al., *Reduced T helper and B lymphocytes in Parkinson's disease.* J Neuroimmunol, 2012. **252**(1-2): p. 95-9.

91. Baba, Y., et al., *Alterations of T-lymphocyte populations in Parkinson disease.* Parkinsonism Relat Disord, 2005. **11**(8): p. 493-8.

92. Bas, J., et al., *Lymphocyte populations in Parkinson's disease and in rat models of parkinsonism.* J Neuroimmunol, 2001. **113**(1): p. 146-52.

93. Kannarkat, G.T., et al., *Common Genetic Variant Association with Altered HLA Expression, Synergy with Pyrethroid Exposure, and Risk for Parkinson's Disease: An Observational and Case-Control Study.* NPJ Parkinsons Dis, 2015. **1**.

94. Hamza, T.H., et al., *Common genetic variation in the HLA region is associated with late-onset sporadic Parkinson's disease.* Nat Genet, 2010. **42**(9): p. 781-5.

95. Jamshidi, J., et al., *HLA-DRA is associated with Parkinson's disease in Iranian population.* Int J Immunogenet, 2014. **41**(6): p. 508-11.

96. Sulzer, D., et al., *T cells from patients with Parkinson's disease recognize alpha-synuclein peptides.* Nature, 2017. **546**(7660): p. 656-661.

97. Zhao, Y., et al., *Association of HLA locus variant in Parkinson's disease.* Clin Genet, 2013. **84**(5): p. 501-4.

98. Chiang, H.L., et al., *Genetic analysis of HLA-DRA region variation in Taiwanese Parkinson's disease.* Parkinsonism Relat Disord, 2012. **18**(4): p. 391-3.

99. Lee, P.-C., et al., *Gene-environment interactions linking air pollution and inflammation in Parkinson's disease.* Environmental Research, 2016. **151**: p. 713-720.

100. Croisier, E., et al., *Microglial inflammation in the parkinsonian substantia nigra: relationship to alpha-synuclein deposition.* J Neuroinflammation, 2005. **2**: p. 14.

101. Imamura, K., et al., *Distribution of major histocompatibility complex class II-positive microglia and cytokine profile of Parkinson's disease brains.* Acta Neuropathol, 2003. **106**(6): p. 518-26.

102. McGeer, P.L., et al., *Reactive microglia are positive for HLA-DR in the substantia nigra of Parkinson's and Alzheimer's disease brains.* Neurology, 1988. **38**(8): p. 1285-91.

103. Harms, A.S., et al., *MHCII is required for alpha-synuclein-induced activation of microglia, CD4 T cell proliferation, and dopaminergic neurodegeneration.* J Neurosci, 2013. **33**(23): p. 9592-600.

104. Jimenez-Ferrer, I., et al., *Allelic difference in Mhc2ta confers altered microglial activation and susceptibility to alpha-synuclein-induced dopaminergic neurodegeneration.* Neurobiol Dis, 2017. **106**: p. 279-290.

105. Cebrian, C., et al., *MHC-I expression renders catecholaminergic neurons susceptible to T-cell-mediated degeneration.* Nat Commun, 2014. **5**: p. 3633.

106. Chu, K., X. Zhou, and B.Y. Luo, *Cytokine gene polymorphisms and Parkinson's disease: a meta-analysis.* Can J Neurol Sci, 2012. **39**(1): p. 58-64.

107. Nie, K., et al., *Polymorphisms in immune/inflammatory cytokine genes are related to Parkinson's disease with cognitive impairment in the Han Chinese population.* Neurosci Lett, 2013. **541**: p. 111-5.

108. San Luciano, M., et al., *GENDER DIFFERENCES IN THE IL6 −174G>C AND ESR2 1730G>A POLYMORPHISMS AND THE RISK OF PARKINSON'S DISEASE.* Neuroscience letters, 2012. **506**(2): p. 312-316.

109. Garcia-Esparcia, P., et al., *Complex deregulation and expression of cytokines and mediators of the immune response in Parkinson's disease brain is region dependent.* Brain Pathol, 2014. **24**(6): p. 584-98.

110. Duke, D.C., et al., *The medial and lateral substantia nigra in Parkinson's disease: mRNA profiles associated with higher brain tissue vulnerability.* Neurogenetics, 2007. **8**(2): p. 83-94.

111. Mogi, M., et al., *Caspase activities and tumor necrosis factor receptor R1 (p55) level are elevated in the substantia nigra from parkinsonian brain.* J Neural Transm (Vienna), 2000. **107**(3): p. 335-41.

112. Boka, G., et al., *Immunocytochemical analysis of tumor necrosis factor and its receptors in Parkinson's disease.* Neurosci Lett, 1994. **172**(1-2): p. 151-4.

113. Cabal-Hierro, L. and P.S. Lazo, *Signal transduction by tumor necrosis factor receptors.* Cellular Signalling, 2012. **24**(6): p. 1297-1305.

114. Gomez-Santos, C., et al., *Dopamine induces TNFalpha and TNF-R1 expression in SH-SY5Y human neuroblastoma cells.* Neuroreport, 2007. **18**(16): p. 1725-8.

115. McGuire, S.O., et al., *Tumor necrosis factor alpha is toxic to embryonic mesencephalic dopamine neurons.* Exp Neurol, 2001. **169**(2): p. 219-30.

Chapter 2: Quality Over Quantity: Advantages of Using Alpha-Synuclein Preformed Fibril Triggered Synucleinopathy to Model Idiopathic Parkinson's Disease

Abstract

Animal models have significantly advanced our understanding of Parkinson's disease (PD). Alpha-synuclein (α-syn) has taken center stage due to its genetic connection to familial PD and localization to Lewy bodies, one pathological hallmark of PD. Animal models developed on the premise of elevated alpha-synuclein via germline manipulation or viral vector-mediated overexpression are used to investigate PD pathophysiology and vet novel therapeutics. While these models represented a step forward compared to their neurotoxicant model predecessors, they rely on overexpression of supraphysiological levels of α-syn to trigger toxicity. However, whereas *SNCA*-linked familial PD is associated with elevated α-syn, elevated α-syn is not associated with idiopathic PD. Therefore, the defining feature of the α-syn overexpression models may fail to appropriately model idiopathic PD. In the last several years a new model has been developed in which α-syn preformed fibrils are injected intrastriatally and trigger normal endogenous levels of α-syn to misfold and accumulate into Lewy body-like inclusions. Following a defined period of inclusion accumulation, distinct phases of neuroinflammation and progressive degeneration can be detected in the nigrostriatal system. In this perspective, we highlight the fact that levels of α-syn achieved in overexpression models generally exceed those observed in idiopathic and even *SNCA* multiplication-linked PD. This raises the possibility that supraphysiological α-syn expression may drive pathophysiological mechanisms not relevant to idiopathic PD. We suggest that synucleinopathy triggered to form within the context of normal α-syn expression represents a more faithful animal model of idiopathic PD and should be used when testing the disease-modifying potential of novel therapeutics.

Introduction

Parkinson's disease (PD) is the second most common neurodegenerative disorder, affecting 7-10 million individuals worldwide. Though PD was first described over 200 years ago by James Parkinson, no therapies currently exist to halt or slow nigrostriatal degeneration despite scores of preclinical studies predicting the success of particular disease-modifying treatment strategies. This "translational abyss" may be due in part to the failure of animal models to faithfully recapitulate human disease and, more specifically, failure to use the appropriate PD animal model.

During the past two decades, numerous preclinical studies have used overexpression of human wildtype or mutant alpha-synuclein (α-syn) in *Drosophila*, rodents and non-human primates to model PD. Overexpression is achieved in these models via transgenic engineering or via injection of viral vectors. However, while these α-syn models represented an advance over neurotoxicant models through the incorporation of α-syn, the mechanism of toxicity and the neuropathology generated differ from idiopathic PD in key respects. Specifically, α-syn overexpression paradigms result in α-syn protein expression levels that far exceed levels associated with idiopathic PD. Such supraphysiological α-syn protein levels can induce exacerbated neuroinflammation. Further, viral vector-mediated α-syn overexpression results in pathology in limited circuitry and can lack a protracted phase of classical Lewy body-like inclusion pathology. We contend that these shortcomings in the α-syn overexpression-based models have hindered our understanding of the pathogenic contributions of normal

endogenous α-syn in idiopathic PD and have handicapped our ability to predict efficacy of novel neuroprotective therapeutics.

Recently, a model of synucleinopathy and nigral degeneration induced by intracerebral administration of sonicated preformed fibrils of α-syn (PFFs) has provided a new platform to study the pathogenic cascade in which normal levels of endogenous α-syn levels are triggered to misfold, template and accumulate. The engagement of physiologic levels of endogenous α-syn in the α-syn PFF model allows for the assessment of differential neural circuit vulnerabilities to α-syn inclusion formation and toxicity. The α-syn PFF model recapitulates many features of human idiopathic PD, namely: a protracted interval of widespread accumulation of insoluble Lewy-like pathology, α-syn inclusion triggered neuroinflammation and degeneration of specific neuronal subpopulations.

In this perspective, we briefly review the pathological features of human idiopathic and *SNCA*-linked familial PD in order to compare these features to those observed in the α-syn PFF model. Ultimately, these sporadic PD and α-syn PFF model features will be placed in the context of the pathology induced by overexpression of α-syn, with a focus on viral vector-mediated α-syn overexpression. We offer up the view point that the synucleinopathy and the inclusion-initiated nigral degeneration resulting from α-syn PFF injection provides a superior platform for comprehending the pathophysiology of idiopathic PD and by extension, a superior platform for evaluating potential neuroprotective therapeutics.

Parkinson's Disease

Alpha-synuclein (α-syn) Expression and Localization in Idiopathic and SNCA-linked Familial PD

While the majority (90-95%) of PD cases do not have an identified genetic component, they share with familial PD a role for the protein α-syn. In the CNS, α-syn accounts for approximately 1% of total protein and is localized primarily in the cytosol of axon terminals, with known roles in membrane bending, synaptic transmission, and plasticity [1, 2]. In 1997 it was first revealed that an Ala53Thr (A53T) substitution in the α-syn gene (*SNCA*) was associated with young onset, autosomal dominant PD [3]. Shortly thereafter it was shown in subjects with idiopathic PD that fibrillar α-syn was a major component of Lewy bodies [4]. Subsequent work identified additional point mutations (A30P, E46K, H50Q, G51D;[5-8]) that increase the risk of PD. The effects of these missense mutations on α-syn protein conformational state, solubility, membrane association, and aggregation kinetics have been extensively studied *in vitro* and *in vivo* [9-12]. In addition to point mutations in *SNCA*, duplications or triplications of wildtype *SNCA* are also causative in familial PD. Collectively, this body of work provides compelling evidence that α-syn plays a central role in the pathophysiology of both familial and idiopathic PD.

As expected, studies of α-syn multiplication carriers demonstrate that α-syn mRNA and protein are elevated in these genetic forms of the disease with 1.5-2-fold increases in abundance reported [13-17]. Notably, *SNCA* triplication carriers exhibit earlier onset and more-rapidly progressing PD compared to duplication carriers or sporadic PD

patients, further lending support that dose-dependent increases in α-syn are a driving factor in disease onset and severity. However, in idiopathic PD the evidence for either elevated α-syn mRNA or α-syn protein is lacking. Analysis of α-syn mRNA levels within individual nigral neurons from early or late idiopathic PD subjects has revealed conflicting results with no differences reported [18, 19], increases reported [20] or decreases reported [21, 22]. Analysis of total α-syn protein levels in postmortem idiopathic PD tissue suggests either a modest transient increase or similar levels to age-matched control [23]. In contrast to *SNCA*-linked familial PD, the concept that increases in α-syn levels drive pathophysiology in idiopathic PD is less supported.

Whereas total expression levels of α-syn appear to distinguish *SNCA* multiplication carriers from idiopathic PD patients, changes in the solubility, membrane association, and abundance of post-translationally modified forms α-syn are similar in both patient subgroups. Investigations beyond a focus on α-syn abundance have identified changes in cellular localization and posttranslational modifications as potential mechanisms of α-syn-mediated toxicity, as reviewed in [10, 24-30]. In idiopathic PD, studies have consistently demonstrated shifts in the ratio of soluble to insoluble α-syn without concurrent changes in total α-syn levels. Specifically: decreases in soluble monomeric α-syn with concurrent increases in soluble phosphorylated α-syn (pSyn) along with increases in membrane-bound α-syn have been observed in particularly vulnerable regions (SN and cortex) in sporadic PD cases [31, 32]. Similar observations have also been made in samples derived from *SNCA* triplication carriers, albeit with increased magnitude and less regional specificity [25]. The fact that both genetic and idiopathic

forms of PD are associated with α-syn phosphorylation and increased membrane interactions suggests a role for these phenomena in PD pathophysiology.

Development of Lewy Pathology and Affected Circuitry

Confirmed diagnosis of PD is not made until Lewy bodies (LBs) and Lewy neurites (LNs) are observed upon post-mortem evaluation. LBs are composed of dozens of proteins, including but not limited to α-syn, neurofilament, p62 and ubiquitin. pSyn staining is the most common immunohistochemical method of LB detection in post-mortem tissue, however, it should be noted that pSyn inclusions likely represent end stage LB development. Immature LBs, termed “pale bodies” are more often observed in early disease stages. Pale bodies are strongly immunoreactive for α-syn and manifest as intracellular diffuse, granular eosinophilic material with ill-defined borders. As disease stage advances, mature cytoplasmic LBs predominate over pale bodies and differ slightly in appearance depending on location in the cortex or brainstem [31-33]. With increasing maturity, LB and LN inclusions display a dense core with radiating filaments, and are strongly Thioflavin-S positive for beta-sheet structure and resistant to digestion by proteinase-K [34, 35]

Although Lewy pathology is widespread in PD brain, it occurs in well-defined regions including the substantia nigra pars compacta, amygdala, olfactory bulb, temporal, frontal and parietal cortices [36]. Braak and colleagues developed a staging scheme for PD based on the location of pSyn LB and LN inclusions. Braak proposed that inclusions are first found in the olfactory bulb and dorsal motor nucleus of the vagus nerve, and follow

an ascending pattern through the brainstem and finally the cortex [37, 38], lending to the debate of PD as a prion-like disease [36, 38, 39]. However, it should be noted that ~50% of cases do not follow this staging scheme [40-43]. Other theories suggest parallel rather than stepwise accumulation of Lewy pathology based on differential vulnerability profiles of various cell types and regions [44].

Neuroinflammation

In recent years, neuroinflammation has been proposed as a contributor to neurodegeneration in PD and a potential target for disease modification. Early observations of post-mortem tissue describe a local increase in inflammatory markers in the SN associated with microglia, notably human-leukocyte antigen-D related (HLA-DR;[45-48]), the human analog for major histocompatibility complex-II (MHC-II; antigen presentation). Not only has increased MHC-II expression been observed, it correlates positively with α-syn burden [49]. More recent work has implicated mutations in HLA-DR in amplified risk for developing PD, and levels of MHC-II are increased in cases of Incidental Lewy Body Disease (Braak stage I-II; [50] suggesting that inflammation may be at least in part, a contributing factor to ongoing degeneration [51]. On a broad level, cytokine measurements from patient biofluids (plasma and CSF) have consistently shown deviations from normal proinflammatory and anti-inflammatory cytokine levels compared to controls, although results are conflicting and may stem from variance in subject disease duration and time of sample collection [52-54]. However, while studies of patient tissue and biofluids have suggested that inflammation is involved in PD, these samples represent a single point in time over long disease duration. It is unclear

whether neuroinflammatory markers that associate with LBs preceed the formation of LBs and if the LB-containing neurons ultimately degenerate. Thus, the time-course of neuroinflammation in relation to α-syn accumulation and aggregation and nigral degeneration in human PD has yet to be determined.

Using the α-syn PFF seeded synucleinopathy to model idiopathic PD

PFF-induced synucleinopathy in the context of normal levels of endogenous α-syn

Given that idiopathic PD is not associated with an increase in total α-syn protein levels, synucleinopathy that arises in the context of normal endogenous α-syn levels would more faithfully recapitulate a key characteristic of the non-genetic form of PD. In contrast, previous models have relied on global overexpression (transgenics) or targeted overexpression (viral vector-mediated) of α-syn (Table 1). The α-syn preformed fibril (PFF) model represents an approach in which synucleinopathy is induced in an environment of normal α-syn protein levels. This was first developed *in vitro* by introduction of α-syn PFFs to primary neuronal cultures. Briefly, α-syn fibrils are generated from recombinant α-syn monomers and sonicated to form smaller ~50 nm fragments which are introduced to cell culture [55]. The PFFs are internalized by neurons, template and recruit endogenous α-syn and accumulate as inclusions of insoluble pSyn [55-57]. The pSyn inclusions ultimately lead to neuronal dysfunction and degeneration. This toxicity is not due to introduction of PFFs *per se* but can be directly linked to the recruitment of endogenous α-syn into inclusions as evidenced by the fact that PFFs do not induce toxicity when applied to α-syn$^{-/-}$ primary neurons [55, 58].

Development of widespread Lewy-like Pathology

The α-syn PFF model has since been extended to wildtype mice [59] and rats [60-62] and most recently non-human primates [63]. These studies demonstrate that direct intracerebral injection of α-syn PFFs leads to accumulation of insoluble pSyn inclusions resembling Lewy pathology, all taking place in an environment of normal endogenous α-syn expression levels. The similarity between α-syn PFF induced pSyn inclusions and human Lewy pathology is particularly striking. At early time points post-injection, pSyn immunoreactive inclusions resemble pale bodies: granular, diffuse and cytoplasmic (Figure 1C). Over time, pSyn inclusions condense into more compact aggregates. The observed pSyn inclusions colocalize with markers commonly observed in human LBs including p62 and ubiquitin, consist of α-syn oligomers and fibrils, and are also Thioflavin-S positive and proteinase-K resistant [60, 61]. Two photon microscopy has confirmed that neurons that form these pSyn inclusions ultimately degenerate [64]. Similarly, the magnitude of pSyn inclusion formation observed in the substantia nigra 2 months following PFF injection can be used to predict the ultimate extent of nigral degeneration observed at 6 months [61]. The protracted course of these aggregation and degeneration events provides investigators the ability to focus on particular phases of the synucleinopathy cascade.

In vivo, the spatial emergence of LB and LN-like pathology is dependent on the location of PFF injection. For example, several groups have demonstrated that intrastriatal injections of PFFs result in pSyn inclusion accumulation in cell bodies of regions innervating the striatum [65]: namely the substantia nigra, agranular insular and motor

cortices, and amygdala [58-62], suggesting that axon terminals internalize the PFFs. The occurrence of pathology in these defined regions supports the concept of retrograde transport and templating of endogenous α-syn within neurons exposed to the injection site, rather than prion-like spread throughout extensive brain networks. Importantly, areas in which pathology is observed are implicated in human PD [36].

Neuroinflammation

In addition to generating widespread pathology, intrastriatal injection of α-syn PFFs allows for investigations to delineate the time course of the inflammatory response in the substantia nigra. Due to the fact that the injection site (striatum) is spatially separated from the substantia nigra, inflammation related to surgical injection is minimized. Intrastriatal injection of PFFs, but not vehicle or other protein controls, induces peak reactive microglial morphology in the substantia nigra at 2 months, corresponding to the time point in which the greatest number of pSyn inclusions are observed [61]. In addition, a pSyn specific increase in MHC-II immunoreactive microglia is observed at this same time point, significantly correlating with pSyn inclusion load. This relationship between MHC-II immunoreactivity and α-syn inclusion burden is reminiscent to what has been reported in idiopathic PD [49] providing face validity to the α-syn PFF model.

Is α-syn overexpression analogous to idiopathic PD?

Reliance on supraphysiological α-syn levels and lack of protracted Lewy-like pathology

Models induced by intranigral injection of adenoassociated (AAV) or lentiviral (LV) vectors overexpressing human wildtype or mutant α-syn often result in dramatic increases in the levels of protein [66-74]. Although final protein levels are titer dependent, many studies report levels of α-syn 2-20x higher than normal endogenous expression levels, as reviewed extensively [75]. As these levels far exceed those observed in either idiopathic, duplication and even SNCA triplication carriers, they raise the potential for pathophysiological mechanisms specific to supraphysiological α-syn expression, mechanisms that may not be relevant to idiopathic PD. Indeed, the downregulation of multiple trophic factor responsive genes is observed with 4-fold, but not lower α-syn overexpression levels [18, 76]. *In vitro* studies show that following transduction, neurons release multiple forms of α-syn [77]. It is therefore likely that α-syn is similarly released from neurons transduced *in vivo*. It is unclear to what extent inclusion-bearing neurons release α-syn, if at all.

Lewy pathology in PD is widespread and likely develops in multiple regions concurrently. In contrast, AAV and LV-mediated overexpression models drive α-syn expression in discrete circuitries, most often the nigrostriatal system. Another consideration is the form of Lewy pathology generated by α-syn overexpression. Although pSyn immunoreactive and proteinase-K resistant inclusions have been reported they are most often small and punctate [74] in contrast to the large, cytoplasmic aggregates seen in human PD and in the α-syn PFF model. Further,

frequently the pSyn inclusions generated following α-syn overexpression are localized to the nucleus (Figure 1B), unlike the cytoplasmic LBs that are the hallmark of PD and are observed in the PFF model. A dramatic rise in cytosolic pSyn has been documented in PD [23], and thus pSyn localized to the nucleus that is observed with viral vector-mediated α-syn overexpression would prevent pSyn's ability to interact with cytoplasmic proteins and structures.

Transgenic models overexpressing wildtype or mutant α-syn consistently display widespread synuclein pathology including proteinase-K resistant inclusions and behavioral deficits [78, 79]. While there are some exceptions [80], the majority of transgenic models do not exhibit robust, protracted nigral degeneration [81, 82]. Thus, while transgenic models are adequate for investigating development of Lewy-like pathology, most fail to recapitulate downstream nigral degeneration and thus have limited translational potential for evaluation of neuroprotective strategies.

Inflammation in AAV and LV-mediated overexpression models: location, location, location

Another feature of viral vector-mediated α-syn overexpression models that is often leveraged is their ability to produce a robust neuroinflammatory response as indicated by microgliosis, MHC-II and CD68 on microglia, in addition to production of proinflammatory cytokines [83-85]. However, there are several considerations when interpreting the disease relevance of the neuroinflammatory response in this paradigm. First, the majority of viral vector models are induced by direct intranigral injection which alone, in the absence of α-syn overexpression, can trigger a pronounced increase in

MHC-II immunoreactive microglia (Figure 1D). This suggests that a significant component of the inflammatory response resulting from intranigral injections of α-syn vectors is due to the injection itself. Further, as previously stated, α-syn overexpression paradigms can result in the release of supraphysiological levels of α-syn into the immediate environment. This secretion of α-syn likely triggers a neuroinflammatory response in the absence of degeneration (Figure 1D) that has little to do with the disease state attempting to be modeled. Lastly, the majority of AAV and LV models overexpress human α-syn, not rodent α-syn, in rats and mice [75, 86]. As rat and mouse α-syn differs from human α-syn by 8 amino acids, it is plausible that overexpression of the foreign human protein may initiate an artificial inflammatory response.

Conclusions

The ability to advance our understanding of pathophysiology in idiopathic PD and predict the efficacy of novel therapeutics is dependent on the fidelity of animal models to the disease state. When modeling idiopathic PD, the presence of LB-like α-syn inclusions within the context of normal endogenous α-syn levels in multiple brain regions, which ultimately results in progressive nigrostriatal degeneration are an essential model feature. While α-syn overexpression models have advanced our understanding of α-syn-mediated toxicity, they depend on focal expression of supraphysiological levels of α-syn in a limited circuitry. In contrast to *SNCA*-linked familial PD, clinicopathologic evidence does not support the concept that increases in α-syn levels drive pathophysiology in idiopathic PD and therefore α-syn overexpression may trigger pathogenic mechanisms that may not be relevant to idiopathic PD. We

propose that widespread accumulation of Lewy body-like inclusions induced by injection of PFFs in the context of normal α-syn levels, ultimately resulting in downstream inflammation and progressive nigral degeneration, more faithfully models the sequence of events in idiopathic PD. Thus, the synucleinopathy induced by α-syn PFF injections represents an exceptional preclinical PD model to investigate the pathogenic contribution of endogenous α-syn, and assess novel disease-modifying therapeutics.

Feature	AAV-Overexpression Models	α-syn PFF Model
Ability to examine impact of α-synuclein inclusions distinct from degeneration	**Difficult** Simultaneous α-syn overexpression and aggregation progresses rapidly to degeneration over the course of weeks	**Straightforward** Distinct interval of inclusion formation followed by degeneration over a protracted time course
Injection artifact	**Confound** Direct injections into the SN produce marked neuroinflammatory response that can make interpretation difficult	**Less of a factor** Direct injections into the striatum have less of an impact within the SN
α-synuclein levels	**Not analogous to idiopathic PD** Continuous supraphysiological α-syn levels produced by forced overexpression are not analogous to idiopathic PD	**Normal endogenous α-syn levels** Pathophysiology results from templating of normal levels of α-syn
Extranigral α-synuclein pathology	**Not present** Pathology limited to the nigrostriatal system	**Wide spread α-syn pathology** Allows for the examination of events outside of nigrostriatal system

Table 2.1: Considerations when modeling idiopathic PD in rodents
Abbreviations: AAV= adenoassociated virus; α-syn= alpha-synuclein, PD= Parkinson's disease; PFFs= alpha-synuclein preformed fibrils; SN= substantia nigra

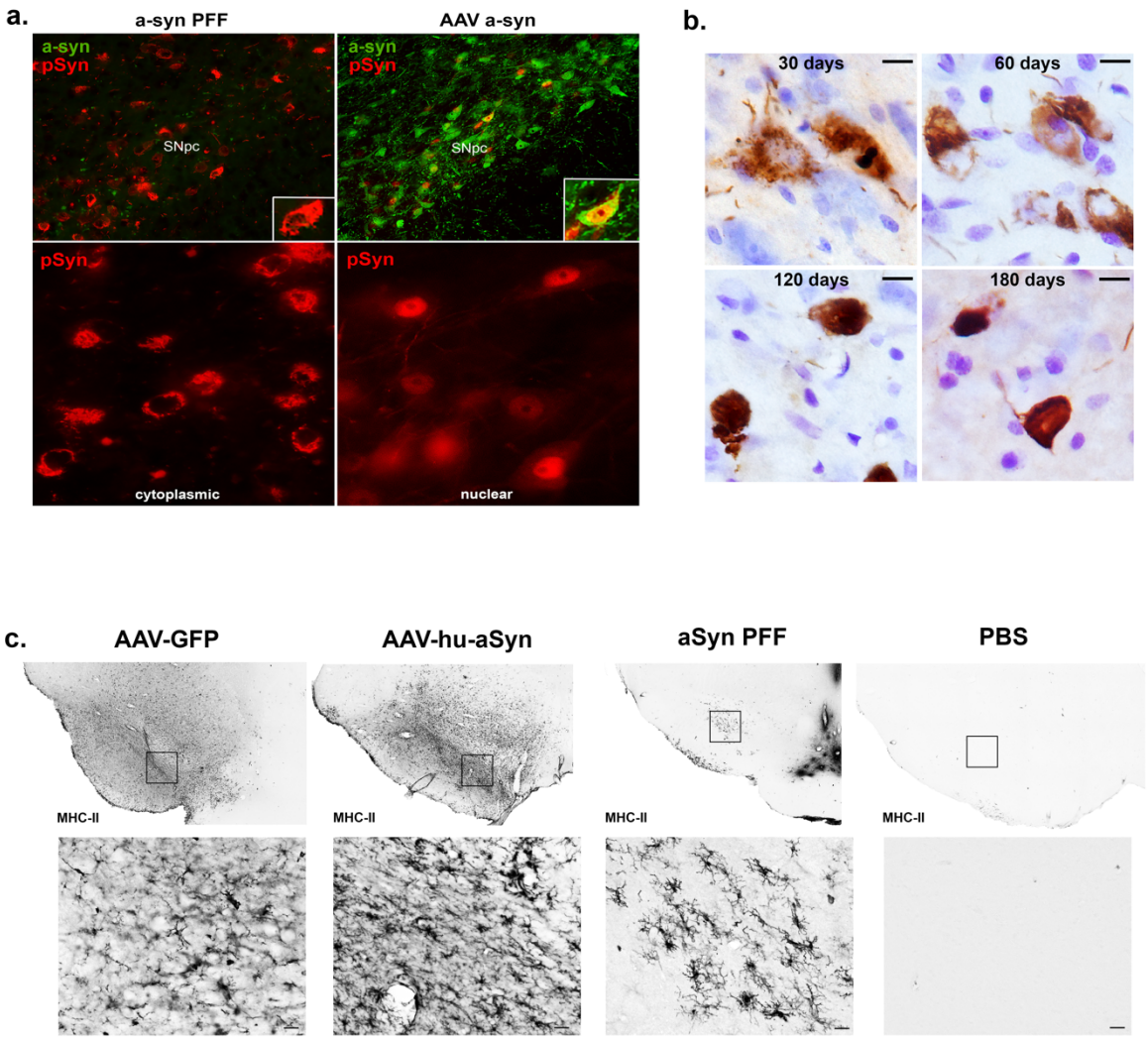

Figure 2.1: Comparison of alpha-synuclein pathology and inflammation between AAV-overexpression and α-syn preformed fibril models
a) Intrastriatal injection of α-syn PFFs results in accumulation of phosphorylated α-syn (pSyn, red) inclusions in the cytoplasm of SNc neurons, similar to cytoplasmic Lewy bodies in PD. **b)** Intranigral delivery of rAAV2/5 expressing human wildtype α-syn results in robust overexpression of human α-syn (green) with relatively few pSyn inclusions (red) in the cytoplasm. pSyn inclusions induced by AAV-mediated overexpression of α-syn are predominantly nuclear. **C)** Evolution of Lewy body-like pSyn inclusion formation in the substantia nigra pars compacta induced by intrastriatal PFF injection. Inclusions follow a similar pattern to that observed in human PD, with immature inclusions appearing diffuse and granular and becoming more dense and compact over time. **D)** Comparison of MHC-II expression 8 weeks following intranigral rAAV2/5 GFP or human wildtype α-syn vector injection or intrastriatal injection of sonicated preformed murine α-syn fibrils or PBS. In all cases no loss of nigral dopamine neurons was observed. Injection of AAV2/5 GFP or human α-syn is associated with robust increases in MHC-II on microglia throughout the mesencephalon, suggesting that the inflammation observed is largely attributable to surgical injection at the transduction site. In

Figure 2.1 cont'd
contrast, intrastriatal injection of PFFs results in MHC-II expression more localized to the SNc, with few to no MHC-II immunoreactive microglia evident in PBS injected animals.
Abbreviations: rAAV2/5= recombinant adenoassociated virus 2/5; α-syn= alpha-synuclein, GFP= green fluorescent protein; MHC-II= major histocompatibility complex-II; PBS= phosphate buffered saline; PFFs= alpha-synuclein preformed fibrils; pSyn = alpha-synuclein phosphorylated at serine129; SNc= substantia nigra pars compacta.

APPENDIX

Supplementary Methods:

Vector construction and intranigral injection

Recombinant adeno-associated viral vector pseudotype 2/5 (rAAV2/5) was used to overexpress human wildtype α-syn (rAAV-hu-α-syn) or green fluorescent protein (GFP) and constructed as previously described [87, 88], resulting in a final titer of 1.8×10^{12} genome copies per ml [88] or 1.8×10^{13} genome copies per ml [87], respectively. Male rats received two unilateral nigral injections of rAAV2/5-hu-α-syn (4µl total; AP −5.3 mm, ML + 2.0 mm, DV −7.2 mm and AP −6.0 mm, ML + 2.0 mm, DV −7.2 mm relative to dura) or rAAV2/5-GFP at a rate of 0.5µl/minute, 2µl per site. Animals were euthanized 8 weeks following injection as described below.

PFF Generation and Intrastriatal Injection

Purification of recombinant, full-length mouse α-syn and in *vitro* fibril assembly and intrastriatal injections were performed as previously described [56, 59, 61]. Prior to sonication, α-syn fibrils were assessed to verify lack of contamination (LAL Assay, (~1 Endotoxin Units /mg), presence of high molecular weight species (sedimentation assay), beta sheet conformation (Thioflavin T) and structure (transmission electron microscopy). Prior to injection, PFFs were thawed, diluted in sterile Dulbecco's PBS (DPBS, 2µg/µl) and sonicated at room temperature using an ultrasonicating homogenizer (300VT; Biologics, Inc., Manassas, VA) with the pulser set at 20%, power output at 30% for 60 pulses at 1 second each. Sonicated PFFs were kept at room temperature throughout the duration of the surgical procedure. Male, 2-month old rats were deeply anesthetized with isoflurane and received two 2µl unilateral intrastriatal

injections (4µl total; AP +1.6, ML +2.4, DV -4.2; AP -1.4, ML +2.0, DV -7.0 from skull) either of sonicated mouse α-syn PFFs (2µg/µl as described previously) or an equal volume of DPBS at a rate at 0.5µl/minute. Injections were administered made using a pulled glass needle attached to a 10 µl Hamilton syringe. After each injection, the needle was left in place for 1 minute, retracted 0.5 mm, left in place for an additional 2 minutes and then slowly withdrawn. Animals were monitored post-surgery and euthanized at monthly intervals up to 6 months.

Immunohistochemistry

All animals were euthanized via pentobarbital overdose (60mg/kg) and intracardially perfused with heparinized 0.9% saline followed by cold 4% paraformaldehyde in 0.1M PO_4. Brains were extracted and post-fixed in 4% PFA for 48 hours and placed in 30% sucrose until sunk. Brains were frozen on a sliding microtome and cut at 40µm. Free-floating sections (1:6 series) were transferred to 0.1M tris buffered saline (TBS). Following washes, endogenous peroxidases were quenched in 3% H_2O_2 for 1 hour and rinsed in TBS. Sections were blocked in 10% normal goat serum/0.5% Triton-X 100 in TBS (NGS, Gibco; Tx-100 Fischer Scientific) for 1 hour. Following block, sections were labeled with the following primary antibodies: mouse anti-human α-syn (transduction verification; Invitrogen, Carlsbad, CA; AHB0261; 1:2000; [87]), mouse anti-phosphorylated α-syn at Serine 129 (pSyn, 81A; Abcam, Cambridge, MA; AB184674; 1:10,000; [61]), or mouse anti-rat major histocompatibility complex-II for antigen presenting microglia (MHC Class II RT1B clone OX-6; BioRad, Hercules, CA; MCA46G, 1:5000; [61]) overnight at 4ºC. Following washes, sections were incubated in

biotinylated secondary antibodies (1:500) against mouse IgG (Millipore, Temecula, CA; AP124B) followed by washes in TBS and 2-hour incubation with Vector ABC standard detection kit (Vector Laboratories, Burlingame, CA; PK-6100). Labeling for pSyn and MHC-II was visualized by development in 0.5 mg/ml 3,3' diaminobenzidine (DAB; Sigma-Aldrich St. Louis, MO; D5637-10G) and 0.03% H_2O_2. Slides were dehydrated in ascending ethanol series then xylenes before coverslipping with Cytoseal (Richard-Allan Scientific, Waltham, MA) and imaged on a Nikon Eclipse 90i microscope with a QICAM camera (QImaging, Surrey, British Colombia, Canada) and Nikon Elements AR (version 4.50.00, Melville, NY).

Immunofluorescence

Free-floating sections (1:6 series) were transferred to 0.1M tris buffered saline (TBS) and washed. Sections were blocked in 10% normal goat serum/0.5% Triton-X 100 in TBS (NGS, Gibco; Tx-100 Fischer Scientific) for 1 hour. Following block, sections were labeled with mouse anti-human α-syn (IgG1; Invitrogen AHB0261; 1:2000) and mouse anti-phosphorylated α-syn (pSyn, 81A; IgG2a; Abcam, Cambridge, MA; AB184674; 1:10,000) overnight at 4ºC. Sections were washed and incubated in secondary antibodies goat anti-mouse against 81A IgG2A (Invitrogen; Carlsbad, CA; A-21135; Alexa Fluor 594) and goat anti-mouse IgG1 against a-syn (Invitrogen; Carlsbad, CA; A-21121; Alexa Fluor 488) at 1:500 in 1% NGS/0.5% Tx-100 for 2 hours. Sections were washed, mounted on subbed slides and coverslipped with VectaShield hardset mounting media (Vector Labs; H1400) and visualized on a on a Nikon Eclipse 90i

microscope with a QICAM camera (QImaging, Surrey, British Colombia, Canada) and Nikon Elements AR (version 4.50.00, Melville, NY).

REFERENCES

REFERENCES

1. Benskey, M.J., R.G. Perez, and F.P. Manfredsson, *The contribution of alpha synuclein to neuronal survival and function - Implications for Parkinson's disease.* J Neurochem, 2016. **137**(3): p. 331-59.

2. Bendor, J.T., T.P. Logan, and R.H. Edwards, *The function of alpha-synuclein.* Neuron, 2013. **79**(6): p. 1044-66.

3. Polymeropoulos, M.H., *Autosomal dominant Parkinson's disease and alpha-synuclein.* Ann Neurol, 1998. **44**(3 Suppl 1): p. S63-4.

4. Spillantini, M.G., et al., *alpha-Synuclein in filamentous inclusions of Lewy bodies from Parkinson's disease and dementia with lewy bodies.* Proc Natl Acad Sci U S A, 1998. **95**(11): p. 6469-73.

5. Somme, J.H., et al., *Initial neuropsychological impairments in patients with the E46K mutation of the alpha-synuclein gene (PARK 1).* J Neurol Sci, 2011. **310**(1-2): p. 86-9.

6. Lesage, S., et al., *G51D alpha-synuclein mutation causes a novel parkinsonian-pyramidal syndrome.* Ann Neurol, 2013. **73**(4): p. 459-71.

7. Kruger, R., et al., *Ala30Pro mutation in the gene encoding alpha-synuclein in Parkinson's disease.* Nat Genet, 1998. **18**(2): p. 106-8.

8. Appel-Cresswell, S., et al., *Alpha-synuclein p.H50Q, a novel pathogenic mutation for Parkinson's disease.* Mov Disord, 2013. **28**(6): p. 811-3.

9. Khalaf, O., et al., *The H50Q mutation enhances alpha-synuclein aggregation, secretion, and toxicity.* J Biol Chem, 2014. **289**(32): p. 21856-76.

10. Jo, E., et al., *alpha-Synuclein membrane interactions and lipid specificity.* J Biol Chem, 2000. **275**(44): p. 34328-34.

11. Dettmer, U., et al., *Parkinson-causing alpha-synuclein missense mutations shift native tetramers to monomers as a mechanism for disease initiation.* Nat Commun, 2015. **6**: p. 7314.

12. Xu, J., et al., *alpha-Synuclein Mutation Inhibits Endocytosis at Mammalian Central Nerve Terminals.* J Neurosci, 2016. **36**(16): p. 4408-14.

13. Olgiati, S., et al., *Early-onset parkinsonism caused by alpha-synuclein gene triplication: Clinical and genetic findings in a novel family.* Parkinsonism Relat Disord, 2015. **21**(8): p. 981-6.

14. Fuchs, J., et al., *Phenotypic variation in a large Swedish pedigree due to SNCA duplication and triplication.* Neurology, 2007. **68**(12): p. 916-22.

15. Farrer, M., et al., *Comparison of kindreds with parkinsonism and alpha-synuclein genomic multiplications.* Ann Neurol, 2004. **55**(2): p. 174-9.

16. Singleton, A.B., et al., *alpha-Synuclein locus triplication causes Parkinson's disease.* Science, 2003. **302**(5646): p. 841.

17. Chartier-Harlin, M.C., et al., *Alpha-synuclein locus duplication as a cause of familial Parkinson's disease.* Lancet, 2004. **364**(9440): p. 1167-9.

18. Su, X., et al., *Alpha-Synuclein mRNA Is Not Increased in Sporadic PD and Alpha-Synuclein Accumulation Does Not Block GDNF Signaling in Parkinson's Disease and Disease Models.* Mol Ther, 2017. **25**(10): p. 2231-2235.

19. Eng-King, T., et al., *Alpha-synuclein mRNA expression in sporadic Parkinson's disease.* Movement Disorders, 2005. **20**(5): p. 620-623.

20. Grundemann, J., et al., *Elevated alpha-synuclein mRNA levels in individual UV-laser-microdissected dopaminergic substantia nigra neurons in idiopathic Parkinson's disease.* Nucleic Acids Res, 2008. **36**(7): p. e38.

21. Neystat, M., et al., *Alpha-synuclein expression in substantia nigra and cortex in Parkinson's disease.* Mov Disord, 1999. **14**(3): p. 417-22.

22. Kingsbury, A.E., et al., *Alteration in α-synuclein mRNA expression in Parkinson's disease.* Movement Disorders, 2004. **19**(2): p. 162-170.

23. Zhou, J., et al., *Changes in the solubility and phosphorylation of alpha-synuclein over the course of Parkinson's disease.* Acta Neuropathol, 2011. **121**(6): p. 695-704.

24. van Rooijen, B.D., M.M. Claessens, and V. Subramaniam, *Membrane interactions of oligomeric alpha-synuclein: potential role in Parkinson's disease.* Curr Protein Pept Sci, 2010. **11**(5): p. 334-42.

25. Tong, J., et al., *Brain alpha-synuclein accumulation in multiple system atrophy, Parkinson's disease and progressive supranuclear palsy: a comparative investigation.* Brain, 2010. **133**(Pt 1): p. 172-88.

26. Oueslati, A., *Implication of Alpha-Synuclein Phosphorylation at S129 in Synucleinopathies: What Have We Learned in the Last Decade?* J Parkinsons Dis, 2016. **6**(1): p. 39-51.

27. Lee, H.J., C. Choi, and S.J. Lee, *Membrane-bound alpha-synuclein has a high aggregation propensity and the ability to seed the aggregation of the cytosolic form.* J Biol Chem, 2002. **277**(1): p. 671-8.

28. Burre, J., M. Sharma, and T.C. Sudhof, *Cell Biology and Pathophysiology of alpha-Synuclein.* Cold Spring Harb Perspect Med, 2018. **8**(3).

29. Barrett, P.J. and J. Timothy Greenamyre, *Post-translational modification of alpha-synuclein in Parkinson's disease.* Brain Res, 2015. **1628**(Pt B): p. 247-253.

30. Auluck, P.K., G. Caraveo, and S. Lindquist, *alpha-Synuclein: membrane interactions and toxicity in Parkinson's disease.* Annu Rev Cell Dev Biol, 2010. **26**: p. 211-33.

31. Irizarry, M.C., et al., *Nigral and cortical Lewy bodies and dystrophic nigral neurites in Parkinson's disease and cortical Lewy body disease contain alpha-synuclein immunoreactivity.* J Neuropathol Exp Neurol, 1998. **57**(4): p. 334-7.

32. Gibb, W.R. and A.J. Lees, *The relevance of the Lewy body to the pathogenesis of idiopathic Parkinson's disease.* J Neurol Neurosurg Psychiatry, 1988. **51**(6): p. 745-52.

33. Stefanis, L., *α-Synuclein in Parkinson's Disease.* Cold Spring Harbor Perspectives in Medicine, 2012. **2**(2): p. a009399.

34. Neumann, M., et al., *Misfolded proteinase K-resistant hyperphosphorylated alpha-synuclein in aged transgenic mice with locomotor deterioration and in human alpha-synucleinopathies.* J Clin Invest, 2002. **110**(10): p. 1429-39.

35. Li, J.Y., et al., *Characterization of Lewy body pathology in 12- and 16-year-old intrastriatal mesencephalic grafts surviving in a patient with Parkinson's disease.* Mov Disord, 2010. **25**(8): p. 1091-6.

36. Halliday, G.M., et al., *Neuropathology underlying clinical variability in patients with synucleinopathies.* Acta Neuropathol, 2011. **122**(2): p. 187-204.

37. Dickson, D.W., *Neuropathology of Parkinson disease.* Parkinsonism & Related Disorders, 2018. **46**: p. S30-S33.

38. Braak, H., et al., *Staging of brain pathology related to sporadic Parkinson's disease.* Neurobiol Aging, 2003. **24**(2): p. 197-211.

39. van de Berg, W.D.J., et al., *Patterns of alpha-synuclein pathology in incidental cases and clinical subtypes of Parkinson's disease.* Parkinsonism & Related Disorders, 2012. **18**: p. S28-S30.

40. Kalaitzakis, M.E., et al., *The dorsal motor nucleus of the vagus is not an obligatory trigger site of Parkinson's disease: a critical analysis of alpha-synuclein staging.* Neuropathol Appl Neurobiol, 2008. **34**(3): p. 284-95.

41. Jellinger, K.A., *A critical reappraisal of current staging of Lewy-related pathology in human brain.* Acta Neuropathol, 2008. **116**(1): p. 1-16.

42. Burke, R.E., W.T. Dauer, and J.P. Vonsattel, *A critical evaluation of the Braak staging scheme for Parkinson's disease.* Ann Neurol, 2008. **64**(5): p. 485-91.

43. Beach, T.G., et al., *Unified staging system for Lewy body disorders: correlation with nigrostriatal degeneration, cognitive impairment and motor dysfunction.* Acta Neuropathol, 2009. **117**(6): p. 613-34.

44. Engelender, S. and O. Isacson, *The Threshold Theory for Parkinson's Disease.* Trends Neurosci, 2017. **40**(1): p. 4-14.

45. McGeer, P.L., et al., *Reactive microglia are positive for HLA-DR in the substantia nigra of Parkinson's and Alzheimer's disease brains.* Neurology, 1988. **38**(8): p. 1285-91.

46. McGeer, P.L., S. Itagaki, and E.G. McGeer, *Expression of the histocompatibility glycoprotein HLA-DR in neurological disease.* Acta Neuropathol., 1988. **76**.

47. McGeer, P.L., et al., *Microglia in degenerative neurological disease.* Glia., 1993. **7**.

48. Imamura, K., et al., *Distribution of major histocompatibility complex class II-positive microglia and cytokine profile of Parkinson's disease brains.* Acta Neuropathol, 2003. **106**(6): p. 518-26.

49. Croisier, E., et al., *Microglial inflammation in the parkinsonian substantia nigra: relationship to alpha-synuclein deposition.* J Neuroinflammation, 2005. **2**: p. 14.

50. Dijkstra, A.A., et al., *Evidence for Immune Response, Axonal Dysfunction and Reduced Endocytosis in the Substantia Nigra in Early Stage Parkinson's Disease.* PLoS ONE, 2015. **10**(6): p. e0128651.

51. Kannarkat, G.T., et al., *Common Genetic Variant Association with Altered HLA Expression, Synergy with Pyrethroid Exposure, and Risk for Parkinson's Disease: An Observational and Case-Control Study.* NPJ Parkinsons Dis, 2015. **1**.

52. Mogi, M., et al., *Interleukin (IL)-1 beta, IL-2, IL-4, IL-6 and transforming growth factor-alpha levels are elevated in ventricular cerebrospinal fluid in juvenile parkinsonism and Parkinson's disease.* Neurosci Lett, 1996. **211**(1): p. 13-6.

53. Lindqvist, D., et al., *Cerebrospinal fluid inflammatory markers in Parkinson's disease – Associations with depression, fatigue, and cognitive impairment.* Brain, Behavior, and Immunity, 2013. **33**: p. 183-189.

54. Eidson, L.N., et al., *Candidate inflammatory biomarkers display unique relationships with alpha-synuclein and correlate with measures of disease severity in subjects with Parkinson's disease.* J Neuroinflammation, 2017. **14**(1): p. 164.

55. Volpicelli-Daley, L.A., et al., *Exogenous alpha-synuclein fibrils induce Lewy body pathology leading to synaptic dysfunction and neuron death.* Neuron, 2011. **72**(1): p. 57-71.

56. Volpicelli-Daley, L.A., K.C. Luk, and V.M. Lee, *Addition of exogenous alpha-synuclein preformed fibrils to primary neuronal cultures to seed recruitment of endogenous alpha-synuclein to Lewy body and Lewy neurite-like aggregates.* Nat Protoc, 2014. **9**(9): p. 2135-46.

57. Luk, K.C., et al., *Exogenous α-synuclein fibrils seed the formation of Lewy body-like intracellular inclusions in cultured cells.* Proceedings of the National Academy of Sciences, 2009. **106**(47): p. 20051-20056.

58. Luk, K.C., et al., *Intracerebral inoculation of pathological α-synuclein initiates a rapidly progressive neurodegenerative α-synucleinopathy in mice.* The Journal of Experimental Medicine, 2012. **209**(5): p. 975-986.

59. Luk, K.C., et al., *Pathological alpha-synuclein transmission initiates Parkinson-like neurodegeneration in nontransgenic mice.* Science, 2012. **338**(6109): p. 949-53.

60. Paumier, K.L., et al., *Intrastriatal injection of pre-formed mouse alpha-synuclein fibrils into rats triggers alpha-synuclein pathology and bilateral nigrostriatal degeneration.* Neurobiol Dis, 2015. **82**: p. 185-99.

61. Duffy, M.F., et al., *Lewy body-like alpha-synuclein inclusions trigger reactive microgliosis prior to nigral degeneration.* J Neuroinflammation, 2018. **15**(1): p. 129.

62. Abdelmotilib, H., et al., *alpha-Synuclein fibril-induced inclusion spread in rats and mice correlates with dopaminergic Neurodegeneration.* Neurobiol Dis, 2017. **105**: p. 84-98.

63. Shimozawa, A., et al., *Propagation of pathological alpha-synuclein in marmoset brain.* Acta Neuropathol Commun, 2017. **5**(1): p. 12.

64. Osterberg, Valerie R., et al., *Progressive Aggregation of Alpha-Synuclein and Selective Degeneration of Lewy Inclusion-Bearing Neurons in a Mouse Model of Parkinsonism.* Cell Reports, 2015. **10**(8): p. 1252-1260.

65. Wall, N.R., et al., *Differential innervation of direct- and indirect-pathway striatal projection neurons.* (1097-4199 (Electronic)).

66. Yamada, M., et al., *Overexpression of alpha-synuclein in rat substantia nigra results in loss of dopaminergic neurons, phosphorylation of alpha-synuclein and activation of caspase-9: resemblance to pathogenetic changes in Parkinson's disease.* J Neurochem, 2004. **91**(2): p. 451-61.

67. Ulusoy, A., et al., *Viral vector-mediated overexpression of alpha-synuclein as a progressive model of Parkinson's disease.* Prog Brain Res, 2010. **184**: p. 89-111.

68. Oliveras-Salvá, M., et al., *rAAV2/7 vector-mediated overexpression of alpha-synuclein in mouse substantia nigra induces protein aggregation and progressive dose-dependent neurodegeneration.* Molecular Neurodegeneration, 2013. **8**: p. 44-44.

69. Mulcahy, P., et al., *Development and characterisation of a novel rat model of Parkinson's disease induced by sequential intranigral administration of AAV-alpha-synuclein and the pesticide, rotenone.* Neuroscience, 2012. **203**: p. 170-9.

70. Lundblad, M., et al., *Impaired neurotransmission caused by overexpression of alpha-synuclein in nigral dopamine neurons.* Proc Natl Acad Sci U S A, 2012. **109**(9): p. 3213-9.

71. Lo Bianco, C., et al., *alpha -Synucleinopathy and selective dopaminergic neuron loss in a rat lentiviral-based model of Parkinson's disease.* Proc Natl Acad Sci U S A, 2002. **99**(16): p. 10813-8.

72. Klein, R.L., et al., *Dopaminergic cell loss induced by human A30P alpha-synuclein gene transfer to the rat substantia nigra.* Hum Gene Ther, 2002. **13**(5): p. 605-12.

73. Kirik, D., et al., *Parkinson-like neurodegeneration induced by targeted overexpression of alpha-synuclein in the nigrostriatal system.* J Neurosci, 2002. **22**(7): p. 2780-91.

74. Ip, C.W., et al., *AAV1/2-induced overexpression of A53T-alpha-synuclein in the substantia nigra results in degeneration of the nigrostriatal system with Lewy-like pathology and motor impairment: a new mouse model for Parkinson's disease.* Acta Neuropathol Commun, 2017. **5**(1): p. 11.

75. Volpicelli-Daley, L.A., et al., *How can rAAV-alpha-synuclein and the fibril alpha-synuclein models advance our understanding of Parkinson's disease?* J Neurochem, 2016. **139 Suppl 1**: p. 131-155.

76. Decressac, M., et al., *Progressive neurodegenerative and behavioural changes induced by AAV-mediated overexpression of alpha-synuclein in midbrain dopamine neurons.* Neurobiol Dis, 2012. **45**(3): p. 939-53.

77. Kim, C., et al., *Neuron-released oligomeric alpha-synuclein is an endogenous agonist of TLR2 for paracrine activation of microglia.* Nat Commun, 2013. **4**: p. 1562.

78. Yamakado, H., et al., *alpha-Synuclein BAC transgenic mice as a model for Parkinson's disease manifested decreased anxiety-like behavior and hyperlocomotion.* Neurosci Res, 2012. **73**(2): p. 173-7.

79. Tanji, K., et al., *Proteinase K-resistant alpha-synuclein is deposited in presynapses in human Lewy body disease and A53T alpha-synuclein transgenic mice.* Acta Neuropathol, 2010. **120**(2): p. 145-54.

80. Nuber, S., et al., *A progressive dopaminergic phenotype associated with neurotoxic conversion of alpha-synuclein in BAC-transgenic rats.* Brain, 2013. **136**(Pt 2): p. 412-32.

81. Matsuoka, Y., et al., *Lack of nigral pathology in transgenic mice expressing human alpha-synuclein driven by the tyrosine hydroxylase promoter.* Neurobiol Dis, 2001. **8**(3): p. 535-9.

82. Fernagut, P.-O. and M.-F. Chesselet, *Alpha-synuclein and transgenic mouse models.* Neurobiology of Disease, 2004. **17**(2): p. 123-130.

83. Sanchez-Guajardo, V., et al., *Microglia acquire distinct activation profiles depending on the degree of alpha-synuclein neuropathology in a rAAV based model of Parkinson's disease.* PLoS One, 2010. **5**(1): p. e8784.

84. Harms, A.S., et al., *MHCII is required for alpha-synuclein-induced activation of microglia, CD4 T cell proliferation, and dopaminergic neurodegeneration.* J Neurosci, 2013. **33**(23): p. 9592-600.

85. Chung, C.Y., et al., *Dynamic changes in presynaptic and axonal transport proteins combined with striatal neuroinflammation precede dopaminergic neuronal loss in a rat model of AAV alpha-synucleinopathy.* J Neurosci, 2009. **29**(11): p. 3365-73.

86. Fischer, D.L., et al., *Viral Vector-Based Modeling of Neurodegenerative Disorders: Parkinson's Disease.* Methods Mol Biol, 2016. **1382**: p. 367-82.

87. Gombash, S.E., et al., *Morphological and behavioral impact of AAV2/5-mediated overexpression of human wildtype alpha-synuclein in the rat nigrostriatal system.* PLoS One, 2013. **8**(11): p. e81426.

88. Fischer, D.L., et al., *Subthalamic Nucleus Deep Brain Stimulation Does Not Modify the Functional Deficits or Axonopathy Induced by Nigrostriatal alpha-Synuclein Overexpression.* Sci Rep, 2017. **7**(1): p. 16356.

Chapter 3: Lewy Body-Like Alpha-Synuclein Inclusions Trigger Reactive Microgliosis Prior To Nigral Degeneration

Abstract

Converging evidence suggests a role for microglia-mediated neuroinflammation in Parkinson's disease (PD). Animal models of PD can serve as a platform to investigate the role of neuroinflammation in degeneration in PD. However, due to features of the previously available PD models, interpretations of the role of neuroinflammation as a *contributor to*- or a *consequence of* neurodegeneration have remained elusive. In the present study, we leveraged the features of synucleinopathy induced in wildtype rats following intrastriatal injection of preformed alpha-synuclein fibrils (α-syn PFFS). Male Fischer 344 rats (N= 114) received unilateral intrastriatal injections of α-syn PFFs, PBS or rat serum albumin with cohorts euthanized at monthly intervals up to six months. Quantification of dopamine neurons, total neurons, phosphorylated α-syn (pS129) aggregates, major histocompatibility complex-II (MHC-II) antigen-presenting microglia and ionized calcium binding adaptor molecule-1 (Iba-1) immunoreactive microglial soma size was performed in the substantia nigra. In addition, the cortex and striatum were also examined for presence of pS129 aggregates and MHC-II antigen-presenting microglia to compare the temporal patterns of pSyn accumulation and reactive microgliosis. Intrastriatal injection of α-syn PFFs to rats resulted in widespread accumulation of phosphorylated α-syn inclusions in several areas that innervate the striatum followed by significant loss (~35%) of substantia nigra pars compacta dopamine neurons within 5-6 months. The peak magnitudes of α-syn inclusion formation, MHC-II expression and reactive microglial morphology were all observed in the SN two months following injection, three months prior to nigral dopamine neuron loss. Surprisingly, MHC-II immunoreactivity in α-syn PFF injected rats was relatively

limited during the later interval of degeneration. Moreover, we observed a significant correlation between substantia nigra pSyn inclusion load and number of microglia expressing MHC-II. In addition, we observed a similar relationship between α-syn inclusion load and number of microglia expressing MHC-II in cortical regions, but not in the striatum. Our results demonstrate that increases in microglia displaying a reactive morphology and MHC-II expression occurs in the substantia nigra in close association with peak numbers of pSyn inclusions, months prior to nigral dopamine neuron degeneration and suggest that reactive microglia may contribute to vulnerability of SNc neurons to degeneration. The rat α-syn PFF model provides an opportunity to examine the innate immune response to accumulation of pathological α-syn in the context of normal levels of endogenous α-syn and provides insight into the earliest neuroinflammatory events in PD.

Introduction

The etiology of Parkinson's disease (PD) is stochastic: a culmination of aging-related changes in brain environment, genetic predispositions, and environmental insults that result in accumulation of alpha-synuclein (α-syn) inclusions (i.e., Lewy bodies) and degeneration of nigrostriatal dopamine neurons [1, 2]. Converging evidence suggests a role for microglia-mediated neuroinflammation in human PD. This theory is supported by observations of increased inflammatory cytokines in both PD patient cerebral spinal fluid (CSF) and plasma [3, 4], and in the patient brain as longitudinal PET imaging has demonstrated early and sustained microglial activation in the basal ganglia [5]. Furthermore, postmortem analyses in PD patients revealed increased expression of inflammatory markers such as human leukocyte antigen (HLA-DR), major histocompatibility complex-II (MHC-II), phagocytic marker CD68, intercellular adhesion molecule-I (ICAM-1), and integrin adhesion molecule (LFA-1) in the substantia nigra [6, 7]. However, a drawback of biofluid and postmortem PD brain samples is that they only provide a static snapshot of events within a longitudinal cascade of PD pathophysiology. This is especially problematic as the overwhelming majority of PD patient samples are collected from individuals who have likely harbored PD-related pathology for decades before, if also not after, diagnosis. This confounds interpretations of the role of neuroinflammation in degeneration in PD and prevents the understanding as to whether neuroinflammation participates as a contributor to nigral degeneration or is simply an artifact of cell death.

One of the most consistent observations in post-mortem PD tissue is an increase in the number of microglia expressing MHC-II (HLA-DR in humans [7-9]) a cell surface protein on antigen presenting cells which is necessary for CD4+ T-cell infiltration. More recently, gene expression changes related to inflammation, including an upregulation of MHC-II, have also been noted in Incidental Lewy Body Disease subjects (Braak stages 1-3 [9, 10]). Additionally, a variant in the HLA-DR gene which encodes for MHC-II is associated with amplified risk for development of PD after pesticide exposure [11]. Increased MHC-II is often concurrently upregulated with genes for proinflammatory cytokines such as tumor necrosis factor (TNF) and interleukin-1 beta (IL-1β) [12]. Moreover, decreased MHC-II expression was shown to attenuate downstream secretion of proinflammatory cytokines [13, 14]. Taken together, it is likely that MHC-II is most closely associated with a proinflammatory phenotype in microglia and may play a contributory role in nigral degeneration in PD. However, while the concept that MHC-II expression on microglia is increased in PD patients is not novel [8], the *temporal pattern* of observed increases in MHC-II in relation to α-syn aggregation and/or nigrostriatal degeneration has been unable to be systematically examined.

Animal models of PD can serve as platforms to investigate the role of neuroinflammation in PD-related cell death and dysfunction. The neuroinflammatory consequences of nigral degeneration and/or α-syn aggregation have been examined previously in various models, including but not limited to: neurotoxicant models (6-hydroxydopamine: 6-OHDA [15, 16]; 1-methyl-4-phenyl-1,2,3,6-tetrahydropyridine: MPTP; [17, 18]), transgenic models expressing human wildtype or mutant α-syn

(A503T, A30P; [19-21]) and viral vector-mediated overexpression of human wild-type or mutated α-syn in the nigrostriatal system [21-27]. However, certain characteristics of these models limit interpretations regarding the specific initiator of the neuroinflammation observed – synuclein inclusions and/or degeneration. Neurotoxicant models (6-OHDA, MPTP) rarely exhibit α-syn pathology [17, 28]. Transgenic models generally do not recapitulate marked nigrostriatal degeneration despite widespread, α-syn pathology [20, 29]. Whereas a robust inflammatory response is observed in association with the elevated α-syn levels, aggregates and nigral degeneration in viral vector-based α-syn overexpression models [21-27, 30-32], the contribution of supraphysiological α-syn levels or the α-syn species difference (human α-syn expressed in rat or mouse) to the neuroinflammatory response is unclear. Importantly, in human sporadic PD, total α-syn levels are not increased, rather phosphorylation and the ratio of soluble to insoluble α-syn increases over time [33-35].

An alternative model of the key features of human sporadic PD such as 1) protracted development of α-syn inclusions under conditions of 2) normal expression levels of endogenous α-syn during an interval that 3) precedes significant nigrostriatal degeneration would offer distinct advantages and allow the time course and potential impact of neuroinflammation to be delineated. Recently, our lab has characterized a rat model of PD that recapitulates this sequence of events, extending previous findings in mice [36, 37]. In this model, nigrostriatal synucleinopathy is induced by intrastriatal injection of sonicated preformed α-syn fibrils (α-syn PFFs) into wildtype rats [36, 38]. The fibrils act as seeds to template and trigger normal levels of *endogenous* α-syn to

accumulate into misfolded hyperphosphorylated, pathological α-syn (Figure 1A). The initial injection of α-syn PFFs *per se* does not directly cause toxicity, given that α-syn pathology and nigral degeneration do not occur in α-syn knockout animals injected with PFFs [37]. In this model we observe widespread accumulation of intraneuronal Lewy neurite-like and Lewy body-like inclusions of phosphorylated α-syn (pSyn) in areas that innervate the striatum. Importantly, the accumulation of intracellular pSyn is gradual and results in loss of striatal dopamine and metabolites in addition to ~40% loss of SNc dopamine neurons over 6 months [36]. Thus, the synucleinopathy produced in the α-syn PFF model provides a unique opportunity to examine the neuroinflammatory consequences of α-syn inclusion accumulation in the context of normal levels of endogenous, intracellular α-syn. In the present study, we systematically investigated the temporal profile of Lewy body-like phosphorylated α-syn inclusion load, reactive microglial morphology, MHC-II antigen presentation, and degeneration in the SN. Importantly, we observe reactive microglia and increased microglial MHC-II expression in association with peak load of SNc pSyn inclusions *months prior to degeneration*, suggesting that neuroinflammation may contribute to nigrostriatal degeneration.

Methods

Animals

Young adult (2 months), male Fischer344 rats (n=114) were used in this study. All animals were provided food and water ad-libitum and housed at the AAALAC approved Van Andel Research Institute vivarium. All procedures were approved and conducted in accordance with Institute for Animal Use and Care Committee (IACUC) at Michigan State University.

Preparation of α-syn PFFs and Verification of Fibril Size

Purification of recombinant, full-length mouse α-syn and in *vitro* fibril assembly was performed as previously described [38-40]. Prior to sonication, α-syn fibrils were assessed to verify lack of contamination (LAL Assay, (~1 Endotoxin Units /mg), high molecular weight (sedimentation assay), beta sheet conformation (Thioflavin T) and structure (electron microscopy). Prior to injection, PFFs were thawed, diluted in sterile Dulbecco's PBS (DPBS, 2μg/μl) and sonicated at room temperature using an ultrasonicating homogenizer (300VT; Biologics, Inc., Manassas, VA) with the pulser set at 20%, power output at 30% for 60 pulses at 1 second each. Following sonication, a sample of the PFFs was analyzed using transmission electron microscopy (TEM). Formvar/carbon coated copper grids (EMSDIASUM, FCF300-Cu) were washed twice with ddH_2O and floated for 1 min. on a 10 μl drop of sonicated α-syn fibrils diluted 1:20 with DPBS. Grids were stained for 1 min. on a drop of 2% uranyl acetate aqueous solution, excess uranyl acetate was wicked away with filter paper, and allowed to dry

before imaging. Grids were imaged on a JEOL JEM-1400 transmission electron microscope. The length of over 500 fibrils per sample were measured to determine average fibril size. The mean length of sonicated mouse α-syn PFFs was estimated to be 51.22 ± 1.31 nm, well within the optimal fibril length previously reported to result in seeding of endogenous phosphorylated α-syn inclusions *in vitro* and *in vivo* (Figure 3.1b-c) [41].

Intrastriatal Injections

Sonicated PFFs were kept at room temperature during the duration of the surgical procedures. All rats were deeply anesthetized with isoflurane received two 2µl unilateral intrastriatal injections (4µl total; AP +1.6, ML +2.4, DV -4.2; AP -1.4, ML +2.0, DV -7.0 from skull) either of sonicated mouse α-syn PFFs (2µg/µl as described previously [36]) or an equal volume of DPBS at a rate at 0.5µl/minute (n=6 per treatment per time point). Injections were administered made using a pulled glass needle attached to a 10 µl Hamilton syringe. After each injection, the needle was left in place for 1 minute, retracted 0.5 mm, left in place for an additional 2 minutes and then slowly withdrawn. Animals were monitored post-surgery and euthanized at predetermined time points (14, 30, 60, 90, 120, 150, and 180 days; Figure 3.1a). In a subsequent experiment, rats received two 2µl unilateral intrastriatal injections either of mouse α-syn PFFs 2ug/ul, DPBS, or rat serum albumin (RSA, Sigma Aldrich, St. Louis, MO; 9048-46-8; 2ug/ul) at the identical coordinates and were euthanized at 2 months post-injection (n=6 per treatment).

Immunohistochemistry

All animals were euthanized via pentobarbital overdose (60mg/kg) and intracardially perfused with heparinized 0.9% saline followed by cold 4% paraformaldehyde in 0.1M PO_4. Brains were extracted and post-fixed in 4% PFA for 48 hours and placed in 30% sucrose until they sunk. For sectioning, brains were frozen on a sliding microtome and cut at 40µm. Free-floating sections (1:6 series) were transferred to 0.1M tris buffered saline (TBS). Following washes, endogenous peroxidases were quenched in 3% H_2O_2 for 1 hour and rinsed in TBS. Sections were blocked in 10% normal goat serum/0.5% Triton-X 100 in TBS (NGS, Gibco; Tx-100 Fischer Scientific) for 1 hour. Following block, sections were immunolabeled with primary antibodies: mouse anti-α-syn fibrils /oligomers (O2; 1:5000, [42]) or mouse anti α-syn fibrils (F2; 1:5000,[42]), pan rabbit-anti α-syn (Abcam, Cambridge, MA; AB15530, 1:1000), mouse anti-phosphorylated α-syn at Serine 129 (pSyn, 81A; Abcam, Cambridge, MA; AB184674; 1:10,000); rabbit anti-tyrosine hydroxylase (TH; Millipore, Temecula, CA; MAB152, 1:4000), rabbit anti-ionized calcium binding adaptor molecule-1 (Iba-1; Wako, Richmond, VA; 019-19741, 1:1000), mouse anti-neuronal nuclei (Neu-N; Millipore, Temecula, CA; MAB 377, 1:5000); or mouse anti-rat major histocompatibility complex-II for antigen presenting microglia (MHC Class II RT1B clone OX-6, BioRad, Hercules, CA; MCA46G, 1:5000) overnight in 1% NGS/0.5% Tx-100/TBS at 4°C. Following washes, sections were incubated in biotinylated secondary antibodies (1:500) against mouse (Millipore, Temecula, CA; AP124B) or rabbit IgG (Millipore, Temecula, CA; AP132B) followed by washes in TBS and 2-hour incubation with Vector ABC standard detection kit (Vector Laboratories, Burlingame, CA; PK-6100). Labeling for pSyn, MHC-II, and TH was

visualized by development in 0.5 mg/ml 3,3' diaminobenzidine (DAB; Sigma-Aldrich St. Louis, MO; D5637-10G) and 0.03% H_2O_2. For dual brightfield visualization of Neu-N and Iba-1, sections were developed according to the manufacturer's instructions using the Vector ImmPACT DAB Peroxidase (Vector Labs, Burlingame, CA; SK-4605) and ImmPACT VIP Peroxidase (Vector Labs, Burlingame, CA; SK-4105) kits, respectively. Slides were dehydrated in ascending ethanol series then xylenes before coverslipping with Cytoseal (Richard-Allan Scientific, Waltham, MA). A subset of pSyn labeled sections were also counterstained with cresyl violet for quantification of *intraneuronal* pSyn inclusions in the SNc.

RNAscope in-situ Hybridization for Iba-1 and MHC-II IHC

40µm thick striatal tissue sections were incubated in Pretreat 1 from the RNAscope Pretreatment Kit (Advanced Cell Diagnostics, Hayward, CA; 310020) for 1 hour. Sections were washed in TBS and then mounted on Vistavision Histobond slides (VWR, Randor, PA; 16004-406) and placed on slide warmer at 60°C overnight. Slides were then incubated for 10 minutes in Pretreat 2 at 99°C, and washed twice in water. Tissue was outlined with Pap Pen (Abcam, Cambridge, UK; ab2601), and incubated with Pretreat 3 in a hybridization oven at 40°C for 15 min, washed twice in water, and incubated with the probe for AIF1 (Iba1; Advanced Cell Diagnostics, Hayward, CA; 457731) for 2 hours in the hybridization oven at 40°C. Six amplification steps with the amplification buffers (Advanced Cell Diagnostics, Hayward, CA; 320600) were then performed in alternating 30- and 15-minute incubation intervals in the hybridization oven per manufacturer instructions. Tissue was developed using the supplied DAB reagent

(Advanced Cell Diagnostics, Hayward, CA; 320600). Tissue was then counterstained for MHC-II (RT1B clone OX-6, BioRad, Hercules, CA; MCA46G, 1:500) in a hybridization chamber, following the same procedures as detailed for other immunohistochemical stains with the exception that the Vector SG reagent (Vector Laboratories, Burlingame, CA) was used as the chromogen. Slides were rinsed in TBS and coverslipped with Cytoseal 60. Images were taken on a Nikon Eclipse 90i microscope with a QICAM camera (QImaging, Surrey, British Colombia, Canada).

Quantification of TH, NeuN, pSyn and MHC-II immunoreactive profiles

Microbrightfield (MBF) Stereoinvestigator (MBF Bioscience, Williston, VT) was used to estimate the total population of THir and NeuNir neurons to determine the time course of TH phenotype loss and overt nigral degeneration. Contours were drawn around the SNc using the 4X objective on every sixth section through the rostrocaudal axis (9-10 sections). A series of counting frames (50μm x 50μm) was systematically and randomly distributed over grid (183 μm x 112 μm) placed over the SNc, allowing for quantification of approximately 20% of the SNc. An investigator blinded to experimental conditions counted THir and NeuNir cells using the optical fractionator probe with a 60x oil immersion objective. Markers were placed on each THir or NeuNir cell in a 1-2 μm z-stack within the counting frame. Between 50-500 objects were counted to generate stereological estimates of the total cell population. The total population estimate was calculated using optical fractionator estimates and variability within animals was assessed via the Gunderson coefficient of error (<0.1). Due to heterogeneity in the distribution of both pSyn and MHC-II immunoreactive profiles within the SN, total

enumeration rather than counting frames was used for quantification. Neurons with intraneuronal pSyn inclusions were defined as profiles of dark, densely stained pSyn immunoreactivity within cresyl violet positive neurons. Contours were drawn around the SNc using the 4X objective on every sixth section through the entire rostrocaudal axis of the SNc (9-10 sections). pSyn inclusions and MHC-IIir microglia were then systematically counted within each contour using the 20X objective. Numbers represent the raw total number of pSyn inclusions or MHC-IIir microglia per animal multiplied by 6 to extrapolate the population estimate.

Microglial Soma Area Analysis

40µm thick nigral tissue sections (1:6 series) from animals injected with α-syn PFFs, RSA, or and DPBS 2 months and 6 months following injection were dual labeled for NeuN and Iba-1 as described above to distinguish the SNc from the SNr. The three nigral sections adjacent to the sections containing the most pSyn inclusions were identified. Z-stack images of the ipsilateral and contralateral SNr bordering the SNc were taken on a Nikon Eclipse 90i microscope with a QICAM camera (QImaging, Surrey, British Colombia, Canada) using the 20x objective and analyzed with Nikon Elements AR (version 4.50.00, Melville, NY). Using the auto-detect feature, each Iba-1ir soma's border was outlined and adjusted accordingly to obtain an accurate quantification of area of the soma, excluding any processes. All microglia in the field of view of each z-stack per section, per rat were quantified with total number of microglia per rat calculated (100-250). Data are expressed as mean Iba-1ir soma area per treatment group. Soma measurements for all microglia per treatment were also grouped into 10µm bins and expressed as a percentage of total microglia counted.

Thioflavin-S Staining

1:12 series was washed in TBS and subsequently mounted on subbed slides to dry (~1 hour). Slides were incubated in 0.5% $KMnO_4$ in TBS for 25 minutes, followed by 5 washes in TBS. Sections were destained in 0.2% $K_2S_2O_5$/0.2% oxalic acid in TBS for 3 minutes followed by incubation in 0.0125% thioflavin-S in 40% EtOH/TBS for 3 minutes and differentiated in 50% EtOH for 15 minutes. Sections were rinsed first in TBS and then dd$H_2$0 before coverslipping with Vectashield Mounting Medium for fluorescence.

Proteinase-K Digestion

1:12 nigral series was washed in TBS. A subset of free floating tissue sections was treated with 10 µg/ml proteinase K (Invitrogen, Carlsbad, CA; 25530015) for 30 minutes at room temperature, followed by 3 washes in TBS and 4 washes in TBS-Tx. Sections were then processed for pan α-syn immunohistochemistry (rabbit anti-α-syn, Abcam, Cambridge, UK; AB15530) as described above, mounted on subbed slides, dehydrated to xylenes, and coverslipped.

Statistics

Statistical analyses were performed using IBM SPSS Statistics (IBM, Armonk, NY) or GraphPad Prism (La Jolla, CA). Statistical significance for all cases was set at $p < 0.05$. Statistical outliers were assessed using the Absolute Deviation from the Median (ADAM) method using the 'very conservative' criterion [43]. To compare numbers of O2 vs. F2 immunoreactive cells (Figure 3.4), THir and NeuNir neurons (Figure 3.5), pSyn α-syn inclusions (Figure 6), MHC-IIir microglia (Figure 5) and Iba-1ir microglia number and size (Figure 3.7) a one-way ANOVA with Tukey's post hoc analyses was used.

Correlation analysis was conducted to investigate the relationship between ipsilateral and contralateral THir neurons (Figure 3.5) and between MHC-IIir and pSyn α-syn inclusions (Figure 3.6).

Results

Sonicated α-syn PFFs are the optimal size for pathology induction in vivo

Prior to intrastriatal injection of mouse α-syn PFFs we investigated the size of the PFFs following sonication using transmission electron microscopy (TEM, Figure 3,1B, C). The mean length of sonicated mouse α-syn PFFs was estimated to be 51.22 ± 1.31 nm, well within the optimal fibril length previously reported to result in seeding of endogenous phosphorylated α-syn inclusions (Figure 3.1d, schematic) in vitro and in vivo [41].

Unilateral intrastriatal injection of α-syn PFFs induces widespread Lewy-like pathology

In our previous work [36] we reported that unilateral intrastriatal injection of mouse α-syn PFFs results in phosphorylated α-syn (pSyn) intraneuronal accumulations in several areas that innervate the striatum [44], most prominently the frontal (primary motor and somatosensory, Layer 5) and insular cortices, amygdala, and SNc. Over time, accumulations increase in number in these regions. In the present study, we observed an identical pattern of pSyn accumulation in rats injected with mouse α-syn PFFs. Specifically, we observe abundant pSyn pathology bilaterally in cortical regions (layers 2/3 of the secondary motor area, insular cortex, and orbital areas; Figure 3.2a). In contrast, we observed unilateral pSyn accumulation in the SNc ipsilateral to the injected striatum, and complete absence of pSyn aggregates in animals injected with and equal volume of PBS or equal volume and concentration of RSA (Supplemental Figure 3.8).

Accumulation of pSyn inclusions followed a distinct temporal pattern depending on the region examined. At 2 months post injection (p.i.), we observed abundant soma and neuritic pSyn inclusions bilaterally in the agranular insular cortex that persisted over the course of 6 months (Supplementary Figure 3.2A). Abundant pSyn accumulations were observed within the ipsilateral SNc at 2 months p.i., which remained ipsilateral and decreased in number over the course of 6 months (Supplementary Figure 3.2D-F). The abundance of pSyn inclusions in the striatum followed an opposite pattern (Supplementary Figure 3.2 G-I). We observed relatively sparse pSyn inclusions in the striatum at 2 months p.i. that were primarily restricted to neurites. At 4 and 6 months p.i., the number of pSyn accumulations in striatal somata increased in abundance and also were observed in the contralateral striatal hemisphere (Supplementary Figure 3.2H-I).

α-syn inclusions in the SNc exhibit oligomeric, fibrillary conformations and Lewy body-like characteristics

The oligomeric form of α-syn is proposed to be one of the toxic species [42, 45-47]. We further characterized the nature of pSyn inclusions within the SNc at 1 month p.i. using conformation-specific antibodies for oligomeric/fibrillar α-syn (O2) or fibrillar-predominant α-syn (F2) and compared that with immunoreactivity to pSyn. (Figure 3.2A-I; [42]). When adjacent sections were quantified using unbiased stereology we observed that 88.2 ± 6.4% of pSyn immunoreactive inclusions exhibited either an oligomeric or fibrillary conformation (O2 only). Furthermore, 56.4 ± 6.04 % of nigral pSyn inclusions were detected as predominately mature, fibrillar aggregates (F2 only) with an estimated

31.7 ± 5.9% of inclusions suggested to be in an oligomeric conformation (O2 only minus F2 only; Figure 3.2J). α-Syn inclusions in the SNc 2 months p.i. displayed Lewy body-like characteristics [48, 49], including resistance to proteinase-K digestion (Figure 3.2 K-L, I) as well as markers for ß-sheet structure as detected by thioflavin-S (Figure 3.2m). Collectively, these results suggest that intrastriatal injection of mouse α-syn PFFs triggers pathological conversion of endogenous α-syn to phosphorylated, oligomeric and fibrillary conformations in the SNc that ultimately result in insoluble, amyloid inclusions resembling Lewy bodies.

PFF-induced synucleinopathy induces significant bilateral loss of SNc neurons

We previously observed that unilateral intrastriatal mouse α-syn PFF injections to rats resulted in bilateral nigrostriatal degeneration of THir SNc neurons within 6 months [36]. To validate this finding in our present cohort we conducted unbiased stereology of THir SNc neurons at 2, 4, 5 and 6 months p.i. in α-syn PFF and PBS injected rats. Injection of PBS did not result in significant loss of THir SNc neurons at any time point ($F_{(7,18)}$ = 1.991, $p > 0.05$) thus PBS injected time points were combined for comparison to PFF-injected rats between identical hemispheres (ipsilateral PBS = 12,518 ± 554; contralateral PBS 11,577 ± 536). Similar to our previous studies, we observed significant, bilateral reduction (~35%) in SNc THir neurons (Figure 3.3A-E). Specifically, the number of SNc THir neurons ipsilateral to α-syn PFF injection at both 5 (8227 ± 1015) and 6 months (8851 ± 1148) p.i. was significantly reduced compared to PBS control rats ($F_{(5, 36)}$ = 4.297, $p < 0.027$, Figure 3.E). Within the contralateral SNc, significantly fewer THir neurons were observed 5 months following α-syn PFF injection

($F_{(5, 36)} = 5.782$, $p < 0.013$) with a non-significant reduction in the contralateral SNc observed at 6 months ($p > 0.05$). A positive correlation existed between the extent of ipsilateral THir SNc neuron loss and the extent of contralateral loss of THir SNc neurons ($r = 0.8855$, $p = 0.0007$, $R^2 = 0.7842$, Figure 3F).

Lastly, to confirm whether reductions in THir neurons induced by PFF injection represented phenotype loss or overt degeneration, unbiased stereology of NeuN-ir neurons in the SNc was conducted in PFF or PBS treated groups at 5 and 6 months p.i.. No significant differences were observed within the corresponding hemisphere between 5 and 6 months due to either PBS or PFF injection (PBS: $F_{(3, 4)} = 1.238$, $p > 0.05$; PFF $F_{(3, 8)} = 0.3986$, $p > 0.05$). Therefore the 5 and 6 month time points were combined into one time point. The number of SNc NeuN-ir neurons ipsilateral to PFF injection was significantly reduced compared to either the ipsilateral or contralateral hemisphere of PBS injected rats ($F_{(3, 16)} = 7.089$, $p < 0.02$). The number of NeuN-ir neurons in the contralateral SNc of PFF injected rats was significantly reduced compared to the ipsilateral SNc of PBS injected rats ($p < 0.0319$). When compared to the contralateral SNc of PBS injected rats, NeuN-ir neurons were reduced yet did not reach significance ($p = 0.0563$, Figure 3.3G-I). Overall our results replicate our previous findings that intrastriatal α-syn PFF injection results in significant bilateral reductions in THir and NeuN-ir SNc neurons over the course of 6 months [36].

In a control experiment, we examined whether intrastriatal injection of an exogenous protein taken up by neurons [50, 51], rat serum albumin (RSA), induced an inflammatory response in the absence of intracellular pSyn accumulation. To rule out

acute toxicity induced by RSA, THir SNc neurons were quantified at 2 months after injection. No significant differences in THir SNc neurons were observed due to PBS, or RSA or PFF injection in either the ipsilateral or contralateral hemisphere ($F_{(5, 26)}$ = 0.3731, $p > 0.05$, Figure 3.3J). These results demonstrate that RSA injection, used as an additional control treatment, did not compromise the survival of THir SNc neurons.

Phosphorylated α-syn inclusions peak in the SNc at 2 months and significantly decrease in number during the 5-6 month interval of SNc degeneration

We determined the time course (1-6 months p.i.) of phosphorylated α-syn (pSyn) accumulation in the SNc following intrastriatal α-syn PFF injection at monthly intervals. pSyn inclusions were observed in the SNc ipsilateral to injection in all α-syn PFF injected rats, with the number of inclusions varying based on time point after injection (Figure 3.4A-D). Inclusions were most abundant at months 1, 2 and 3, with all three time points exhibiting significantly higher α-syn inclusions compared to the interval of SNc degeneration at months 4, 5 and 6 (Figure 3.3E, G; Figure 4D; $F_{(5, 18)} = 2.251$, $p \leq 0.001$). The number of intraneuronal α-syn inclusions in the SNc was significantly greater at 2 months p.i. compared to all other time points except the 1 month time point (Figure 4D; $p \leq 0.006$). At 2 months approximately 2220 ± 148.6 SNc neurons possessed pSyn inclusions. By comparison, a loss of ≈ 3804 THir SNc neurons ipsilateral to PFF injection was observed at 5-6 months. These results suggest that pSyn inclusion formation in the SNc between 1-3 months after PFF-injection precedes degeneration of the SNc neurons at 5-6 months p.i.

MHC-II immunoreactive (MHC-IIir) microglia increase in the SNc in association with accumulation of α-syn inclusion, but are decreased during the interval of degeneration

MHC-II expression on microglia is associated with co-expression of pro-inflammatory genes such as TNF, IL-1β, and CD80 as well as proinflammatory cytokine secretion [12-14]. We quantified MHC-II immunoreactive (MHC-IIir) microglia within an adjacent series of SNc tissue sections at months 1, 2, 3, 4, 5 and 6 after unilateral α-syn PFF or PBS intrastriatal injection in order to examine neuroinflammation. Double labeling for MHC-II protein and Iba-1 mRNA confirmed the identity of MHC-IIir cells to be microglia (Figure 3.4E).

MHC-IIir microglia were observed in the SNc ipsilateral to injection in both α-syn PFF and PBS control rats at all time points. No MHC-IIir microglia were observed in the contralateral SNc. However, the magnitude of MHC-IIir microglia varied over time and followed a nearly identical pattern to that observed with pSyn inclusion accumulation. At the one-month time point no significant differences were observed between the number of MHC-IIir microglia in the ipsilateral SNc of PBS controls compared to α-syn PFF injected rats ($F_{(11, 45)} = 17.45$, $p > 0.05$), presumably reflecting a non-specific response to injection (Figure 3.4I). However, significantly higher numbers of MHC-IIir microglia were observed in the ipsilateral SN of α-syn PFF-injected rats compared to PBS injected control rats at months 2, 4 and 5 ($p < 0.006$, Figure 3.4F, G and I). The peak of MHC-IIir microglia occurred in the SN 2 months following α-syn PFF injection ($p < 0.02$ compared to PFF injected rats all other time points), corresponding to the time point when the greatest number of SNc neurons possess α-syn aggregates (Figure 3.4 D, G

and I). In contrast, significantly fewer MHC-IIir microglia were observed in PFF injected rats at months 5 and 6, corresponding to the interval of SNc THir neuron loss, although these numbers were still greater than PBS-injected controls (Figure 3.3E and Figure 3.4I). There was a positive correlation between the number of MHC-IIir microglia and the number of SNc neurons possessing pS129 α-syn inclusions in the SN ($r = 0.8858$, $p = 0.0015$, $R^2 = 0.7846$, Figure 3.4J, months 2, 4 and 6).

To confirm these findings, we repeated injections in a separate cohort of animals with rat serum albumin (RSA) as an additional control group for neuronal uptake of exogenous protein in the absence of pSyn accumulation, as PBS injection only controls for needle insertion into the parenchyma. As in previous cohorts, α-syn PFF injection resulted in a significant increase in MHC-IIir microglia in the SN at 2 months p.i. (Figure 3.4K, $p \leq 0.0006$). Injection of RSA resulted in similar numbers of MHC-IIir microglia as observed in PBS-injected control rats. No acute neurotoxicity was observed in RSA injected animals at 2 months p.i. (Figure 3.3I). Collectively, these results reveal that the preponderance of MHC-II expression in SN microglia is associated with pSyn α-syn inclusions at early time points, however is significantly attenuated during the interval of THir SNc degeneration.

pSyn inclusions in the SNc are associated with a reactive microglial morphology in the adjacent SNr

The number and distribution of MHC-IIir microglia in the SN suggested that not all microglia were expressing MHC-II. We next used Iba-1 immunoreactivity to examine the entire microglia population within an adjacent series of SN tissue sections at 2 and 6

months after α-syn PFF, RSA or PBS intrastriatal injection (Figure 3.5). Quantitation of the number of Iba-1 immunoreactive (Iba-1ir) microglia in the adjacent SNr revealed no significant differences in microglial number due to α-syn PFF, RSA or PBS injection at either 2 months (Figure 3.5A) or 6 months p.i. (2 months: $F_{(3, 16)} = 0.2637$, $p > 0.05$; 6 months: $F_{(3, 10)} = 0.2427$, $p > 0.05$). No significant differences were observed in microglial soma area in the SNr due to intrastriatal RSA injections at the 2 month time point ($F_{(3, 16)} = 0.256$, $p = 0.855$, Figure 3.5B). At the 2 month time point coinciding with the peak of pSyn α-syn inclusion accumulation in the SNc, we observed an appreciable increase in the soma size and thickness and number of microglial processes in the SNr of PFF injected rats compared to a more classically quiescent microglial morphology observed in control injected rats. Specifically, in the ipsilateral SNr of rats two months following α-syn PFF injection the average microglia cell body area was significantly larger compared to PBS-injected rats ($F_{(3, 16)} = 4.016$, $p = 0.02$, Figure 3.5C, D, E). Microglia soma area varied in all conditions between ≈ 10 – 200 μm^2, with a significantly greater percentage of microglia > 70 μm^2 observed in the SNr of rats possessing SNc pSyn α-syn inclusions at 2 months compared to rats injected with PBS (Figure 3.5F-H, $F_{(2, 12)} = 4.613$, $p = 0.03$).

At six months p.i., a time point corresponding to the time point of very few pSyn α-syn inclusions and immediately following loss of SNc neurons, no significant differences in microglia soma size were observed between α-syn PFF and PBS injected rats ($F_{(3, 10)} = 2.089$, $p > 0.05$, Figure 3.5I-M). Of note, the average microglial soma area in PBS injected rats at 6 months (rats 8 months of age) was significantly larger than PBS-

injected rats at 2 months (4 months of age) suggesting an age-related increase ($F_{(3, 12)}$ = 37.00, p <0.001). The distribution of microglia soma areas between PFF and PBS rats 6 months following injection also appeared similar (Figure 3.5L, M) with an apparent age-related effect [52-54] reflected in a greater percentage of microglia > 70 μm^2 in 8-month-old rats compared to 4-month-old rats.

Overall, our finding that the peak time point of SNc pSyn α-syn inclusions is associated with a significant increase in microglia soma size suggests that synucleinopathy in the SNc triggers early disturbances in local microglia. The interval in which we observe this synucleinopathy-induced reactive microglial morphology is 3 months prior to loss of SNc neurons (Figure 3.3E, G) suggesting that reactive microglia have the potential to contribute to vulnerability of SNc neurons to degeneration.

We also examined a series of sections throughout the SN and striatum at 2, 4, and 6 months p.i. in α-syn PFF and PBS injected rats for presence of cluster of differentiation 68 (CD68) which labels both phagocytic microglia and infiltrating macrophages. While a few CD68-ir cells were observed in blood vessels, no CD68-ir cells were observed in the parenchyma during any of the time points examined (data not shown). The lack of CD68 immunoreactivity in the parenchyma of the SN or striatum at any time point suggests that the magnitude of synucleinopathy and subsequent degeneration produced in the α-syn PFF model does not trigger microglial phagocytic activity.

MHC-IIir microglia in the agranular insular cortex are associated with the accumulation of α-syn inclusions

We also examined the time course of pSyn inclusion accumulation and MHC-II expression on microglia in the agranular insular cortex, as this region possesses

compacta; SNr= substantia nigra pars reticulata. SEM = standard error of the mean. abundant Lewy-body like pathology in our model and is implicated in non-motor symptoms in PD [55]. At 2 months p.i. we observe abundant pSyn inclusions primarily localized to the somata (Figure 3.6A), with increased neuritic pathology evident by 4 months (Figure 6B). Interestingly, an observable decrease in both neuritic and somata inclusions is evident by 6 months (Figure 3.6C). We observe a similar temporal pattern of MHC-IIir microglia as described for the SN: the highest number of MHC-IIir microglia are observed at 2 months p.i., when pSyn inclusions first peak, and a decrease in MHC-IIir microglia in association with reductions in the number of pSyn inclusions. Interestingly, a decrease in MHC-IIir microglia is observed between 2 and 4 months p.i. when pSyn pathology becomes more abundant with the appearance of neuritic inclusions. These observations suggest that MHC-II is upregulated as a *first response* to *formation* of pSyn inclusions and is not sustained over time, despite secondary increase in synuclein burden. Few to no MHC-IIir microglia were observed in PBS injected animals (Figure 3.6G-L), strengthening the concept that MHC-IIir on microglia is induced by initial accumulation of pSyn.

MHC-IIir microglia in the striatum are not associated with the accumulation of α-syn inclusions

Lastly, we examined the time course of accumulation of pSyn inclusions and number of MHC-IIir microglia in the striatum in rats that received unilateral α-syn PFF or PBS

intrastriatal injection. As reported previously [36], the pattern of pSyn α-syn inclusion accumulation in the striatum is strikingly different from accumulation in the SNc. At 2 months, α-syn inclusions in cell bodies in the ipsilateral striatum are relatively sparse and pSyn α-syn immunoreactivity appeared primarily localized to neurites, presumably in terminals from the SNc (Supplementary Figure 3.10A, Appendix). Over the course of the 4 months, pSyn α-syn inclusions in cell bodies in the striatum increase in number, involving the contralateral hemisphere as well, with the greatest number of pSyn α-syn inclusions observed in the ipsilateral striatum at the 6-month time point (Supplementary Figure 3.10C, Appendix). In adjacent striatal tissue sections, we examined the temporal pattern of MHC-IIir microglia following unilateral α-syn PFF or PBS intrastriatal injection. Early after injection, at 2 weeks, 1 month and 2 months, abundant MHC-IIir microglia were observed in the ipsilateral striatum in proximity to the injection sites in both PFF- and PBS-injected rats (Supplementary Figure 3.10D, G, Appemdix). No differences were observed between treatment groups at the 1 month time point but the magnitude of the MHC-II response appeared slightly larger in PFF-injected rats compared to the PBS-injected rats at the 2-month time point. However, at 4 and 6 months, during the interval of continuing accumulation of pSyn α-syn inclusions in the striatum, the number of MHC-IIir microglia decreased dramatically with no differences observed in the small number of MHC-IIir microglia observed in both treatment groups (Supplementary Figure 3.10E, F, H, I. Appendix). These results suggest that the acute microglial response to the PFF injectate may differ from the acute response to the surgical injection alone, but that the subsequent increase α-syn inclusion load within neurons in the striatum does not trigger a second wave of microglial MHC-II immunoreactivity.

Discussion

In the present study, intrastriatal injection of α-syn PFFs to rats resulted in widespread accumulation of phosphorylated α-syn inclusions in several areas that innervate the striatum, as previously reported in rats and mice [36, 56]. Further examination of the inclusions formed in the SNc revealed that they share many key features with Lewy bodies and were most abundant between months 1-3 after intrastriatal α-syn PFF injection, peaking at 2 months. The magnitude of ipsilateral SNc neurons bearing α-syn inclusions 1-3 months after α-syn PFF injection approximated the magnitude of loss of ipsilateral SNc neurons observed at 5-6 months, suggesting a direct relationship between α-syn inclusion accumulation and degeneration of SNc neurons. Synucleinopathy specific MHC-II expression in the ipsilateral SNc similarly peaked in the SN at 2 months and was associated with a reactive microglial morphology, characterized by significantly larger soma size, 3 months prior to degeneration. Surprisingly, MHC-II immunoreactivity in α-syn PFF injected rats was significantly decreased during the period of SNc degeneration (5-6 months). Overall, the temporal pattern of peak Lewy body-like inclusion formation was associated with peak neuroinflammation in the SN, both of which appear months prior to loss of SNc neurons. These results suggest that and increase in MHC-II may be a first-response mechanism to initial accumulation of intracellular α-syn and that reactive microglia have the potential to contribute to vulnerability of SNc neurons to degeneration (Figure 3.7, left). Given the role of microglia as professional phagocytes and antigen presenting cells, the absence of a second wave of reactive microglial morphology and decrease in MHC-IIir microglia during the interval of ongoing degeneration was surprising. This result may be

explained by the protracted and mild magnitude of cell death at the terminal end point studied (~35% at 6 months p.i.) in contrast to the severity of degeneration in post-mortem PD samples (50-90% at diagnosis [57]). Additionally, a limitation of rodent models is that DAergic neurons do not possess neuromelanin, a potent microglial activator [58-60], therefore the contribution of the inflammatory response in humans may in fact be underestimated by findings from animal models. Furthermore, Iba-1 morphology and MHC-II are only two specific markers out of many possible indices of inflammation (cytokines, toll like receptor expression, etc…) Therefore, we cannot completely rule out the involvement of other inflammatory mediators during the interval of degeneration. Our results specifically point to involvement of antigen presentation by microglia induced by intraneuronal inclusions of pSyn. Further studies investigating what peptides are being presented by MHC-IIir microglia (α-syn, membrane of dying neurons, etc…) and the enhanced expression of other inflammatory mediators such as toll-like receptor signaling are warranted.

Within the agranular insular cortex, we observe pSyn primarily localized to the somata at 2 months, followed by an increase in neuritic pathology by 4 months, and a significant decrease overall in pSyn immunoreactivity at 6 months (Figure 3.7, right). This suggests that similar to the SN, neurons in the agranular insular cortex harboring inclusions die over the course of 6 months. Moreover, a similar pattern of MHC-II expression on microglia is observed: numbers of MHC-IIir microglia peak when pSyn pathology is most abundant and decrease over time. Although this has not been systematically quantified in the present study, future studies investigating inflammation and degeneration in this

area following intrastriatal α-syn PFF injection are warranted, as the insula has been implicated in the manifestations of non-motor symptoms in human PD [55, 61, 62].

Within the striatum, the site of α-syn PFF injection, we observed a distinctly different pattern of accumulation of α-syn inclusions compared to the SNc (Supplementary Figure 3J). We observed a dissociation between α-syn inclusion load and MHC-II immunoreactivity in the striatum (Supplementary Figure 3.10). The procedure of intrastriatal injection itself triggered an acute increase in MHC-II immunoreactive microglia that appeared to be slightly enhanced by the presence of the PFF injectate; however, the presence of MHC-II decreased dramatically over time in all conditions despite an ever increasing α-syn inclusion load. Compared to the SNc, the accumulation of α-syn inclusions in the striatum is delayed with no loss of striatal neurons observed at 6 months [36] and it is unknown whether degeneration of striatal neurons ultimately occurs at later time points. It is unclear whether α-syn inclusion load increases and peaks past the 6-month time point and whether the presence of MHC-II immunoreactive microglia may have similarly tracked with a future peak. The results in the striatum illustrate the necessity of determining the role of an acute inflammatory response to local injection and that the magnitude of this response may prevent the reactive microgliosis associated with pathological α-syn inclusions. Further, these striatal results suggest that α-syn inclusions do not automatically trigger reactive microgliosis and that other factors including rate of inclusion formation, impending cytotoxicity, local environment or microglia and astrocyte density [41] may be involved in determining the neuroinflammatory cascade of events.

In response to persistent neuronal stress and protein accumulation such as α-syn aggregation, microglia can become chronically activated, proliferate, migrate, secrete pro-inflammatory cytokines and reactive oxygen species and ultimately contribute to neuronal injury in an uncontrolled, feed-forward manner [19, 63-66]. Microglia can also phagocytose both living and dead neurons [67-69]. The observation that α-syn inclusion triggered MHC-II expression on microglia in the SN prior to degeneration indicates that neuroinflammation may contribute to the mechanism of pathophysiology. However, it is unlikely that microglial activation is the sole arbiter of degeneration given that neuronal death can result from α-syn PFF induced intraneuronal inclusions in cultures in the absence of microglia [39]. A more likely scenario involves neuroinflammation contributing to or accelerating nigrostriatal degeneration with properties unique to the nigral environment [70-75] adding to the cascade of events. Future studies investigating the secretion of proinflammatory and anti-inflammatory cytokines in the SN at time points prior to- and following nigral degeneration is warranted.

Human PD studies examining neuroinflammation suggest involvement of both the local brain immune response and the adaptive immune system in PD [76-78]. In the present study, we did not examine the possibility of peripheral immune cell infiltration beyond phagocytic CD68+ macrophages, which were not detected in the parenchyma in PFF injected animals at any stage, and data from human tissue regarding the presence of CD68+ macrophages in human PD is limited [8]. However, microglia are considered to be the principle antigen-presenting cell within the brain and MHC-II expression is

associated with the recognition of CD4+ T-helper cells. It is possible that CD4+ T-cells participate in the response to α-syn inclusions in the SN; however, whether the net effect of CD4+ T-cells is neurodegenerative or neuroprotective requires further systematic evaluation [79]. In addition, MHC-I expression by SNc neurons was observed in association with α-syn overexpression [80] and may similarly be expressed by α-syn inclusion-bearing SNc neurons. In addition, it was recently shown that T lymphocytes isolated from PD patients recognize specific α-syn peptides [81], strengthening the concept that neuroinflammation can be induced by α-syn and potentially involved early in PD progression.

While the concept that MHC-II is involved in PD and correlates with α-syn burden [8] has existed for several decades, our results are the first to systematically evaluate the time course of *endogenous* pSyn accumulation and microglial MHC-II expression prior to- and after nigrostriatal degeneration has occurred. Our results indicate that MHC-II expression in the SNc is increased at early time points in which SNc neurons possess pSyn inclusions, and is relatively sparse during the interval of nigral degeneration, suggesting that MHC-II is a response to initial inclusion formation. Future studies investigating the direct impact of increased or decreased MHC-II expression on the magnitude of degeneration, and what role, if any, peripheral T cells play in disease progression are warranted. Our results and the well-characterized rat α-syn PFF model will facilitate future studies to provide key mechanistic insights into the specific relationship between pathological α-syn inclusions, neuroinflammation and degeneration in sporadic PD

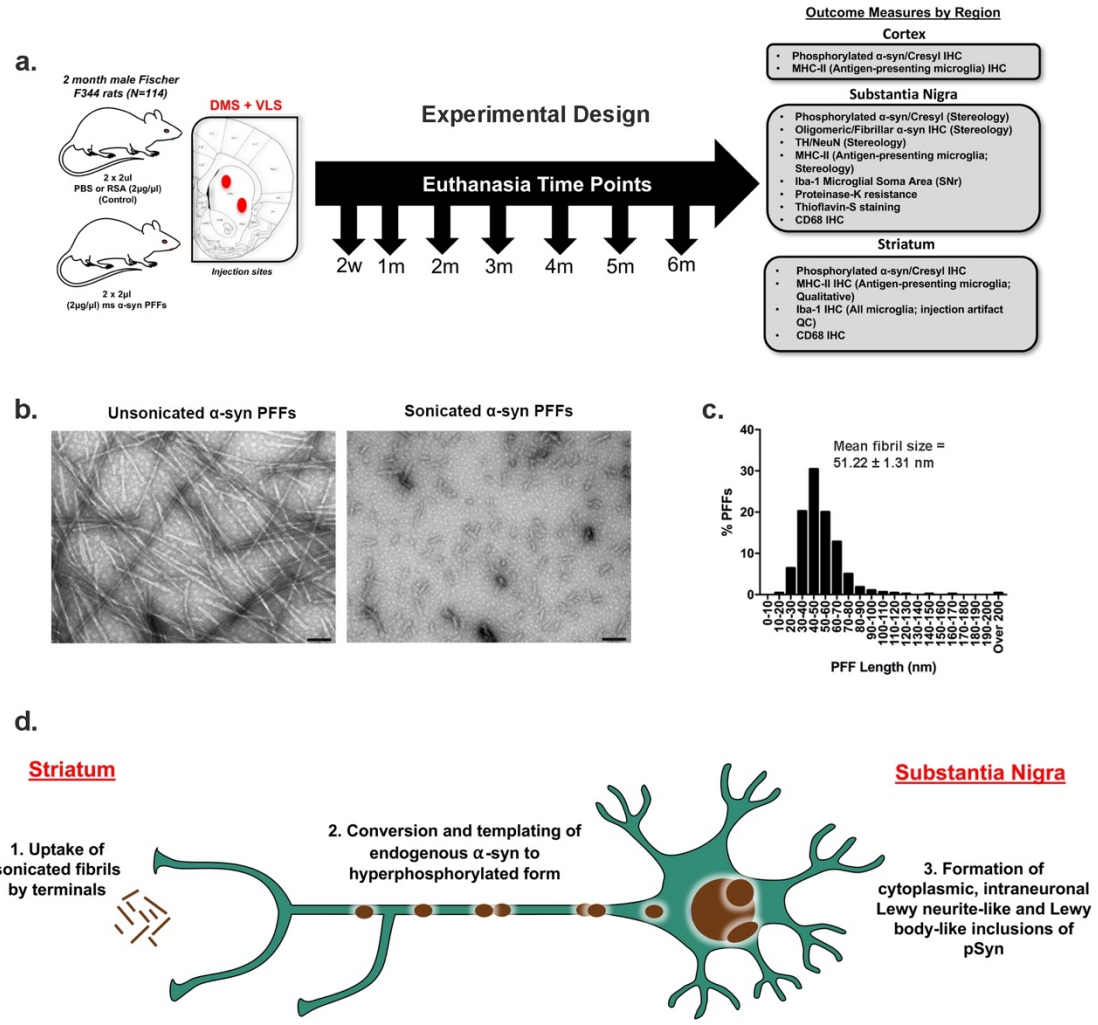

Figure 3.1: Experimental Design and PFF Quality Control
(a) Experimental Design: Two month old male Fischer344 rats (N=114) received two unilateral intrastriatal injections of either sonicated α-syn PFFs, Dulbecco's PBS (PBS), or rat serum albumin (RSA; follow-up study only). Cohorts of rats were euthanized at an early time point (2 weeks) and monthly intervals thereafter. Brains were removed and processed for immunohistochemical measures of pathology as detailed. **(b)** Electron micrographs of unsonicated *(left)* α-syn PFFs and sonicated α-syn PFFs *(right);* Scale bars =100nm. **(c)** Measurement distribution of ~500 sonicated PFFs prior to injection; mean fibril size = 51.22 ±1.31 nm. **(d)** Schematic of PFF model of synucleinopathy. Sonicated α-syn fibrils are injected into the striatum and taken up by nigrostriatal terminals *(1)*, after which they template and convert endogenous α-syn to a hyperphosphorylated, pathological form *(2)*, ultimately accumulating into Lewy neurite- and Lewy body-like inclusions *(3)*.
Abbreviations: α-syn = alpha-synuclein; PFFs= pre-formed alpha-synuclein fibrils; PBS = phosphate buffered saline; µl = microliter; µg = microgram; DMS = dorsal medial striatum; VLS = ventrolateral striatum; IHC = immunohistochemistry; pSyn = α-syn phosphorylated at Serine129; MHC-II = major histocompatibility complex-II; Iba-1= ionized calcium-binding adaptor

Fig. 3.1 cont'd.
molecule 1; TH = tyrosine hydroxylase; NeuN = Neuronal nuclei; CD68 = cluster of differentiation 68; QC = quality contro

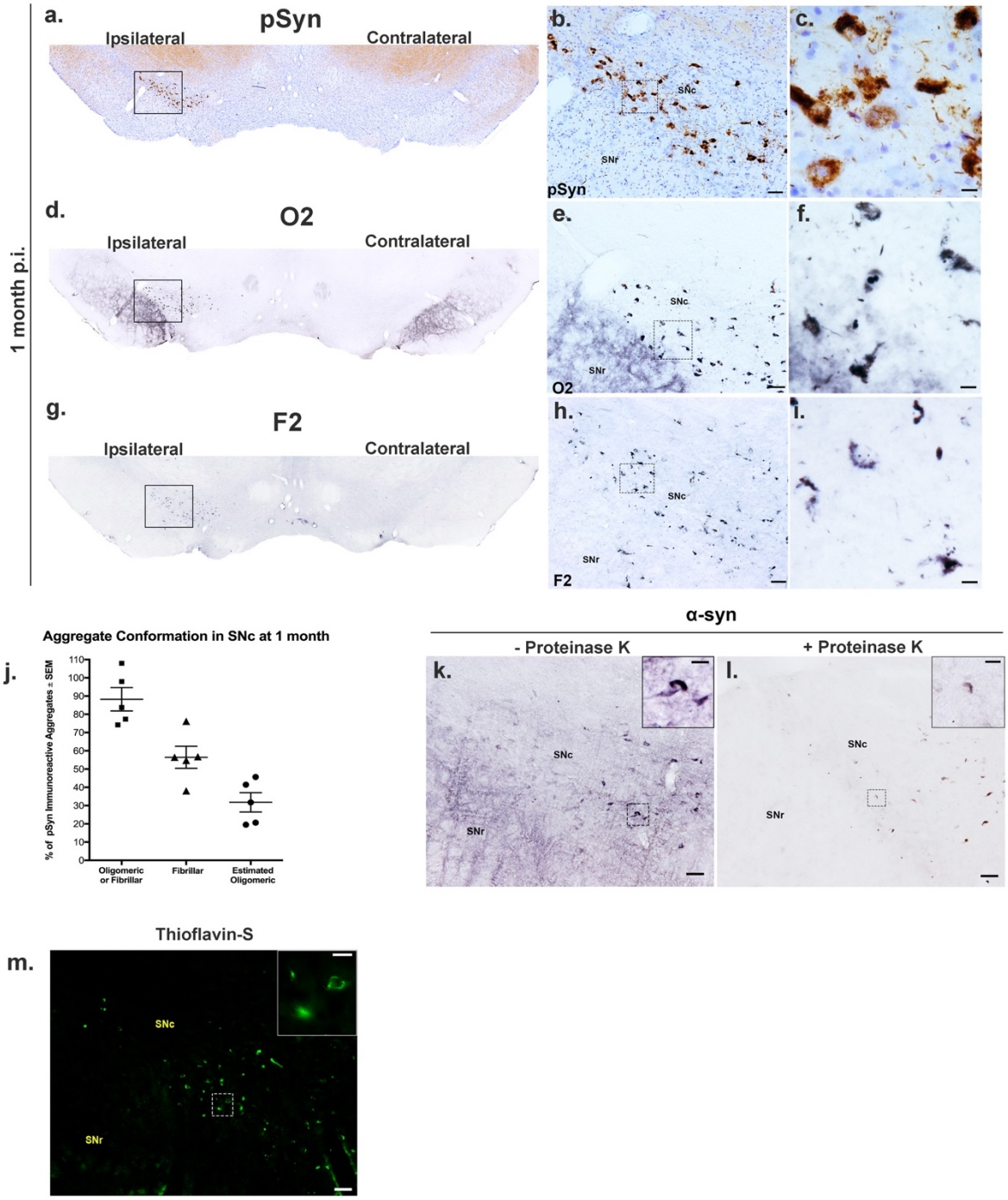

Figure 3.2: α-syn inclusions in the SNc exhibit oligomeric and fibrillary conformations and Lewy body-like characteristics

(a-c) Representative images of Lewy-body-like intraneuronal pSyn inclusions in the substantia nigra pars compacta (SNc) at 1 month p.i. show pathology is localized to the ipsilateral SNc. **(d-f)** Adjacent SN tissue sections stained for O2 (oligomeric/fibrillar α-syn conformation specific) and F2 **(g-i)** (fibrillar specific conformation) α-syn reveal that many intraneuronal inclusions possess mature, fibrillar inclusions of α-syn. **(j)** Percent of pSyn inclusions with either \ oligomeric/fibrillar (O2) or predominantly fibrillar (F2) immunoreactivity and estimated proportion of pSyn inclusions that are oligomeric only. Data represent mean ± SEM. Scale bars (b, e, h) =

Fig. 3.2 cont'd
50μm, (c, f, i) = 10 μm. **(k)** Endogenous α-syn immunoreactivity in the SNc and SNr. **(l)** Adjacent tissue sections exposed to proteinase-K reveal absence of soluble α-syn in the SNr and the presence of insoluble, neuronal inclusions of α-syn in the SNc. **(m)** Thioflavin-S fluorescence of amyloid structure present in SNc neurons. Scale bars **(k, l, m)** = 50μm, (Insets) = 25μm. Abbreviations: α-syn = alpha-synuclein; p.i. = post injection; pSyn= α-syn phosphorylated at Serine129; O2= oligomeric/fibrillar α-syn antibody; F2= fibrillar α-syn only antibody; SNc =substantia nigra pars compacta; SNr; substantia nigra pars reticulata; SEM = standard error of the mean.

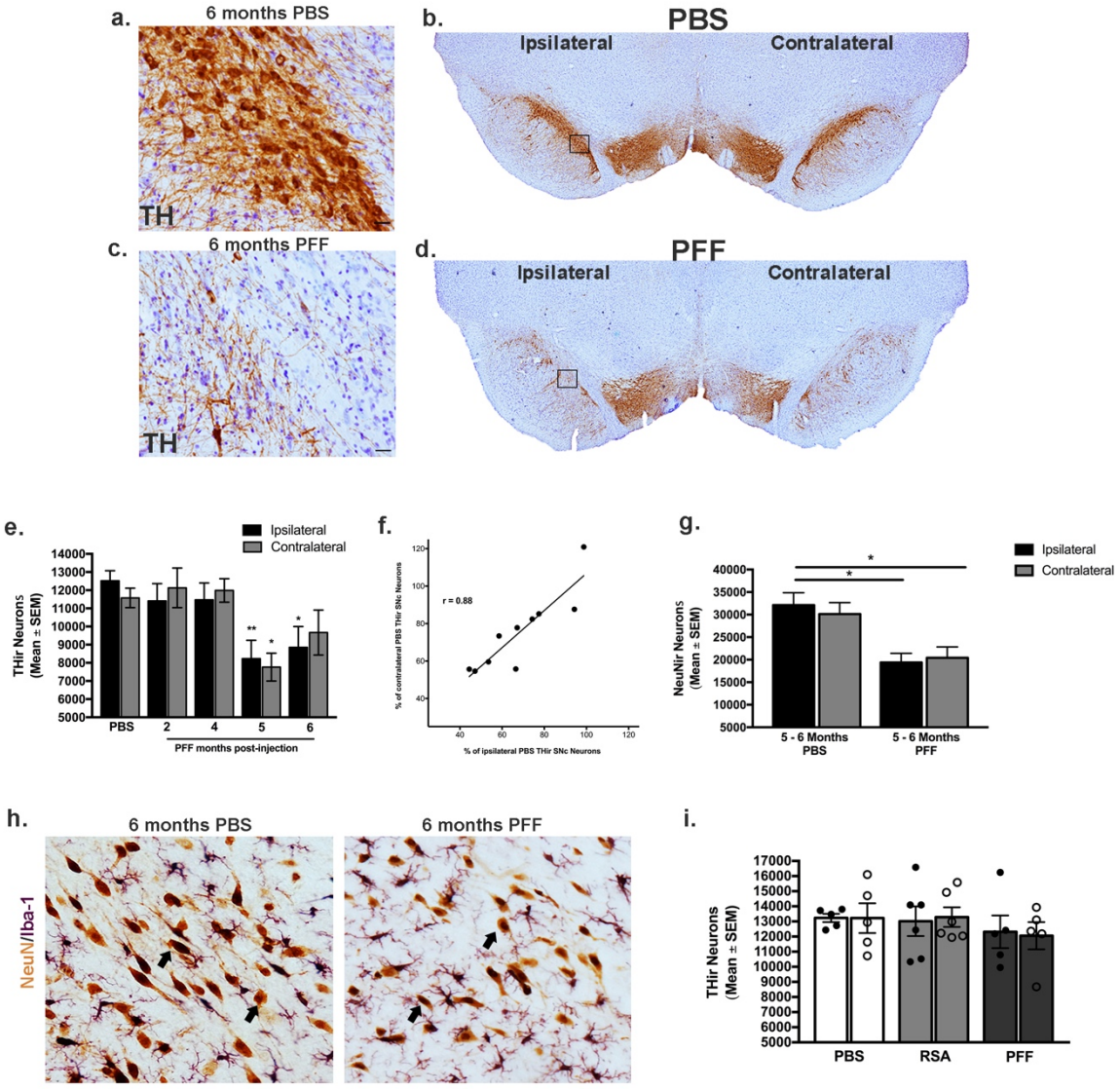

Figure 3.3: α-syn PFF-seeded synucleinopathy induces protracted, significant bilateral loss of SNc dopamine neurons

(a-d) Unilateral intrastriatal α-syn PFF injection induces visible loss of THir neurons (brown) in the SN at 6 months compared to an age-matched, PBS injected control. Scale bars (A,C) = 25μm. **(e)** Stereological assessment of THir neuron loss at 2, 4, 5, and 6 months following α-syn PFF or saline injection. Significant ipsilateral reduction in THir neurons was observed at 5 and 6 months post injection compared to saline injected controls with significant contralateral loss at 5 months *p<0.027 compared to respective PBS hemisphere, **p < 0.013 compared to respective PBS hemisphere **(f)** Correlation between extent of ipsilateral THir neuron loss and contralateral loss as compared to PBS control; (r = 0.8855, p = 0.0007, R^2 = 0.7842). **(g)** Stereological assessment of NeuNir neurons reveals overt degeneration distinct from loss of TH phenotype, *p< 0.03 compared to ipsilateral PBS. **(h)** Representative IHC of NeuNir neurons (brown, arrows) in the SNc in PBS *(left)* and PFF injected *(right)* animals 6 months p.i. **(i)** Stereological assessment of THir neurons at 2 months p.i. reveals no significant acute toxicity from injection of rat serum albumin (RSA). Data represent mean ± SEM.

Fig. 3.3 con'td
Abbreviations: PFF = pre-formed alpha-synuclein fibrils p.i. = post injection; Ipsilateral = ipsilateral hemisphere relative to injection; contralateral = contralateral hemisphere relative to injection; SNc = substantia nigra pars compacta; SNr; substantia nigra pars reticulata; Neu-Nir = Neuronal Nuclei

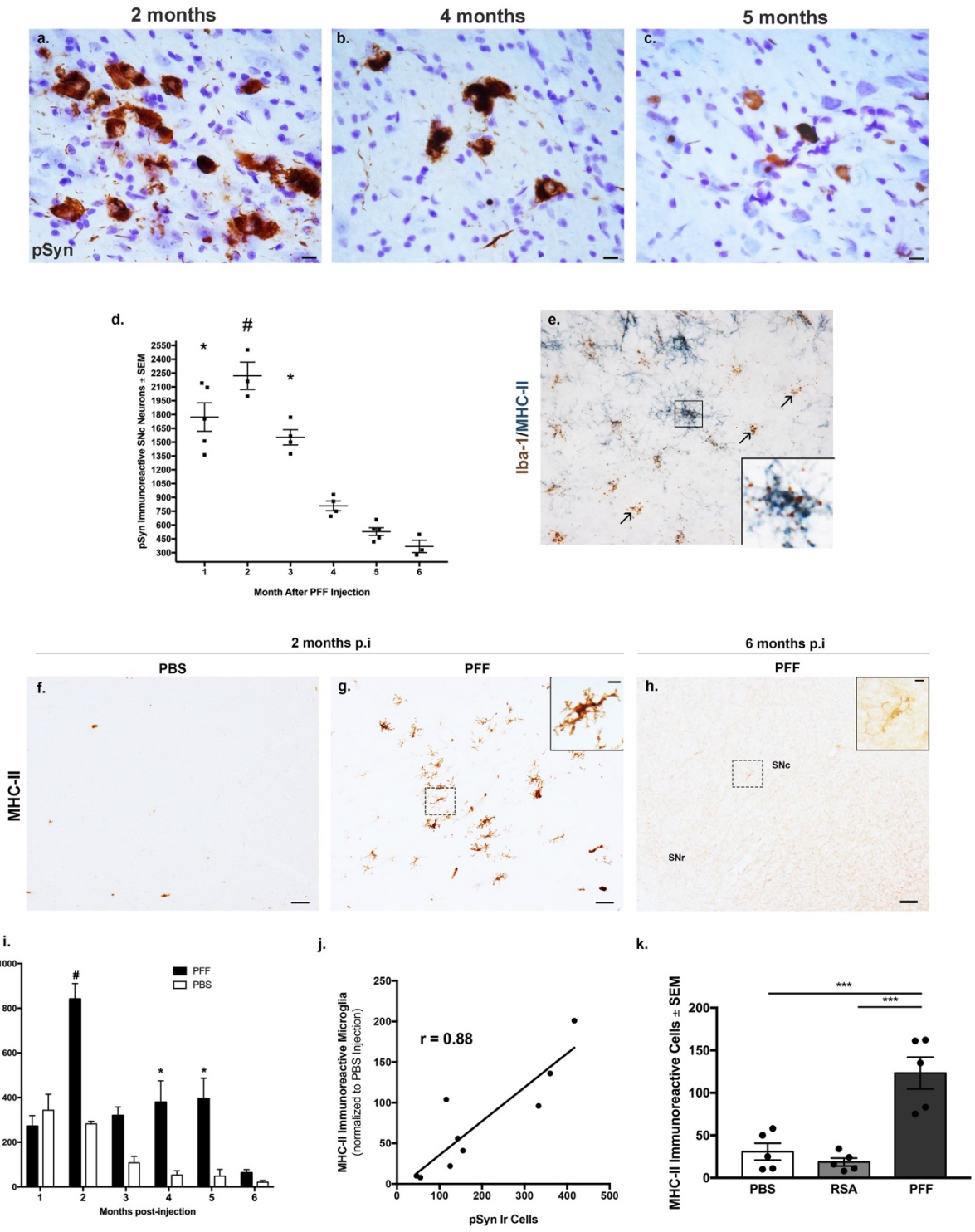

Figure 3.4: Antigen-presenting MHC-II immunoreactive (MHC-IIir) microglia increase in the SNc in association with peak accumulation of α-syn inclusions, but are limited during the interval of degeneration

(a-c) Representative images of pSyn inclusions in the SNc at 2, 4 and 5 months p.i.; Scale bar (A-C) = 10µm. **(d)** Stereological assessment of pS129 containing neurons in the substantia

Figure 3.4 cont'd.
nigra in PFF animals at 1, 2, 3, 4, 5, and 6 months p.i.; *p≤0.001 compared to 4, 5, 6, months. #p ≤ 0.006 compared to 3, 4, 5, 6 months. pSyn inclusions decrease over time in association with neuronal loss. **(e)** Major-histocompatibility complex-II (MHC-II; blue) protein colocalizes with ionized calcium binding adaptor molecule 1 mRNA (brown) within microglia. **(f-g)** Representative images of MHC-II antigen-presenting microglia in the SN at 2 months in PBS and PFF injected rats and 6 months post-PFF injection **(h)**; Scale bar F-H = 50 μm, Insets= 10μm**. (i)** Stereological assessment of MHC-IIir microglia in the SN reveals MHC-IIir microglia are significantly higher in PFF vs. PBS animals at 2, 4, and 5 months *p<0.006. More MHC-IIir microglia are evident in 2 month PFF animals vs. all other PFF time points #p<0.02. Notably, MHC-IIir microglia peak at the same time pSyn aggregation peaks **(d, i)**. **(j)** Number of MHC-II immunoreactive microglia correlated with number of SNc neurons with intraneuronal pSyn inclusions ($r = 0.8858$, $p = 0.0015$, $R^2 = 0.7846$). **(k)** In a follow-up study, intrastriatal injection of rat serum albumin (RSA) does not impact numbers of MHC-IIir microglia compared to PBS $p > 0.05$. Injection of PFFs in this second cohort confirmed previous observations of a significant increase in MHC-IIir microglia compared to PBS or RSA at 2 months p.i. *** p ≤ 0.0006. Abbreviations: p.i. = post injection; PFFs= pre-formed alpha-synuclein fibrils; PBS = phosphate buffered saline; RSA = rat serum albumin. MHC-II= major-histocompatibility complex-II; Iba-1= ionized calcium binding adaptor molecule 1; -ir=immunoreactive; SNc = substantia nigra pars compacta; SEM = standard error of the mean.

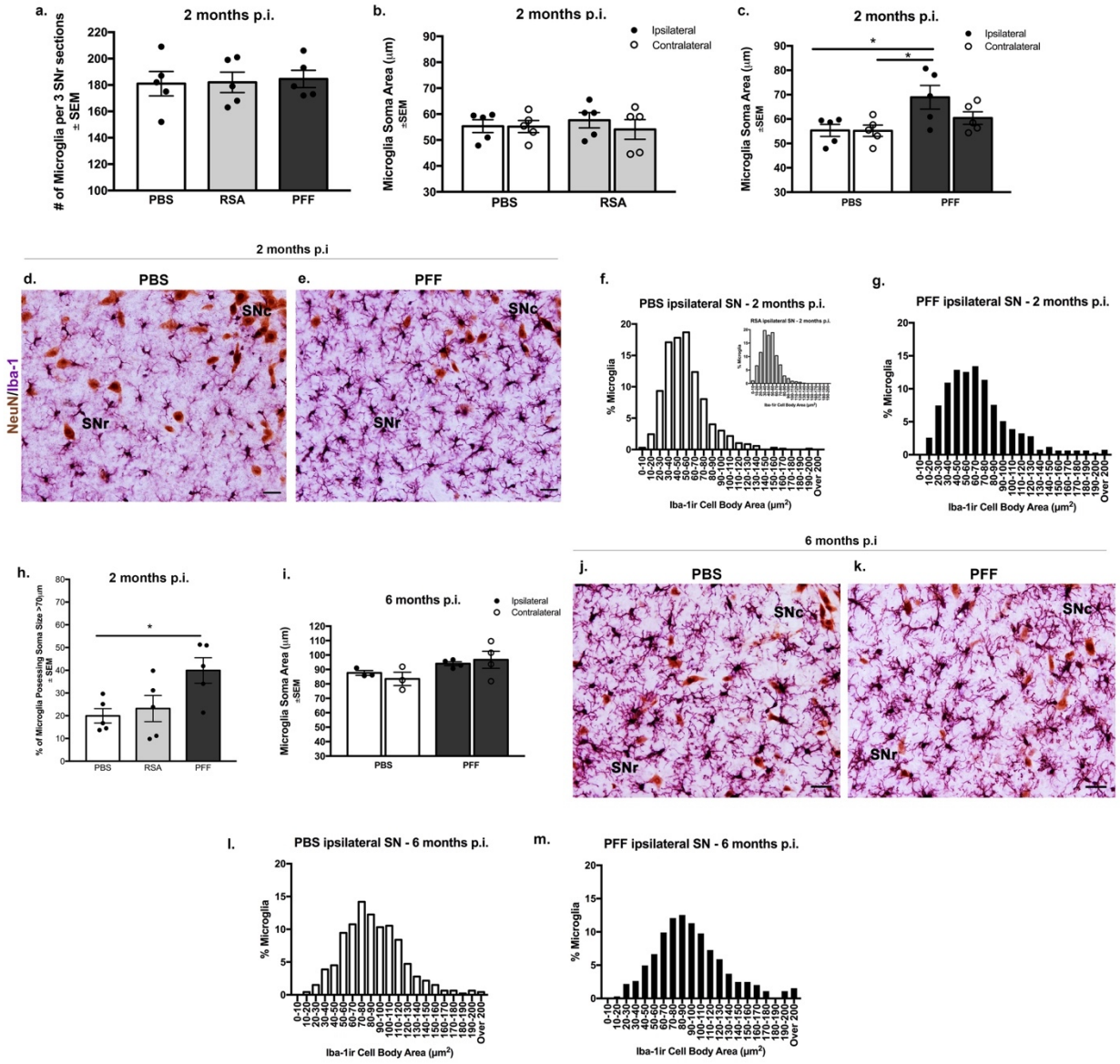

Figure 3.5: SNr microglia exhibiting reactive morphology are associated with pSyn inclusion-bearing neurons in the SNc

(a) Total number of microglia did not differ between PBS, RSA and PFF-injected animals, $p > 0.05$. **(b)** Microglia soma area in the ipsilateral and contralateral SNr did not differ significantly between animals receiving intrastriatal injections of PBS or RSA, $p > 0.05$. **(c)** Microglia soma area was significantly increased at 2 months in the ipsilateral SNr, when peak numbers of pSyn aggregates are present in nearby SNc neurons as compared to PBS-injected animals, $^*p = 0.02$. **(d-e)** Representative images of SN sections dual labeled for Iba-1 immunoreactive microglia (purple) and NeuN-ir neurons (brown) 2 months following either intrastriatal PBS or α-syn PFF injected rats. α-syn PFF-injected rats exhibit larger cell bodies and increased number and thickness of processes. **(f, inset)** Distribution of microglia soma area measurements 2 months following intrastriatal PBS or RSA injection illustrated as a percent of total microglia quantified. **(g)** Distribution of microglia soma area measurements 2 months following α-syn PFF injection illustrated as a percent of total microglia quantified. **(h)** Percent of total microglia

Figure 3.5 cont'd.
quantified for soma area analysis with cell body areas >70 µm at 2 months. Microglia in PFF-injected rats possessed significantly more microglia with cell bodies larger than >70 µm compared to PBS-injected rats, *p = 0.03. **(l)** At 6 months p.i. microglia soma area in the ipsilateral and contralateral SNr did not differ significantly between rats receiving either PBS or α-syn PFF intrastriatal injections, during the interval of ongoing degeneration in the SNc of PFF injected animals, p > 0.05. **(j-k)** Representative images of SN sections dual labeled for Iba-1 immunoreactive microglia (purple) and NeuN-ir neurons (brown) at 6 months p.i. exhibit a hyper ramified morphology, regardless of treatment. **(l-m)** Distribution of microglia soma area measurements 6 months p.i in PBS and PFF injected rats as a percent of total microglia quantified. Scale Bars (D-E, J-K) = 25µm. Data represent mean ± SEM.
Abbreviations: p.i. = post injection; PFFs= pre-formed alpha-synuclein fibrils; PBS = phosphate buffered saline; RSA = rat serum albumin.; Iba-1= ionized calcium binding adaptor molecule 1; ir=immunoreactive; NeuN-ir = Neuronal Nuclei immunoreactive; Ipsilateral = ipsilateral hemisphere relative to injection; contralateral = contralateral hemisphere relative to injection; SNc = substantia nigra pars compacta; SNr= substantia nigra pars reticulata. SEM = standard error of the mean.

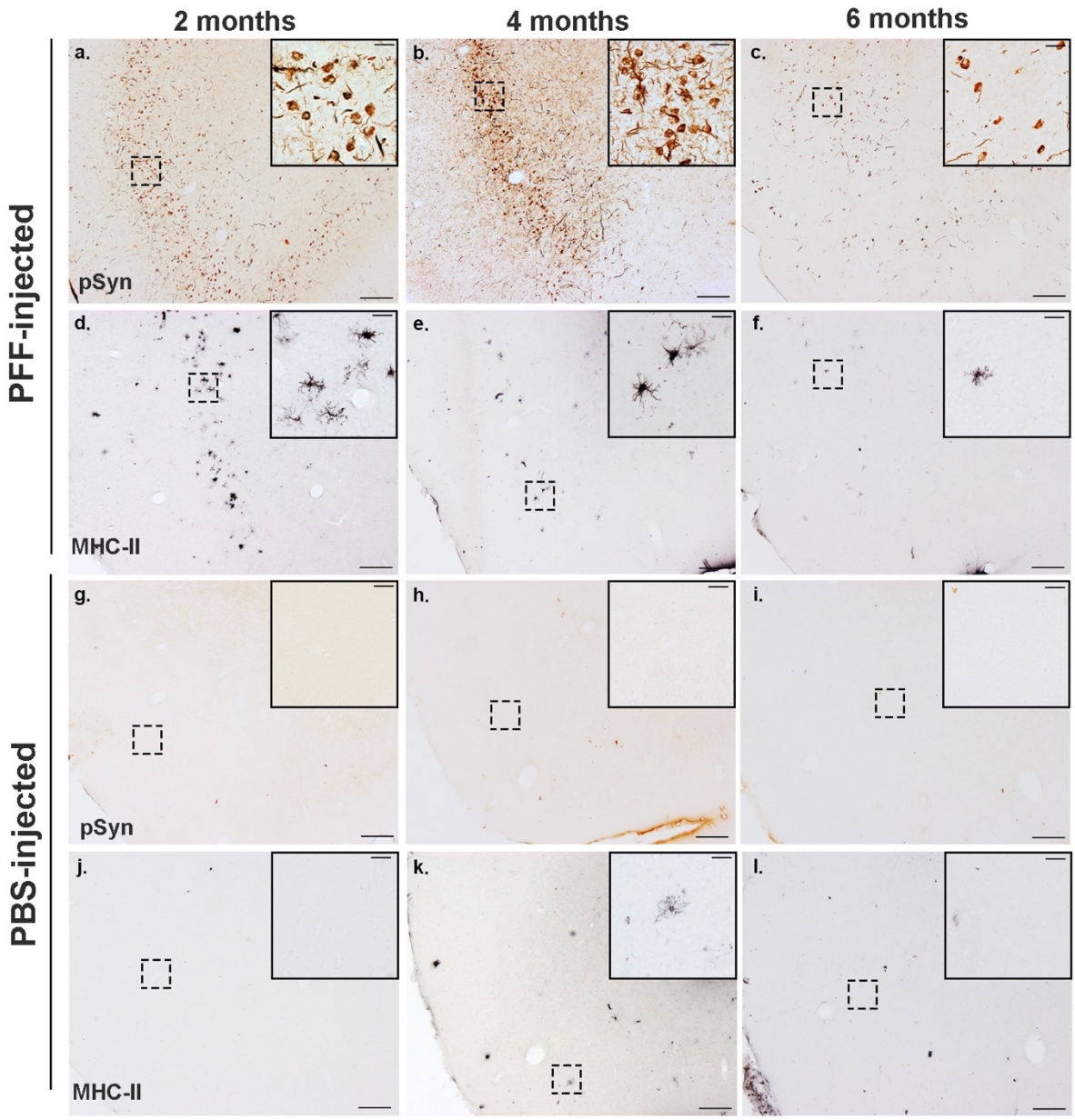

Figure 3.6: Microglia expressing MHC-II are associated with pSyn inclusions in the agranular insular cortex

(a-c) Representative images of pSyn accumulation in the agranular insular cortex at 2, 4 and 6 months p.i. Pathology is primarily localized to the soma at 2 months **(a)**, with increased neuritic pathology by 4 months **(b)** and an observable decrease overall by 6 months, possibly due to death of neurons. **(c)**. No pSyn inclusions were observed in PBS-injected animals **(g-i)**. **(d-f)** A similar pattern was observed in MHC-II expression on microglia. Peak numbers of MHC-IIir microglia were observed at 2 months p.i. **(d)**, decreased at 4 months **(e)** and virtually absent by 6 months **(f).** **(j-l)** Few to no MHC-IIir microglia were observed in PBS injected animals at any time point, suggesting that MHC-II expression occurs in response to accumulation of pSyn inside neurons. Abbreviations: p.i. = post injection; pSyn = α-syn phosphorylated at Serine129; PFFs= pre-formed alpha-synuclein fibrils; PBS = phosphate buffered saline; MHC-II= major-histocompatibility complex-II;; -ir=immunoreactive.

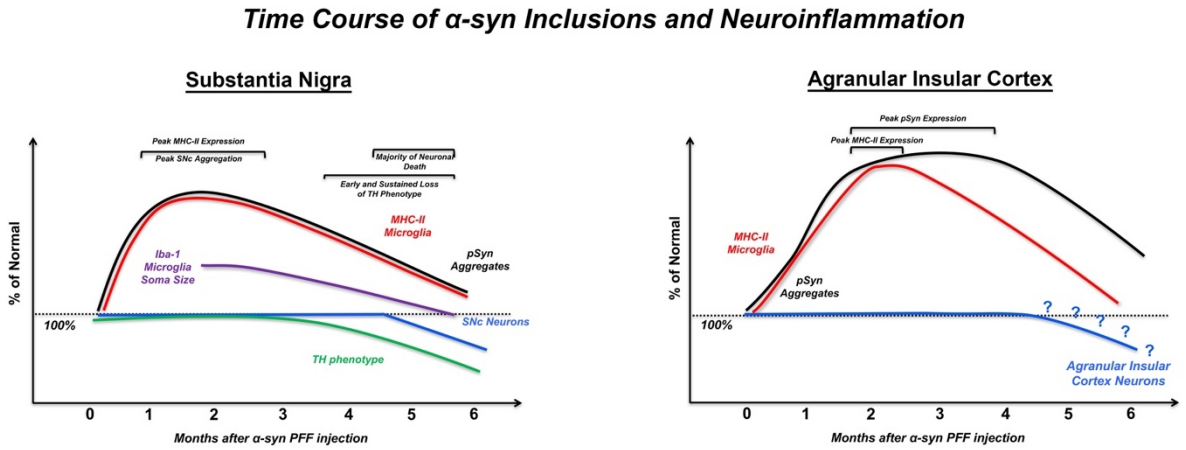

Figure 3.7: Regional timelines of synucleinopathy, neuroinflammation, and degeneration in the substantia nigra and agranular insular cortex following intrastriatal α-syn PFF injection

(Left): Early accumulation of phosphorylated inclusions of α-syn (peak at 2 months) in the substantia nigra leads to loss of TH phenotype and eventual loss of nigrostriatal dopamine neurons by 5-6 months p.i. In the SN, the pattern of microgliosis similarly follows that of pSyn: microglia in the adjacent SNr exhibit a reactive morphology at 2 months p.i. when nearby SNc neurons possess the greatest number of SNc pSyn inclusions. Interestingly, MHC-IIir antigen presenting microglia in the SNc also peak at 2 months p.i., again coinciding with the greatest number of pSyn intraneuronal inclusions and decrease over time to near non-detectable levels during the interval of degeneration, suggesting a relationship between pathological α-syn and inflammation.

(Right): Early accumulation of pSyn inclusions occurs between 2 and 4 months, with inclusions primarily localized to the somata at 2 months, an increase in neuritic inclusions at 4 months, and an observable decrease of overall pSyn pathology at 6 months, suggesting that similar to the SN, neurons in the agranular insular cortex harboring inclusions eventually die off. MHC-II immunoreactivity follows a similar pattern to that observed in the SN, with peak expression observed at 2 months p.i., and decreased over the course of 6 months.

APPENDIX

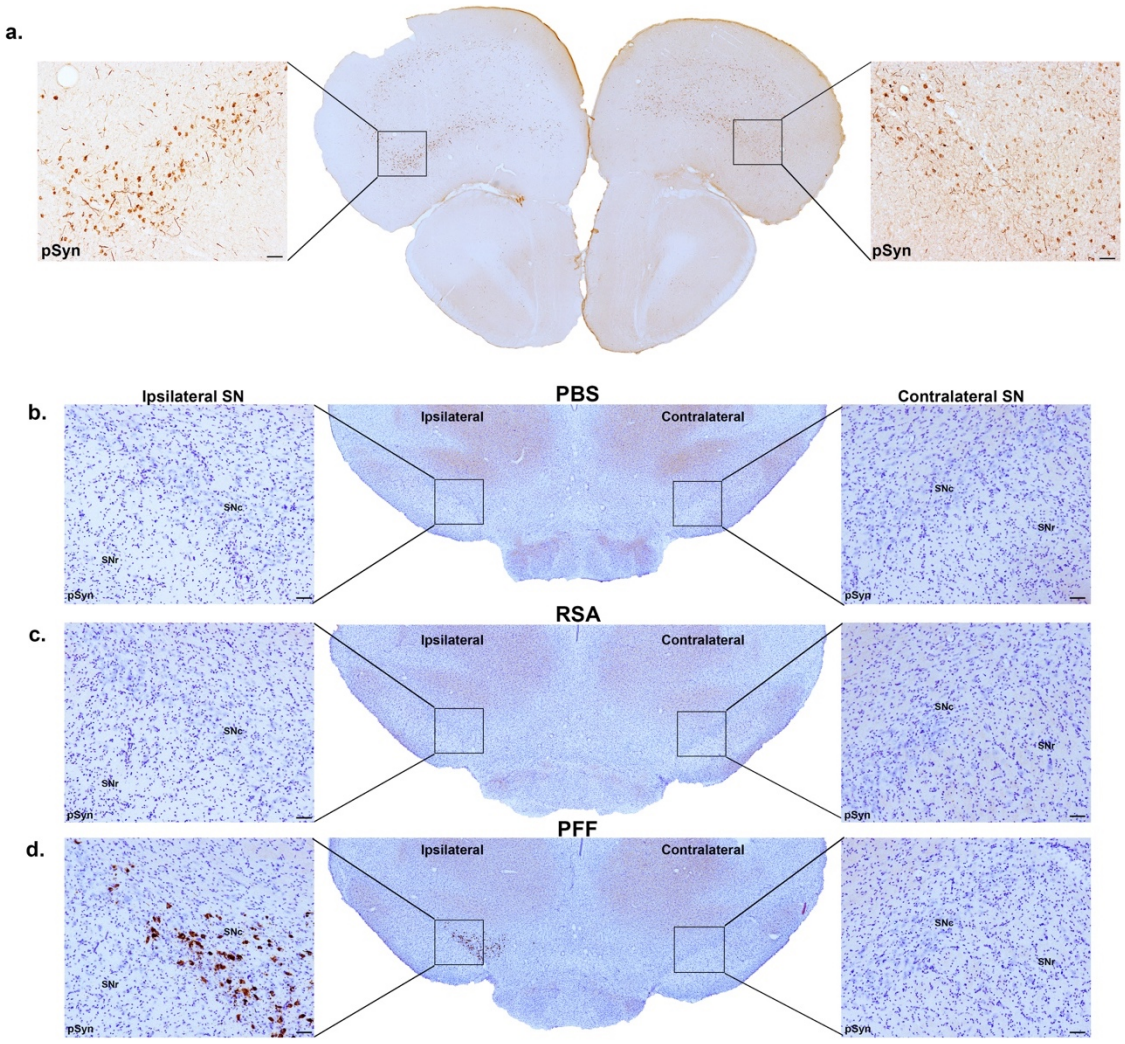

Figure 3.8: Unilateral intrastriatal injection of α-syn PFFs, but not RSA or PBS, induces bilateral cortical and unilateral SNc Lewy-body like inclusions of phosphorylated α-syn (pSyn)

(a) pSyn pathology is observed bilaterally in cortical areas after unilateral injection of α-syn PFFs, namely in layers 2/3, orbital and agranular insular cortices. **(b)** Injection of PBS or **(c)** RSA did not induce pSyn accumulation. **(d)** pSyn accumulation in the ipsilateral substantia nigra pars compacta (SNc) at 2 months post-injection, with no evidence of pSyn inclusions in the contralateral SNc. Scale bars (A-D) = 50 μm

Abbreviations: α-syn = alpha-synuclein; PFFs= pre-formed alpha-synuclein fibrils; PBS = phosphate buffered saline; RSA = rat serum albumin; pSyn = α-syn phosphorylated at serine 129

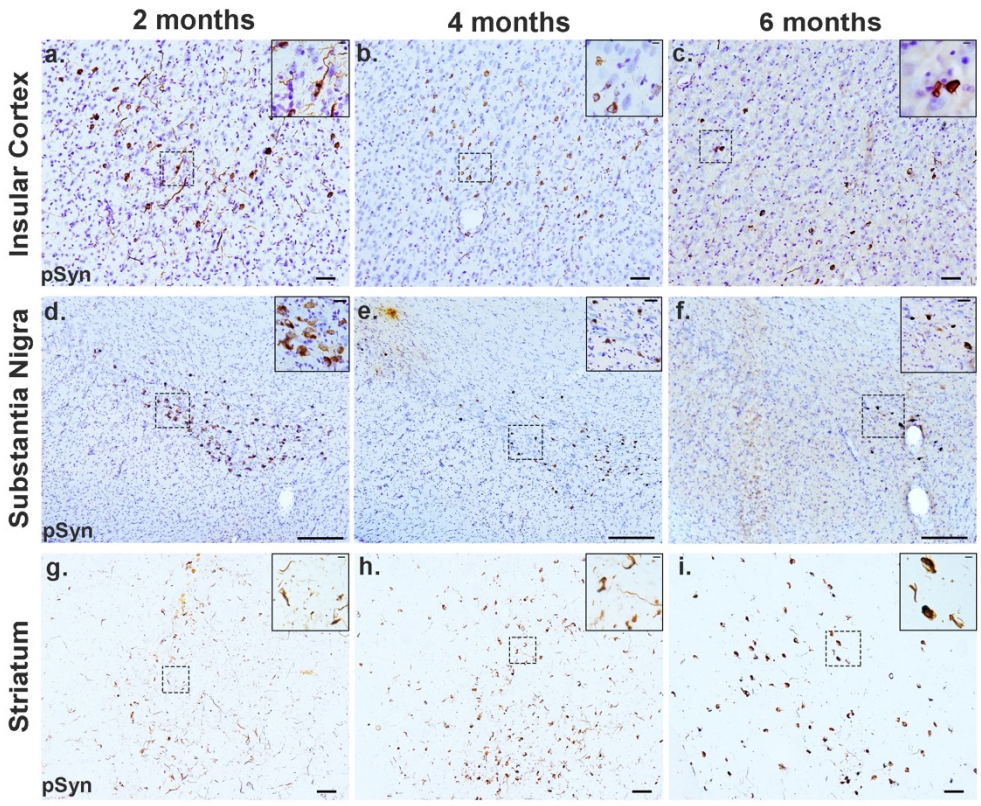

Figure 3.9: Unilateral intrastriatal injection of α-syn PFFs induces widespread accumulation of Lewy-body like inclusions of phosphorylated α-syn (pSyn)
Representative images illustrating the time course of pSyn pathology in regions innervating the striatum. **(a-c)** pSyn pathology in the ipsilateral agranular insular cortex localized to both the soma and neurites at 2 months p.i. (post-injection) that over time becomes primarily localized to the soma; Scale bar = 50μm, inset = 10μm. **(d-f)** Ipsilateral accumulation of pSyn in the substantia nigra peaks at 2 months and becomes less abundant over time as neurons degenerate; Scale bar = 200μm, inset = 25μm. **(g-i)** In contrast to other areas, pSyn in the striatum is primarily localized to neurites at 2 months and becomes more abundant and localized to the soma over time, Scale bar = 50μm, inset = 10μm.
Abbreviations: α-syn = alpha-synuclein; PFFs= pre-formed alpha-synuclein fibrils; pSyn= α-syn phosphorylated at Serine129; p.i.= post injection.

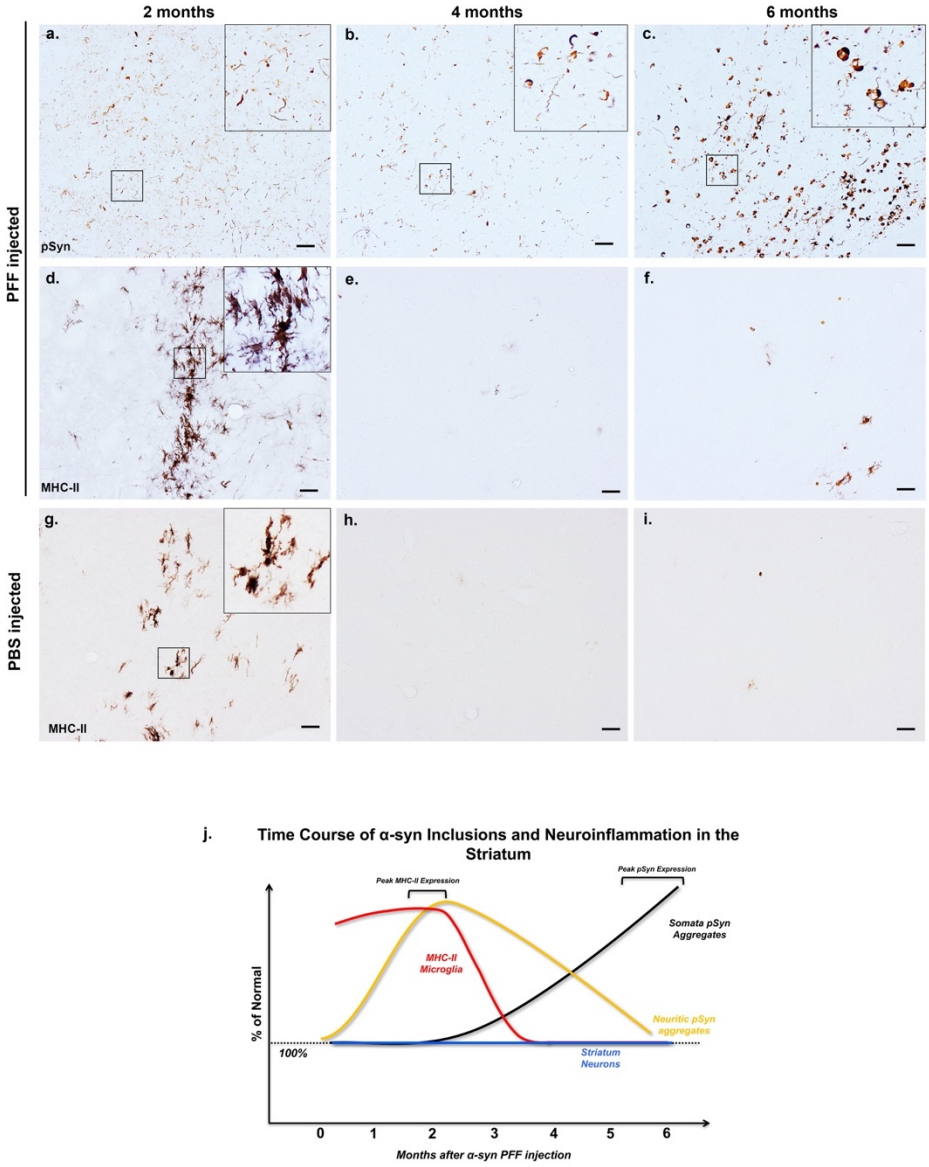

Figure 3.10: Antigen-presenting MHC-IIir microglia are not associated with peak of intraneuronal inclusions of pSyn in the striatum

Progression of pSyn pathology and MHC-IIir microglia in the striatum. **(a)** At 2 months p.i., pSyn inclusions are localized to neurites, presumably representing terminals from the SNc. **(b-c)** Over time pSyn inclusions become primarily localized to the soma of striatal neurons. **(d)** Abundant MHC-IIir microglia in the striatum primarily localized around the α-syn PFF injection site at 2 months. **(e-f)** MHC-IIir microglia in the striatum are largely absent during continuing accumulation of intraneuronal pSyn inclusions at 4 months **(e)** and 6 months **(f)** p.i. **(g)** Intrastriatal injection of PBS results abundant MHC-IIir microglia in the striatum localized near the site of injection at 2 months p.i., although appearing less abundant than MHC-IIir microglia in the striatum of α-syn PFF rats at the same time point **(d)**. **(h)** MHC-IIir microglia are similarly absent from the parenchyma by 4 months **(h)** and 6 months p.i **(i).** Scale bars A-I**=**50 μm.

Figure 3.10 cont'd
Abbreviations: p.i. = post injection; PFFs= pre-formed alpha-synuclein fibrils; PBS = phosphate buffered saline; pSyn= α-syn phosphorylated at Serine129, MHC-IIir= major-histocompatibility complex-II immunoreactive.

REFERENCES

REFERENCES

1. Collier, T.J., N.M. Kanaan, and J.H. Kordower, *Aging and Parkinson's disease: Different sides of the same coin?* Movement Disorders, 2017. **32**(7): p. 983-990.

2. Collier, T.J., J.H. Kanaan Nm Fau - Kordower, and J.H. Kordower, *Ageing as a primary risk factor for Parkinson's disease: evidence from studies of non-human primates.* (1471-0048 (Electronic)).

3. Mogi, M., et al., *Interleukin (IL)-1 beta, IL-2, IL-4, IL-6 and transforming growth factor-alpha levels are elevated in ventricular cerebrospinal fluid in juvenile parkinsonism and Parkinson's disease.* Neurosci Lett, 1996. **211**(1): p. 13-6.

4. Lindqvist, D., et al., *Cerebrospinal fluid inflammatory markers in Parkinson's disease – Associations with depression, fatigue, and cognitive impairment.* Brain, Behavior, and Immunity, 2013. **33**: p. 183-189.

5. Gerhard, A., et al., *In vivo imaging of microglial activation with [11C](R)-PK11195 PET in idiopathic Parkinson's disease.* Neurobiol Dis, 2006. **21**(2): p. 404-12.

6. McGeer, P.L., et al., *Reactive microglia are positive for HLA-DR in the substantia nigra of Parkinson's and Alzheimer's disease brains.* Neurology, 1988. **38**(8): p. 1285-91.

7. Imamura, K., et al., *Distribution of major histocompatibility complex class II-positive microglia and cytokine profile of Parkinson's disease brains.* Acta Neuropathol, 2003. **106**(6): p. 518-26.

8. Croisier, E., et al., *Microglial inflammation in the parkinsonian substantia nigra: relationship to alpha-synuclein deposition.* J Neuroinflammation, 2005. **2**: p. 14.

9. Dijkstra, A.A., et al., *Evidence for Immune Response, Axonal Dysfunction and Reduced Endocytosis in the Substantia Nigra in Early Stage Parkinson's Disease.* PLoS ONE, 2015. **10**(6): p. e0128651.

10. Braak, H., et al., *Staging of brain pathology related to sporadic Parkinson's disease.* Neurobiol Aging, 2003. **24**(2): p. 197-211.

11. Kannarkat, G.T., et al., *Common Genetic Variant Association with Altered HLA Expression, Synergy with Pyrethroid Exposure, and Risk for Parkinson's Disease: An Observational and Case-Control Study.* NPJ Parkinsons Dis, 2015. **1**.

12. Spiller, K.L., et al., *The role of macrophage phenotype in vascularization of tissue engineering scaffolds.* (1878-5905 (Electronic)).

13. Harms, A.S., et al., *MHCII is required for alpha-synuclein-induced activation of microglia, CD4 T cell proliferation, and dopaminergic neurodegeneration.* J Neurosci, 2013. **33**(23): p. 9592-600.

14. Liu, X., et al., *Intracellular MHC class II molecules promote TLR-triggered innate immune responses by maintaining activation of the kinase Btk.* Nature Immunology, 2011. **12**: p. 416.

15. Cicchetti, F., et al., *Neuroinflammation of the nigrostriatal pathway during progressive 6-OHDA dopamine degeneration in rats monitored by immunohistochemistry and PET imaging.* Eur J Neurosci, 2002. **15**(6): p. 991-8.

16. Koprich, J.B., et al., *Neuroinflammation mediated by IL-1beta increases susceptibility of dopamine neurons to degeneration in an animal model of Parkinson's disease.* J Neuroinflammation, 2008. **5**: p. 8.

17. Forno, L.S., et al., *Similarities and differences between MPTP-induced parkinsonsim and Parkinson's disease. Neuropathologic considerations.* Adv Neurol, 1993. **60**: p. 600-8.

18. Kurkowska-Jastrzebska, I., et al., *The inflammatory reaction following 1-methyl-4-phenyl-1,2,3, 6-tetrahydropyridine intoxication in mouse.* Exp Neurol, 1999. **156**(1): p. 50-61.

19. Gao, H.M., et al., *Neuroinflammation and alpha-synuclein dysfunction potentiate each other, driving chronic progression of neurodegeneration in a mouse model of Parkinson's disease.* Environ Health Perspect, 2011. **119**(6): p. 807-14.

20. Gomez-Isla, T., et al., *Motor dysfunction and gliosis with preserved dopaminergic markers in human alpha-synuclein A30P transgenic mice.* Neurobiol Aging, 2003. **24**(2): p. 245-58.

21. Koprich, J.B., et al., *Expression of human A53T alpha-synuclein in the rat substantia nigra using a novel AAV1/2 vector produces a rapidly evolving pathology with protein aggregation, dystrophic neurite architecture and nigrostriatal degeneration with potential to model the pathology of Parkinson's disease.* Mol Neurodegener, 2010. **5**: p. 43.

22. Yamada, M., et al., *Overexpression of alpha-synuclein in rat substantia nigra results in loss of dopaminergic neurons, phosphorylation of alpha-synuclein and activation of caspase-9: resemblance to pathogenetic changes in Parkinson's disease.* (0022-3042 (Print)).

23. Ulusoy, A., et al., *Viral vector-mediated overexpression of alpha-synuclein as a progressive model of Parkinson's disease.* (1875-7855 (Electronic)).

24. Theodore, S., et al., *Targeted overexpression of human alpha-synuclein triggers microglial activation and an adaptive immune response in a mouse model of Parkinson disease.* (0022-3069 (Print)).

25. Oliveras-Salvá, M., et al., *rAAV2/7 vector-mediated overexpression of alpha-synuclein in mouse substantia nigra induces protein aggregation and progressive dose-dependent neurodegeneration.* Molecular Neurodegeneration, 2013. **8**: p. 44-44.

26. Gombash, S.E., et al., *Morphological and behavioral impact of AAV2/5-mediated overexpression of human wildtype alpha-synuclein in the rat nigrostriatal system.* PLoS One, 2013. **8**(11): p. e81426.

27. Fischer, D.L., et al., *Viral Vector-Based Modeling of Neurodegenerative Disorders: Parkinson's Disease.* (1940-6029 (Electronic)).

28. Simola, N., A.R. Morelli M Fau - Carta, and A.R. Carta, *The 6-hydroxydopamine model of Parkinson's disease.* (1029-8428 (Print)).

29. Matsuoka, Y., et al., *Lack of nigral pathology in transgenic mice expressing human alpha-synuclein driven by the tyrosine hydroxylase promoter.* Neurobiol Dis, 2001. **8**(3): p. 535-9.

30. Ip, C.W., et al., *AAV1/2-induced overexpression of A53T-α-synuclein in the substantia nigra results in degeneration of the nigrostriatal system with Lewy-like pathology and motor impairment: a new mouse model for Parkinson's disease.* Acta Neuropathologica Communications, 2017. **5**: p. 11.

31. Sanchez-Guajardo, V., et al., *Microglia acquire distinct activation profiles depending on the degree of alpha-synuclein neuropathology in a rAAV based model of Parkinson's disease.* PLoS One, 2010. **5**(1): p. e8784.

32. Thakur, P., et al., *Modeling Parkinson's disease pathology by combination of fibril seeds and α-synuclein overexpression in the rat brain.* Proceedings of the National Academy of Sciences, 2017.

33. Farrer, M., et al., *Comparison of kindreds with parkinsonism and alpha-synuclein genomic multiplications.* Ann Neurol, 2004. **55**(2): p. 174-9.

34. Su, X., et al., *Alpha-Synuclein mRNA Is Not Increased. LID - S1525-0016(17)30179-X [pii] LID - 10.1016/j.ymthe.2017.04.018 [doi] FAU - Su, Xiaomin.* (1525-0024 (Electronic)).

35. Zhou, J., et al., *Changes in the solubility and phosphorylation of alpha-synuclein over the course of Parkinson's disease.* (1432-0533 (Electronic)).

36. Paumier, K.L., et al., *Intrastriatal injection of pre-formed mouse alpha-synuclein fibrils into rats triggers alpha-synuclein pathology and bilateral nigrostriatal degeneration.* Neurobiol Dis, 2015. **82**: p. 185-99.

37. Luk, K.C., et al., *Intracerebral inoculation of pathological α-synuclein initiates a rapidly progressive neurodegenerative α-synucleinopathy in mice.* The Journal of Experimental Medicine, 2012. **209**(5): p. 975-986.

38. Polinski, N.K., et al., *Best Practices for Generating and Using Alpha-Synuclein Pre-Formed Fibrils to Model Parkinson's Disease in Rodents. LID - 10.3233/JPD-171248 [doi].* (1877-718X (Electronic)).

39. Volpicelli-Daley, L.A., K.C. Luk, and V.M. Lee, *Addition of exogenous alpha-synuclein preformed fibrils to primary neuronal cultures to seed recruitment of endogenous alpha-synuclein to Lewy body and Lewy neurite-like aggregates.* Nat Protoc, 2014. **9**(9): p. 2135-46.

40. Volpicelli-Daley, L.A., et al., *Exogenous alpha-synuclein fibrils induce Lewy body pathology leading to synaptic dysfunction and neuron death.* Neuron, 2011. **72**(1): p. 57-71.

41. Tarutani, A., et al., *Effect of Fragmented Pathogenic α-Synuclein Seeds on Prion-like Propagation.* Journal of Biological Chemistry, 2016.

42. Vaikath, N.N., et al., *Generation and characterization of novel conformation-specific monoclonal antibodies for alpha-synuclein pathology.* (1095-953X (Electronic)).

43. Leys, C., et al., *Detecting outliers: Do not use standard deviation around the mean, use absolute deviation around the median.* Journal of Experimental Social Psychology, 2013. **49**(4): p. 764-766.

44. Wall, N.R., et al., *Differential innervation of direct- and indirect-pathway striatal projection neurons.* (1097-4199 (Electronic)).

45. Kim, C., et al., *Neuron-released oligomeric alpha-synuclein is an endogenous agonist of TLR2 for paracrine activation of microglia.* Nat Commun, 2013. **4**: p. 1562.

46. Wan, O.W. and K.K. Chung, *The role of alpha-synuclein oligomerization and aggregation in cellular and animal models of Parkinson's disease.* (1932-6203 (Electronic)).

47. Winner, B., et al., *In vivo demonstration that alpha-synuclein oligomers are toxic.* (1091-6490 (Electronic)).

48. Li, J.Y., et al., *Characterization of Lewy body pathology in 12- and 16-year-old intrastriatal mesencephalic grafts surviving in a patient with Parkinson's disease.* (1531-8257 (Electronic)).

49. Tanji, K., et al., *Proteinase K-resistant alpha-synuclein is deposited in presynapses in human Lewy body disease and A53T alpha-synuclein transgenic mice.* (1432-0533 (Electronic)).

50. Liu, Z., et al., *Neuronal uptake of serum albumin is associated with neuron damage during the development of epilepsy.* (1792-0981 (Print)).

51. Rey, N.L., et al., *Widespread transneuronal propagation of alpha-synucleinopathy triggered in olfactory bulb mimics prodromal Parkinson's disease.* (1540-9538 (Electronic)).

52. Conde, J.R. and W.J. Streit, *Effect of aging on the microglial response to peripheral nerve injury.* (1558-1497 (Electronic)).

53. Streit, W.J., *Microglia and neuroprotection: implications for Alzheimer's disease.*

54. Streit, W.J., et al., *Dystrophic microglia in the aging human brain.* (0894-1491 (Print)).

55. Christopher, L., et al., *Uncovering the role of the insula in non-motor symptoms of Parkinson's disease.* (1460-2156 (Electronic)).

56. Luk, K.C., et al., *Pathological alpha-synuclein transmission initiates Parkinson-like neurodegeneration in nontransgenic mice.* Science, 2012. **338**(6109): p. 949-53.

57. Kordower, J.H., et al., *Disease duration and the integrity of the nigrostriatal system in Parkinson's disease.* (1460-2156 (Electronic)).

58. Viceconte, N., et al., *Neuromelanin activates proinflammatory microglia through a caspase-8-dependent mechanism.* (1742-2094 (Electronic)).

59. Zhang, W., et al., *Neuromelanin activates microglia and induces degeneration of dopaminergic neurons: implications for progression of Parkinson's disease.* (1476-3524 (Electronic)).

60. Zhang, W., et al., *Human neuromelanin: an endogenous microglial activator for dopaminergic neuron death.* (1945-0508 (Electronic)).

61. Maillet, A., et al., *The prominent role of serotonergic degeneration in apathy, anxiety and depression in de novo Parkinson's disease.* (1460-2156 (Electronic)).

62. Cerasa, A., et al., *Cortical volume and folding abnormalities in Parkinson's disease patients with pathological gambling.* (1873-5126 (Electronic)).

63. Block, M.L. and J.S. Hong, *Microglia and inflammation-mediated neurodegeneration: multiple triggers with a common mechanism.* Prog Neurobiol, 2005. **76**(2): p. 77-98.

64. Gao, H.M., et al., *Neuroinflammation and oxidation/nitration of alpha-synuclein linked to dopaminergic neurodegeneration.* J Neurosci, 2008. **28**(30): p. 7687-98.

65. Hwang, O., *Role of oxidative stress in Parkinson's disease.* Exp Neurobiol, 2013. **22**(1): p. 11-7.

66. Wilshusen, R.A. and R.L. Mosley, *Innate and Adaptive Immune-Mediated Neuroinflammation and Neurodegeneration in Parkinson's Disease*, in *Neuroinflammation and Neurodegeneration*, P.K. Peterson and M. Toborek, Editors. 2014, Springer New York: New York, NY. p. 119-142.

67. Hong, S., et al., *Complement and microglia mediate early synapse loss in Alzheimer mouse models.* Science, 2016.

68. Solga, A.C., et al., *RNA-sequencing reveals oligodendrocyte and neuronal transcripts in microglia relevant to central nervous system disease.* (1098-1136 (Electronic)).

69. Park, J.Y., et al., *Microglial phagocytosis is enhanced by monomeric alpha-synuclein, not aggregated alpha-synuclein: implications for Parkinson's disease.* (1098-1136 (Electronic)).

70. Farooqui, T. and A.A. Farooqui, *Lipid-mediated oxidative stress and inflammation in the pathogenesis of Parkinson's disease.* Parkinsons Dis, 2011. **2011**: p. 247467.

71. Kim, W.G., et al., *Regional difference in susceptibility to lipopolysaccharide-induced neurotoxicity in the rat brain: role of microglia.* J Neurosci, 2000. **20**(16): p. 6309-16.

72. Zhang, K. and R.J. Kaufman, *From endoplasmic-reticulum stress to the inflammatory response.* Nature, 2008. **454**(7203): p. 455-462.

73. Zhang, W., et al., *Human neuromelanin: an endogenous microglial activator for dopaminergic neuron death.* Frontiers in bioscience (Elite edition), 2013. **5**: p. 1-11.

74. Andringa, G., et al., *Mapping of rat brain using the Synuclein-1 monoclonal antibody reveals somatodendritic expression of alpha-synuclein in populations of neurons homologous to those vulnerable to Lewy body formation in human synucleopathies.* J Neuropathol Exp Neurol, 2003. **62**(10): p. 1060-75.

75. Urrutia, P.J., N.P. Mena, and M.T. Núñez, *The interplay between iron accumulation, mitochondrial dysfunction, and inflammation during the execution step of neurodegenerative disorders.* Frontiers in Pharmacology, 2014. **5**: p. 38.

76. Brochard, V., et al., *Infiltration of CD4+ lymphocytes into the brain contributes to neurodegeneration in a mouse model of Parkinson disease.* (0021-9738 (Print)).

77. Jiang, S., et al., *The correlation of lymphocyte subsets, natural killer cell, and Parkinson's disease: a meta-analysis.* (1590-3478 (Electronic)).

78. Kustrimovic, N., et al., *Dopaminergic Receptors on CD4+ T Naive and Memory Lymphocytes Correlate with Motor Impairment in Patients with Parkinson's Disease.* (2045-2322 (Electronic)).

79. Carson, M.J., B. Thrash Jc Fau - Walter, and B. Walter, *The cellular response in neuroinflammation: The role of leukocytes, microglia and astrocytes in neuronal death and survival.* (1566-2772 (Print)).

80. Cebrian, C., et al., *MHC-I expression renders catecholaminergic neurons susceptible to T-cell-mediated degeneration.* Nat Commun, 2014. **5**: p. 3633.

81. Sulzer, D., et al., *T cells from patients with Parkinson's disease recognize alpha-synuclein peptides.* (1476-4687 (Electronic)).

Chapter 4: Synucleinopathy- And Age-Dependent Alterations in Inflammatory Cytokine Levels in CSF and Plasma

Introduction

The majority of Parkinson's disease (PD) patients are diagnosed following the emergence of motor symptoms, after approximately 50% of nigrostriatal dopamine neurons have been lost, diminishing the potential for disease-modification. Thus, the importance of identifying biomarkers in easily accessible biofluids in the early stages of disease has become increasingly recognized [1]. Alterations in pro- and anti-inflammatory cytokines in post mortem tissue and CSF and plasma from PD patients have been well-documented, albeit with some conflicting results reported in biofluids (**Summarized in Table 4.1** [2-8]). These discordant results likely stem from several sources of variability including differences in disease duration and time of sample collection [7]. Nonetheless, evidence from human biofluids suggests that alterations in inflammatory cytokines in both the CNS and plasma are associated with PD.

Increased production of proinflammatory cytokines and chemokines microglia in the aged brain (reviewed in [9-11]) and astrocytes [12, 13] can result in increased blood-brain barrier (BBB) permeability by inducing expression of adhesion molecules on endothelial cells and disrupting tight junctions, thereby inducing migration of lymphocytes [14, 15]. Leakiness of the BBB places the brain in jeopardy of exposure to neurotoxic factors and thus represents a risk or contributor to age-related neurodegenerative diseases [16-20]. To date, no studies examining inflammatory cytokines in CSF in normal, healthy aging have been conducted, though measurement of inflammatory cytokines in serum has suggested an increase in proinflammatory mediators such as interleukin-6 (IL-6) and CD40L with age [21, 22]. Therefore, the first

set of experiments examined the cytokine profile in CSF and plasma in the context of normal aging in the rat. Importantly, we observe significant increases in tumor necrosis factor (TNF) and keratinocyte chemoattractant (KC/GRO; CXCL1) in CSF and plasma in the context of normal aging.

Decreased integrity of the BBB has been established in patients with Parkinson's disease and thus may be a contributor to ongoing degeneration via aberrant diffusion of toxins, cytokines/chemokines and migration of peripheral leukocytes [14, 19, 23, 24]. While previous studies have identified abnormal levels of cytokines in biofluids of subjects with established PD, samples from *de novo* PD patients also represent a time point in which a significant number of nigral DA neurons have already degenerated [25], precluding the ability to investigate disturbances in immune response that may occur early in the disease prior to degeneration. The previous temporal characterization of pSyn accumulation, MHC-II expression and microglial morphological changes, and nigrostriatal degeneration in the rat PFF model as described in Chapter 3 [26, 27] allow us to investigate changes in CSF and plasma cytokine levels both in early stages of synucleinopathy, and after the onset of nigral degeneration. In the CSF we observe increased IL-6 in rats with nigral pSyn inclusions as well as significant correlations between nigral pSyn inclusion burden and tumor necrosis factor (TNF) and interferon gamma (IFN-$\boldsymbol{\gamma}$). Lastly, we observe increases in TNF, keratinocyte chemoattractant (KC/GRO), and interleukin-5 (IL-5) in CSF and in IL-6 in plasma, following degeneration, analogous to findings in human PD. Our results suggest that disturbances in specific

Cytokine	Name	Function	Increased or Decreased in Human PD	Stable across 24 hours? (Eidson 2017)
IFN-γ	Interferon Gamma	Enhances MHC-I expression; MHC-II expression on B cells and macrophages; antigen presentation; Ig class switching	Increased (CSF, Reale et al. 2009) Decreased (serum, Eidson et al. 2017); CSF levels correlate with UPDRS Score (Eidson et al. 2017) Decreased (plasma, Rocha et al. 2016)	Yes (serum)
IL-1β	Interleukin-1 Beta	Prostaglandin secretion; T cell and macrophage activation	Increased (CSF, Reale et al. 2009) Increased (blood, Qin et al. 2017) Increased (CSF, plasma, Blum-Degen et al. 1995)	Unknown
IL-4	Interleukin 4	B cell differentiation; decreases production of Th1 cels, macrophages, IFN-γ; enhances expression of IgE and IgG1	Decreased (plasma, Rocha et al. 2016)	Unknown
IL-5	Interleukin 5	B cell growth factor; eosinophil growth	***Unknown in CSF, serum***	Unknown
IL-6	Interleukin 6	Acute phase response; differentiation of B cells into Ig secreting cells	Decreased (plasma, Rocha et al. 2016) Increased (CSF, Blum-Degen et al. 1995) Increased (CSF, Mogi et al. 1994)	No (serum)
KC/GRO (CXCL1)	Keratincyte Chemoattractant	Neutrophil activation	***Unknown in CSF, serum***	Unknown
IL-10	Interleukin 10	Decreases cytokine production	Increased (blood, Qin et al. 2017) Decreased (plasma, Rocha et al. 2016)	Unknown
IL-13	Interleukin 13	Regulation of B-cell proliferation, macrophage activation; Decreases cytokine production and Th1 cells	***Unknown in CSF, serum***	Unknown
TNF-α	Tumor Necrosis Factor Alpha	Inducer of apoptosis; enhancement of endothelium adhesiveness for leukocytes via VCAM-1 and ICAM-1 expression	Increased (CSF, Reale et al. 2009) Increased (blood, Qin et al. 2017) No difference (CSF, Eidson et al 2017 Decreased (serum, Eidson et al. 2017) Decreased (plasma, Rocha et al. 2016)	Yes (serum) ; No (CSF)

Table 4.1: Cytokine expression in biofluids of PD patients
Several studies have investigated the expression of inflammatory cytokines in CSF, plasma, and whole blood of PD patients. Differential expression is observed for some cytokines depending on which biofluid is assayed, and some studies report opposite results from assaying the same biofluid. Cytokine functions adapted from *[28]*

cytokines are triggered by pSyn inclusion, analogous to very early-stage PD, and become significantly elevated following nigral degeneration.

Methods

Animals

Male Fischer344 were used in this study. All animals were provided food and water ad-libitum and housed at the AAALAC approved Van Andel Research Institute vivarium or Grand Rapids Research Center vivarium. All procedures were approved and conducted in accordance with Institute for Animal Use and Care Committee (IACUC) at Michigan State University.

Groups:

Cohort 1 (Aging cohort): A total of 16 male Fischer F344 rats were used at the following ages: 4 months (n=5), 8 months (n=5) and 20 months (n=6) [29-31]. Naïve rats at 4 months and 8 months of age correspond to ages of Cohort 2 animals sacrificed at 2 and 4 months post-injection, respectively. CSF and plasma were collected from all animals.
Cohort 2 (Synucleinopathy cohort): A total of 52 male Fischer F344 rats received two-site unilateral injections of either PBS or 8 or 16 total µg mouse α-syn PFFs and euthanized at 2, 4 and 6 months post-injection based on our previous temporal characterization of α-syn accumulation and nigral degeneration. CSF was taken from all animals at all time points. Plasma was taken from the 6-month time point only.

Preparation of α-syn PFFs and Verification of Fibril Size

PFF preparation was conducted as described in Chapter 3 [26, 27, 32-34]. Purification of recombinant, full-length mouse α-syn and in *vitro* fibril assembly was performed as previously described. Prior to sonication, α-syn fibrils were assessed to verify lack of contamination (LAL Assay, (~1 Endotoxin Units /mg)), high molecular weight (sedimentation assay), beta sheet conformation (Thioflavin T) and structure (electron microscopy). Prior to injection, PFFs were thawed, diluted in sterile Dulbecco's PBS (PBS, 2μg/μl or 4 μg/μl) and sonicated at room temperature using an ultrasonicating homogenizer (300VT; Biologics, Inc., Manassas, VA) with the pulser set at 20%, power output at 30% for 60 pulses at 1 second each. Following sonication, a sample of the PFFs was analyzed using transmission electron microscopy (TEM). Formvar/carbon coated copper grids (EMSDIASUM, FCF300-Cu) were washed twice with ddH_2O and floated for 1 min. on a 10 μl drop of sonicated α-syn fibrils diluted 1:20 with PBS. Grids were stained for 1 min. on a drop of 2% uranyl acetate aqueous solution, excess uranyl acetate was wicked away with filter paper, and allowed to dry before imaging. Grids were imaged on a JEOL JEM-1400 transmission electron microscope. The length of over 500 fibrils per sample were measured to determine average fibril size to ensure fibril length was of optimal size for seeding *in vivo.*

Intrastriatal Injection of α-syn PFFs

Sonicated PFFs were kept at room temperature during the duration of the surgical procedures. All rats in Cohort 1 were deeply anesthetized with isoflurane and received two 2μl unilateral intrastriatal injections either of sonicated mouse α-syn PFFs (8μg total protein or 16 μg total protein in 4 μl total injectate; AP +1.6, ML +2.0, DV -4.0; AP +0.1,

ML +4.2, DV -5.0 from skull) or an equal volume of PBS at a rate at 0.5µl/minute. Injections were administered using a pulled glass needle attached to a 10 µl Hamilton syringe. After each injection, the needle was left in place for 1 minute, retracted 0.5 mm, left in place for an additional 2 minutes and then slowly withdrawn. Animals were monitored post-surgery and euthanized at predetermined time points (2 months, 4 months, and 6 months post injection).

Euthanasia and biofluid collection

All animals received I.P. injection of 30mg/kg Beuthanasia (Henry Schein, Columbus OH) and were placed into a stereotaxic frame. CSF (~100 µl) was collected via cisterna magna puncture [35] and blood collected via cardiac puncture, transferred to plasma collections tubes (BD catalog info) and kept on ice. Animals were perfused with 0.9% heparinized saline followed by 0.9% saline. Brains were immersion fixe in 4% PFA for 48 hours and placed in 30% sucrose until sunk. CSF was centrifuged at 10,000 *g* for 10 min. at 4ºC to pellet any contaminating red blood cells, and the supernatant was transferred to a 1.5ml collection tube. Blood was centrifuged at 3,000 *g* for 5 min. at 4ºC and the top layer of plasma was transferred to a tube. CSF and plasma samples were frozen at -80ºC until analysis.

MesoScale Mupltiplex ELISA for Inflammatory Cytokines

Measurement of interferon gamma (IFN-γ), interleukin-10 (IL-10), interleukin-13 (IL-13), interleukin-1 beta (IL-1β), interleukin-4 (IL-4), interleukin-5 (IL-5), interleukin-6 (IL-6), keratinocyte chemoattractant (KC/GRO, CXCL1) and tumor necrosis factor (TNF) was

conducted with the 96 well MesoScale V-Plex Proinflammatory Panel 2 Rat kit (MSD, Rockville MD, K15059D-1) on the MSD SECTOR Imager 2400-A (Meso Scale Diagnostics, LLC, Rockville, MD) per the manufacturers' instructions. CSF (diluted 1:2) and plasma (diluted 1:4) samples were run in duplicate, and the signal generated was compared to the standard curve for each anylate and subsequently converted to the calculated concentration mean (pg/ml) which was used for final calculations.

Immunohistochemistry and Stereological Analysis in the SNc

Extensive stereological quantification of SNc neurons possessing α-syn inclusions phosphorylated Serine 129 (pSyn), SNc neurons (neuronal nuclei, Neu-N) and ; tyrosine hydroxylase (TH) immunoreactive SNc neurons was conducted as described previously [36].

Immunofluorescence in the Agranular Insular Cortex

Free floating cortical sections (1:6 series) were transferred to 0.1M tris buffered saline (TBS) containing 0.5% Triton X-100 (Tx100; TBS-Tx). Following washes, sections were incubated in 10% NGS/TBS-Tx and blocked for 1 hour. Following block, sections were double immunolabled with primary antibodies against mouse anti-phosphorylated α-syn at Serine 129 (pSyn, 81A; Abcam, Cambridge, MA; AB184674; 1:15,000) and rabbit anti-ionized calcium binding adaptor molecule-1 (Iba-1; Wako, Richmond, VA; 019-19741, 1:1000) overnight at 4ºC. Following primary incubation, sections were washed and incubated in secondary antibodies goat anti-rabbit (AlexaFluor 488; Invitrogen, Carlsbad, CA; A-11008) and goat anti-mouse (AlexaFluor 568; AbCam, Cambridge,

MA; ab175473) 1:500 in 1% NGS/0.5% Tx-100 for 2 hours. Sections were washed, mounted on subbed slides and coverslipped with VectaShield hardset mounting media (Vector Labs; H1400) and visualized on a on a Nikon Eclipse 90i microscope with a QICAM camera (QImaging, Surrey, British Colombia, Canada) and Nikon Elements AR (version 4.50.00, Melville, NY).

Inclusion Criteria for Examination of Inflammatory Cytokine Levels

All naïve rats (Cohort 1) and control rats injected with PBS (Cohort 2) were included for examination of inflammatory cytokine levels. Rats injected α-syn PFFs (Cohort 2) were included for examination of inflammatory cytokine analysis only if they possessed >1600 pSyn aggregates in the SNc. The 1600 pSyn aggregate cut off was determined by the distribution of data points which revealed a cluster of rats at the bottom of the distribution of SNc pSyn aggregates at 2 or 4 months (**Figure 4.7a, Appendix**), exhibiting virtually no spread and no apparent relationship between pSyn load and cytokine levels (**Figure 4.7b-c, Appendix**). Therefore, to examine the impact of pSyn inclusion load on inflammatory cytokines only rats possessing >1600 pSyn aggregates in the SNc were included for analysis. This resulted in the exclusion of 4 of 10 rats at the 2 month p.i. time point and 2 of 11 rats at the 4 month p.i. time point, all rats that had been injected with the lower total quantity of α-syn PFFs (8μg). Due to the fact that no rats possessed more than 1600 pSyn aggregates in the SNc at 6 months no correlation analysis between pSyn inclusion load and cytokine levels was performed for this time point. However, correlations were performed between cytokine levels and

magnitude of degeneration (24.64% - 52.82%) as determined by stereological counts of THir neurons.

Statistics

Statistical analyses were performed using GraphPad Prism (La Jolla, CA). Statistical significance for all cases was set at $p < 0.05$. Statistical outliers were assessed using the absolute Deviation from the Median (ADAM) method using the 'very conservative' criterion [37]. Comparisons between 2 groups were analyzed using a Student's t-test. For comparisons of 3 or more, a one-way ANOVA with Tukey's post hoc analyses was used. Correlation analysis was conducted to investigate the relationship between pSyn inclusion number and cytokine levels. For cytokine levels that were below detection limit (BDL) or below fit curve (BFC) in which no value was given, the calculated low at which the standard curve crosses the X axes was substituted.

Results

TNF and KC/GRO are significantly increased in CSF with aging

To investigate the relationship of biofluid cytokine levels with advancing age, levels of IFN-γ, IL-10, IL-13, IL-1β, IL-4, IL-5, IL-6, KC/GRO, and TNF were measured. As morphological and functional changes in microglia have been reported with aging [9-11, 38, 39] we first stained sections of agranular insular cortex from 4, 8, and 20-month old male rats, based on our previous observation that microglia increase MHC-II expression in the presence of pSyn. No gross changes in cell body size, shape, or extent of branching were observed between microglia from different age groups **(Figure 4.1a)**.

As expected, I these naïve rats no pSyn immunoreactivity was observed. In CSF, KC/GRO ($F_{(2, 12)}$ = 14.50, p = 0.006) was significantly increased in CSF at 20 months (70.47 ± 19.53 pg/ml) compared to 4 months (34.81 ± 2.52 pg/ml) and 8 months (33.07 ± 8.56 pg/ml), p<0.002. Additionally, TNF ($F_{(2, 12)}$ = 77.28, p<0.0001*)* was significantly increased in CSF at 20 months (1.51 ± 0.18 pg/ml) compared to 4 months (0.40 ± 0.10 pg/ml) and 8 months (0.59 ± 0.17 pg/ml), p<0.0001. In plasma, TNF ($F_{(2, 13)}$ = 9.51, p<0.003) was significantly increased at 20 months (4.73 ± 0.99 pg/ml) compared to 4 months (3.03 ± 0.45 pg/ml) and 8 months (3.05 ± 0.64 pg/ml). No other significant age-related differences were observed in cytokine levels in CSF or plasma (p>0.05).

Intrastriatal α-syn PFF injection results in cortical pSyn inclusions

Previous analysis of the cohort of rats used in this study demonstrated widespread accumulation of pSyn inclusions in the SNc, amygdala, motor and insular cortices [36]. Given our previous findings demonstrating increased MHC-II expression in the agranular insular cortex, we wanted to examine microglial morphology in this area. To examine the morphological characteristics (soma size, thickness and number of branches) and abundance of microglia surrounding pSyn inclusions in the agranular insular cortex we performed dual label immunofluorescence. Abundant pSyn inclusions were evident in α-syn PFF-injected rats, with no inclusions observed following control PBS injections (**Figure 4.3a)**. Microglial processes were observed in close proximity to pSyn inclusions **(Figure 4.3a, inset),** however no qualitative differences between the morphological characteristics and quantity of microglia were readily apparent between PBS and PFF injected animals. The time course of SNc pSyn accumulation and

degeneration in this cohort has been well-described in this cohort in our previous study [26, 27]. pSyn accumulation in the SNc is greatest at 2 months and decreases over time in association with cell loss (**Figure 4.2a;**[26, 27, 36]). Furthermore, significant nigral cell loss between 24.64% - 52.82% is observed in the ipsilateral SNc at 6 months post-injection (**Figure 4.2b** [36]).

CSF IFN-γ positively correlates with pSyn inclusion load at 2 months p.i., 3 months prior to nigral degeneration

Two separate approaches were used to examine the impact of α-syn PFF induced pSyn inclusions on CSF cytokine levels. First, group differences were examined between α-syn PFF and control PBS injected rats. Second, correlation analysis was conducted to determine any relationship between the magnitude of pSyn inclusions in the SNc within individual rats, as previously determined [36], and CSF cytokine levels. No significant group differences in cytokine levels due to either PFF or PBS treatment were observed at 2 months p.i. (*p >0.05,* **Table 4.2, Figure 4.3b**). In general, IL-1β, IL-13, and IL-4 fell below the fit curve BFC or BDL regardless of treatment (**Table 4.2**). Extensive variability in the number of SNc pSyn inclusions was observed within the α-syn PFF injected rats, prompting a correlation analysis to examine the relationship between SNc pSyn inclusion number and cytokine levels. There was a positive correlation between levels of IFN-γ and number of SNc pSyn inclusions ($r = 0.82$, $p= 0.0463$, $R^2= 0.67$; **Figure 4.3c**). Although rats possessing more pSyn inclusions appeared to have higher IL-6 and TNF CSF levels, no significant correlations were detected (IL-6: $r = 0.68$, $p= 0.13$, $R^2= 0.47$, **Figure 4.3d;** TNF: $r = 0.62$, $p= 0.19$, $R^2= 0.38$; **Figure 4.3e**).

At 4 months, at the onset of degeneration, IL-6 is significantly increased in CSF from α-syn PFF-injected rats, TNF and IFN-γ levels positively correlate with pSyn inclusions

Abundant pSyn inclusions were detected in the agranular insular cortex of α-syn PFF-injected rats 4 months after injection. However, no observable changes in microglia number or morphology were observed between PBS and PFF-injected animals (**Figure 4.4a).** Similar to 2 months p.i., IL-1β and IL-4 were BFC or BDL regardless of treatment, however increased variability in cytokines in PFF animals was observed compared to 2 months (**Table 4.3, Figure 4.3b**). α-syn PFF induced synucleinopathy was associated with significantly higher CSF IL-6 compared to PBS-injected rats at 4 months p.i. (p = 0.007, **Table 4.3, Figure 4.4b)**. Within individual PFF-injected rats, increased levels of pSyn inclusions was not associated with IL-6 CSF levels as no correlation was observed (r = 0.02, R^2 = 0.0002, p = 0.97). No additional significant between group differences in CSF cytokine levels were detected ($p > 0.05$), however CSF IL-10 trended toward being increased in rats injected with PFFs (PFF: 6.12 ± 0.80 pg/ml, PBS: 3.79 pg/ml ± 0.84 pg/ml, p =0.07). Correlation analysis was conducted to determine any relationship between the magnitude of pSyn inclusions in the SNc within individual PFF-injected rats at 4 months [26, 36] and CSF cytokine levels. Both CSF IFN-γ and TNF were positively correlated to SNc pSyn inclusion number (IFN: r = 0.79, R^2 = 0.62, p = 0.01; TNF: r = 0.69, R^2 = 0.47, p = 0.04, Figure 5.3c, e).

At 6 months, during the interval of degeneration, IL-5, KC/GRO, and TNF are significantly increased in CSF from α-syn PFF-injected rats

No changes in microglial abundance were observed between PBS and PFF-injected animals at 6 months p.i, during the interval of degeneration, though microglia in PFF-

injected animals appeared to have fewer branches (**Figure 4.5a**). Levels of IL-1β, IL-13, and IL-4 were generally BFC or BDL (**Table 4.4**) and variability within 6 month PFF samples appeared to be less compared to 4 month samples. Levels of three cytokines were significantly increased in the CSF from α-syn PFF-injected rats compared to PBS controls (**Table 4.4, Figure 4.5b**): IL-5 (PBS: all BDL, 3.42 ± 0 pg/ml, PFF: 5.12 ± 0.67 pg/ml, $p = 0.02$), KC/GRO (PBS: 23.25 ± 2.04 pg/ml, PFF 29.91 ± 0.95 pg/ml, $p = 0.01$), and TNF (PBS: 0.28 ± 0.06 pg/ml, PFF: 0.49 ± 0.03 pg/ml, $p = 0.01$). Correlation to pSyn inclusion number was not conducted at this time point due to the decrease in pSyn inclusions in association with degeneration. Increased magnitude of degeneration ranging from 24.64% - 52.82% loss of SNc neurons [36] did not correlate with any increase in CSF cytokines (**Figure 4.9, Appendix**).

At 6 months, during the interval of degeneration, IL-6 is significantly increased in plasma from α-syn PFF-injected rats

In addition to CSF, plasma was also collected from rats 6 months after either α-syn PFF or control PBS injection (Table 5.5). Cytokines were detected in higher amounts in plasma at 6 months p.i. compared to CSF at the same time point, however, IL-1β similarly remained BDL. Plasma IL-6 was significantly increased in α-syn PF-injected rats at 6 months p.i. compared to controls (PBS: 46.23 ± 9.81 pg/ml, PFF: 77.45 ± 6.45 pg/ml, $p < 0.02$). No other differences in plasma cytokines due to PFF treatment were observed, however IL-4 (PBS: 4.54 ± 0.16 pg/ml, PFF: 4.91 ± 0.13, $p = 0.08$) and IL-5 (PBS: BDL, 3.39 ± 0, PFF: 6.66 ± 1.43, $p = 0.07$) displayed a trend towards an increase in the plasma of PFF compared to PBS-injected rats. Increased magnitude of

degeneration ranging from 24.64% - 52.82% loss of SNc neurons [36] did not correlate with any increase in plasma cytokines (**Figure 4.10, Appendix**).

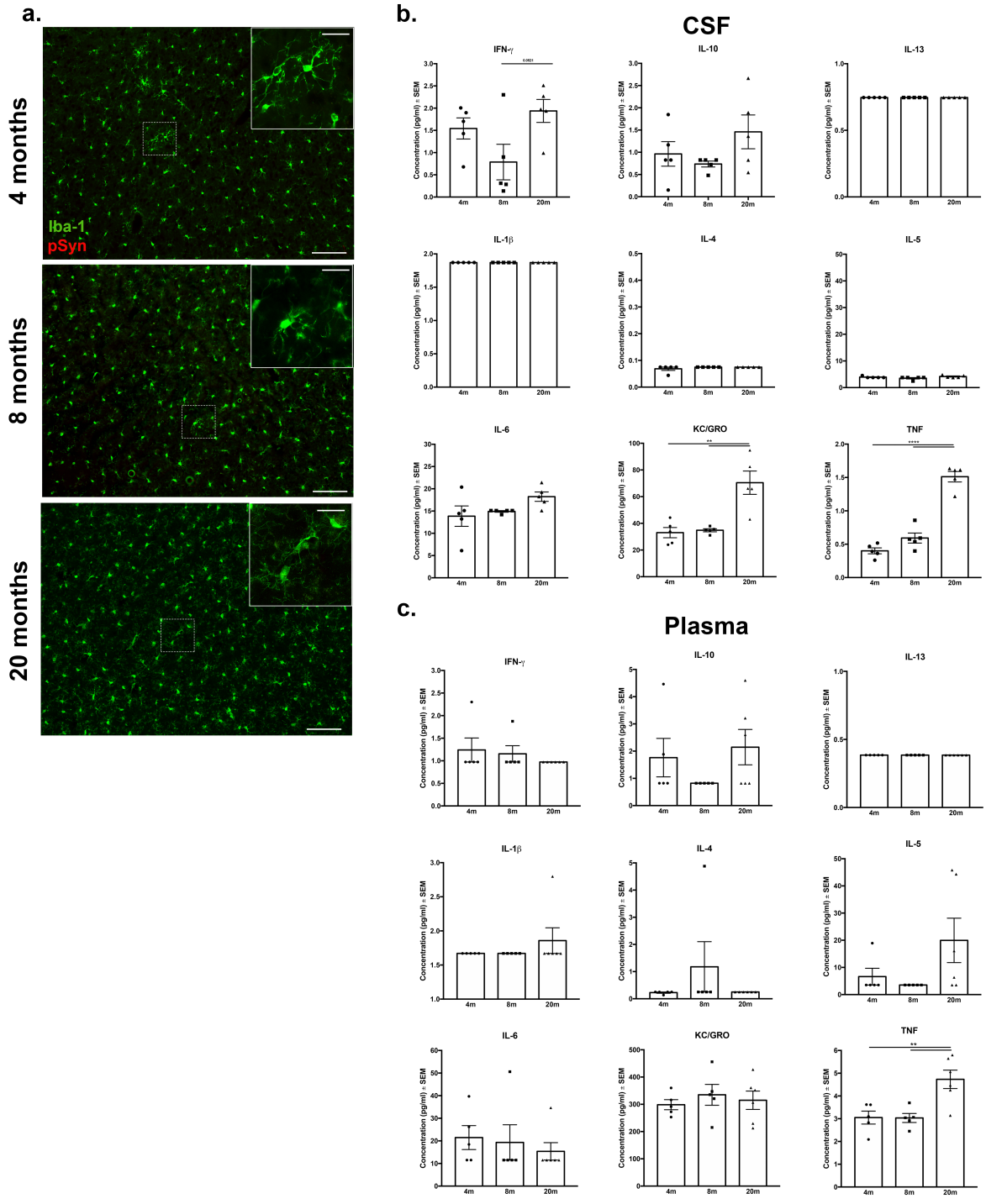

nigra

Figure 4.1: TNF and KC/GRO are significantly increased with normal aging
(a) No gross differences in microglia are observed in the agranular insular cortex at 4, 8 and 20 months. Note lack of staining for pSyn. (b) Of the nine cytokines analyzed, KC/GRO was

significantly increased in CSF at 20 months (70.47 ± 19.53 pg/ml) compared to 4 months (34.81 ± 2.52 pg/ml) and 8 months (33.07

Figure 4.1: cont'd.

± 8.56 pg/ml) ***p*<0.002. TNF was also significantly increased in CSF at 20 months (1.51 ± 0.18 pg/ml) compared to 4 months (0.40 ± 0.10 pg/ml) and 8 months (0.59 ± 0.17 pg/ml) ****p<0.0001. **(c)** TNF was significantly increased at 20 months in plasma **p≤ 0.007, (4.73 ± 0.99 pg/ml) compared to 4 months (3.03 ± 0.45 pg/ml) and 8 months (3.05 ± 0.64 pg/ml).

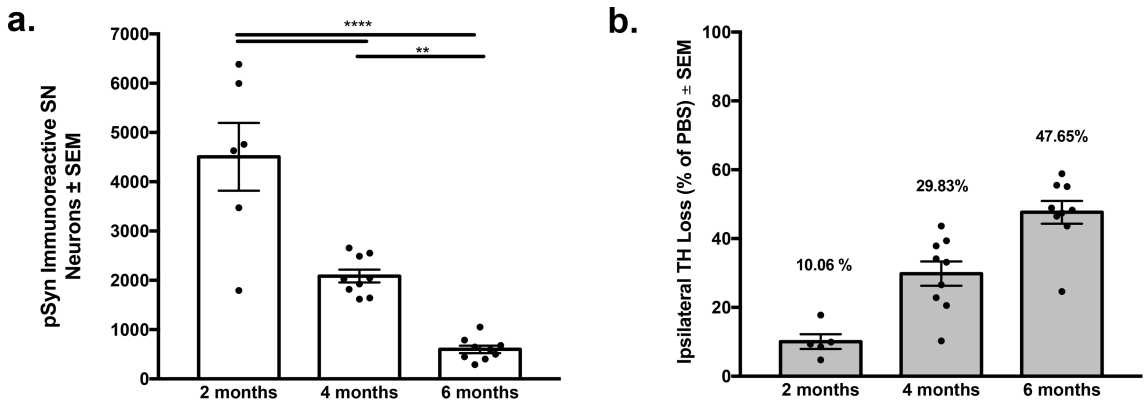

Figure 4.2: Time course of pSyn inclusions and TH neuron loss in the SN
(a) pSyn inclusion number in the ipsilateral SN following intrastriatal injection of PFFs. Inclusion number was significantly higher at 2 months compared to 4 and 6 months (p<0.0001), 4 months significantly higher than 6 months (p=0.0043). (b) Magnitude of ipsilateral TH loss compared to PBS control at 2, 4, and 6 months p.i. displays protracted, progressive nature of degeneration.

Cytokine	Detection Range (pg/ml)	Treatment	Mean Concentration (pg/ml) +/- SEM	p value
IFN-γ	1.97 - 6973.69	PFF	2.76 ± 0.52	0.61
		PBS	3.26 ± 0.72	-
IL-10	2.99 - 25621.81	PFF	3.92 ± 0.67	0.20
		PBS	2.90 ± 0.09	-
IL-13	0.75 - 1859.70	PFF	0.65 ± 0.13	0.12
		PBS	0.39 ± 0.08	-
IL-1β	3.74 - 14026.79	PFF	2.24± 0.82	0.26
		PBS	BDL	-
IL-4	0.40 - 1185.06	PFF	0.10 ± 0.02	0.43
		PBS	0.46 ± 0.37	-
IL-5	3.74 - 10879.22	PFF	6.95 ± 0.20	0.26
		PBS	6.15 ± 0.57	-
IL-6	1.36 - 3247.76	PFF	12.53 ± 3.35	0.31
		PBS	8.38 ± 2.24	-
KC/GRO	0.42 - 3236.77	PFF	34.51 ± 1.06	0.09
		PBS	53.52 ± 8.78	-
TNF	0.35 - 1282.30	PFF	0.61 ± 0.06	0.67
		PBS	0.58 ± 0.04	-

Table 4.2: CSF Cytokine levels at 2 months post-injection
No cytokines were significantly increased in PFF animals compared to PBS controls at 2 months p.i. Abbreviations: BDL = Below detection limit; pg/ml = picogram per milliliter; SEM = standard error of the mean

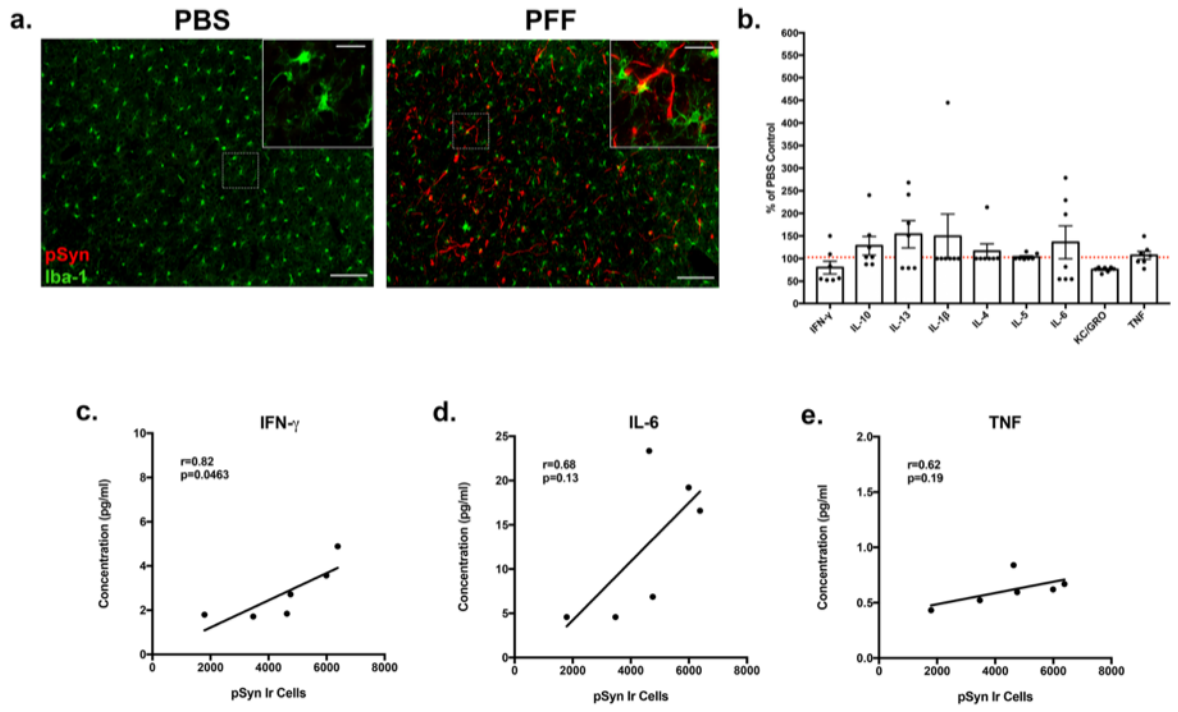

Figure 4.3: IFN-γ in CSF is associated with pSyn inclusion load at 2 months p.i., prior to nigral degeneration

(a) No gross changes in microglia number or morphology were observed in agranular insular cortex sections in PBS and PFF injected animals. However, microglial processes are shown in close proximity to pSyn immunoreactive neurites (PFF inset). (b) No differences in levels of inflammatory cytokines were observed at 2 months p.i. compared to PBS controls, however, considerable variability was noted within the PFF injected groups. (c) IFN-γ is positively correlated with number of pSyn-ir cells in the SN. (d-e) Although variable, levels of IL-6 and TNF did not significantly correlate with pSyn-ir cells in the SN. Abbreviations: BDL = Below detection limit; -ir = immunoreactive; pg/ml = picogram per milliliter; p.i. = post-injection; pSyn: α-syn at Serine 129; SEM = standard error of the mean; SN = substantia nigra

Cytokine	Detection Range (pg/ml)	Treatment	Mean Concentration (pg/ml) +/- SEM	p value
IFN-γ	1.97 - 6973.69	PFF	2.93 ± 0.79	0.14
		PBS	1.36 ± 0.26	-
IL-10	2.99 - 25621.81	PFF	6.12 ± 0.80	0.07
		PBS	3.80 ± 0.84	-
IL-13	0.75 - 1859.70	PFF	0.94 ± 0.17	0.42
		PBS	0.76 ± 0.19	-
IL-1β	3.74 - 14026.79	PFF	1.817 ± 0.36	0.40
		PBS	BDL	-
IL-4	0.40 - 1185.06	PFF	BDL	0.26
		PBS	BDL	-
IL-5	3.74 - 10879.22	PFF	8.06 ± 1.04	0.40
		PBS	BDL	-
IL-6*	1.36 - 3247.76	PFF	14.32 ± 1.92	0.007
		PBS	BDL	-
KC/GRO	0.42 - 3236.77	PFF	35.88 ± 6.07	0.64
		PBS	32.25 ± 0.94	-
TNF	0.35 - 1282.30	PFF	0.71 ± 0.06	0.77
		PBS	0.68 ± 0.09	-

Table 4.3: CSF Cytokine levels at 4 months post-injection
IL-6 was significantly increased in PFF animals compared to PBS controls at 4 months p.i. Abbreviations: BDL = Below detection limit; pg/ml = picogram per milliliter; p.i. = post-injection; SEM = standard error of the mean.

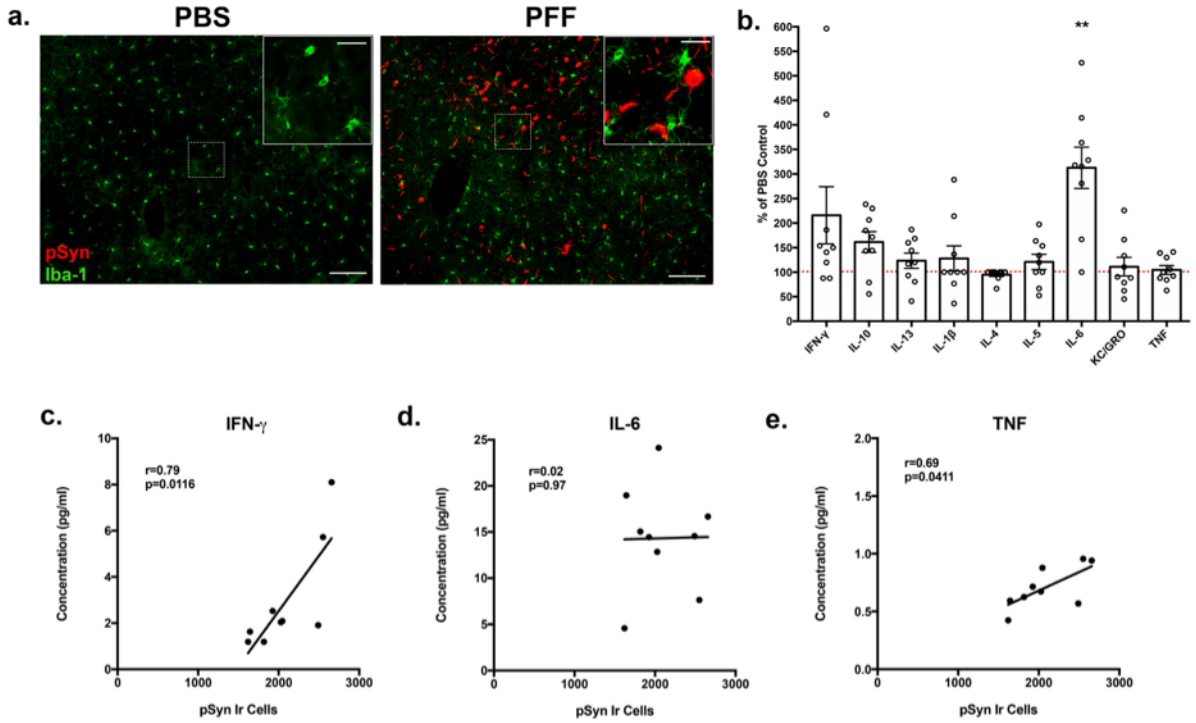

Figure 4.4: IL-6 is significantly increased and IFN-γ and TNF in CSF are associated with pSyn inclusion load at 4 months p.i., prior to nigral degeneration.
(a) No changes in morphology or number of microglia were observed in the agranular insular cortex between PBS and PFF injected animals at 4 months p.i. (b) Increased variability within PFF groups is observed at 4 months p.i. at the onset of degeneration. Notably, IL-6 is significantly increased compared to PBS controls (p = 0.007). (c) IFN-γ is positively correlated to pSyn-ir cells in the SN. (d) While levels of IL-6 are significantly increased in PFF-injected animals compared to PBS, IL-6 did not significantly correlate to pSyn-ir cell number. (d) TNF is positively correlated to pSyn-ir cell number. Abbreviations: BDL = Below detection limit; -ir = immunoreactive; pg/ml = picogram per milliliter; p.i. = post-injection; pSyn: α-syn at Serine 129; SEM = standard error of the mean; SN = substantia nigra.

Cytokine	Detection Range (pg/ml)	Treatment	Mean Concentration (pg/ml) ± SEM	p value
IFN-γ	1.79 - 7064.95	PFF	1.20 ± 0.11	0.11
		PBS	1.00 ± 0.02	-
IL-10	8.01 - 25595.40	PFF	1.44 ± 0.12	0.88
		PBS	1.45 ± 0.003	-
IL-13	0.65 - 1852.43	PFF	0.46 ± 0.06	0.08
		PBS	BDL	-
IL-1β	5.24 - 13760.13	PFF	3.28 ± 0.27	0.33
		PBS	BDL	-
IL-4	0.38 - 1179.16	PFF	BDL	0.94
		PBS	BDL	-
IL-5*	4.20 -10447.31	PFF	5.46 ± 0.61	0.02
		PBS	BDL	-
IL-6	3.76 - 13365.88	PFF	7.00 ± 1.09	0.16
		PBS	5.00 ± 0.14	-
KC/GRO*	0.70 - 3191.24	PFF	29.81 ± 0.95	0.01
		PBS	23.25 ± 2.04	-
TNF*	0.36 - 1314.95	PFF	0.49 ± 0.03	0.01
		PBS	0.28 ± 0.06	-

Table 4.4: CSF Cytokine levels at 6 months post-injection
IL-5, KC/GRO, and TNF were significantly increased in PFF animals compared to PBS controls at 4 months p.i. Abbreviations: BDL = Below detection limit; pg/ml = picogram per milliliter; SEM = standard error of the mean.

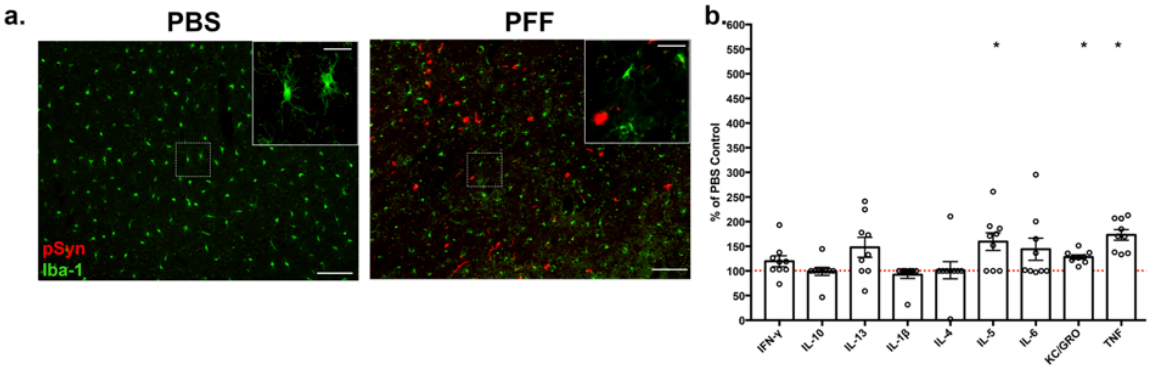

Figure 4.5: IL-5, KC/GRO and TNF are significantly increased in CSF during the interval of degeneration

(a) While no changes in microglial number are observed in the agranular insular cortex of PBS or PFF injected animals, microglia in PFF-injected animals appear to have smaller, dystrophic cell bodies and processes and less extensive branching at 6 months p.i. (b) IL-5, KC/GRO, and TNF are significantly increased compared to PBS controls at 6 months p.i., the interval of ongoing degeneration.

Abbreviations: BDL = Below detection limit; -ir = immunoreactive; pg/ml = picogram per milliliter; p.i. = post-injection; pSyn: α-syn at Serine 129; SEM = standard error of the mean; SN = substantia nigra.

Cytokine	Detection Range (pg/ml)	Treatment	Mean Concentration (pg/ml) ± SEM	p value
IFN-γ	1.65 - 7085.95	PFF	10.61 ± 0.49	0.72
		PBS	10.03 ± 1.49	-
IL-10	7.67 - 25890.53	PFF	108.10 ± 2.80	0.10
		PBS	100.6 ± 3.234	-
IL-13	0.72 - 13499.90	PFF	9.12 ± 0.47	0.23
		PBS	7.57 ± 1.15	-
IL-1β	4.30 - 13499.90	PFF	BDL	N/A
		PBS	BDL	-
IL-4	0.37 - 1184.70	PFF	4.91 ± 0.12	0.08
		PBS	4.54 ± 0.16	-
IL-5	3.69 - 10980.48	PFF	6.67 ± 1.43	0.07
		PBS	BDL	-
IL-6*	1.85 - 12424.84	PFF	77.45 ± 6.49	0.02
		PBS	46.23 ± 9.81	-
KC/GRO	1.05 - 3212.37	PFF	301.3 27.22	0.35
		PBS	334.1 ± 20.15	-
TNF	0.38 - 1346.40	PFF	3.85 ± 0.12	0.27
		PBS	3.55 ± 0.22	-

Table 4.5: Plasma cytokine levels at 6 months post-injection
Interleukin-6 is significantly increased in PFF compared to PBS-injected animals.
Abbreviations: BDL = Below detection limit; pg/ml = picogram per milliliter; SEM = standard error of the mean.

Discussion

To our knowledge, this is the first study to investigate the profile of inflammatory cytokines in CSF and plasma in the context of normal rodent aging and in a Parkinson's disease animal model. Additionally, the time course of synucleinopathy followed by protracted degeneration afforded by PFF injection allows for the unique opportunity to investigate early changes in inflammatory mediators in biofluids for the first time.

To summarize, we observe significant increases in TNF and KC/GRO in the context of normal rodent aging, concurrent with the concept that the CNS becomes increasingly proinflammatory with age and less protected by a deteriorating BBB. Interestingly, increased TNF has been implicated in increasing BBB permeability in a number of diseases via induced expression of molecules which promote recruitment and adhesion of T-cells to the endothelium, followed by migration into the parenchyma [40-44] and thus may represent a contributor to age-related degeneration.

In the context of synucleinopathy, we observed no group differences in CSF cytokines at 2 months p.i., when pSyn burden in the SN and cortical regions is greatest. However, the variability of pSyn accumulation between animals at this time point masked group differences. However, a positive correlation between SN pSyn-ir cell number and levels of IFN-γ was observed, which may be related to increased MHC-II expression in the SN as described in Chapter 3 [26], as IFN-γ increases MHC-I and MHC-II expression [45] and has been shown to contribute to neurotoxicity in PD models [46-48].

At 4 months p.i. positive correlations between SN pSyn-ir cell number and IFN-γ and TNF were observed with increased significance compared to 2 months, and levels of IL-6 were significantly increased. At 6 months p.i., all cytokines in CSF and plasma failed to correlate with magnitude of degeneration. However, CSF levels of IL-5, KC/GRO, and TNF and plasma levels of IL-6 were significantly increased in PFF-injected animals. Data on the involvement of IL-5 and KC/GRO in human PD is lacking and requires further investigation.

Our study detected levels of two commonly PD-associated cytokines following degeneration, TNF and IL-6. To our surprise, we failed to detect IL-1β at reliable levels at any time point. Polymorphisms in the IL-1β gene have been implicated in risk of sporadic PD [49-51] and protein levels are consistently detected in patient biofluids [2, 5]. It is possible that IL-1β does not reach detectable levels until pathology has been ongoing for an extended period of time, or may reflect differences in response of the rat vs. human immune system.

Collectively, our results demonstrate that early changes in CSF cytokines are particularly variable and related to Lewy pathology. Therefore, it is unlikely that cytokine(s) alone can constitute a reliable biomarker for earlier disease detection. While the majority of biofluid studies in patients correlate cytokines to α-syn and/or tau levels within the same biofluid [7, 52], we were limited by sample volume in this study which precluded this tandem analysis. However, the advantage of animal models is that we were able to correlate to pathology within the brain, which is currently not

possible in patients. Future studies aimed at developing imaging ligands for α-syn pathology in the brain may provide insight on the relationship between CSF/plasma cytokines that is more tightly linked to ongoing synucleinopathy and degeneration.

Furthermore, the significant increase in total individual cytokines (pg/ml) and the collective number of differentially secreted cytokines during the interval of degeneration suggests that a certain duration and threshold of pSyn load, degeneration and potentially other detrimental processes (oxidative stress, parenchymal inflammation) must be reached before group differences between synucleinopathy and control samples are detected. As biofluid data from PD patients represents a period after diagnosis, when degeneration has reached a magnitude of at least 50%, our 6 month results are in agreement with this concept.

Our results point to aging-related and early synucleinopathy-specific associations to proinflammatory cytokines that have previously been assayed in PD but unable to be investigated in early stages prior to degeneration. Development of tools to diagnose patients at earlier disease stages may aid in developing anti-inflammatory therapies targeted at cytokines for disease modification.

APPENDIX

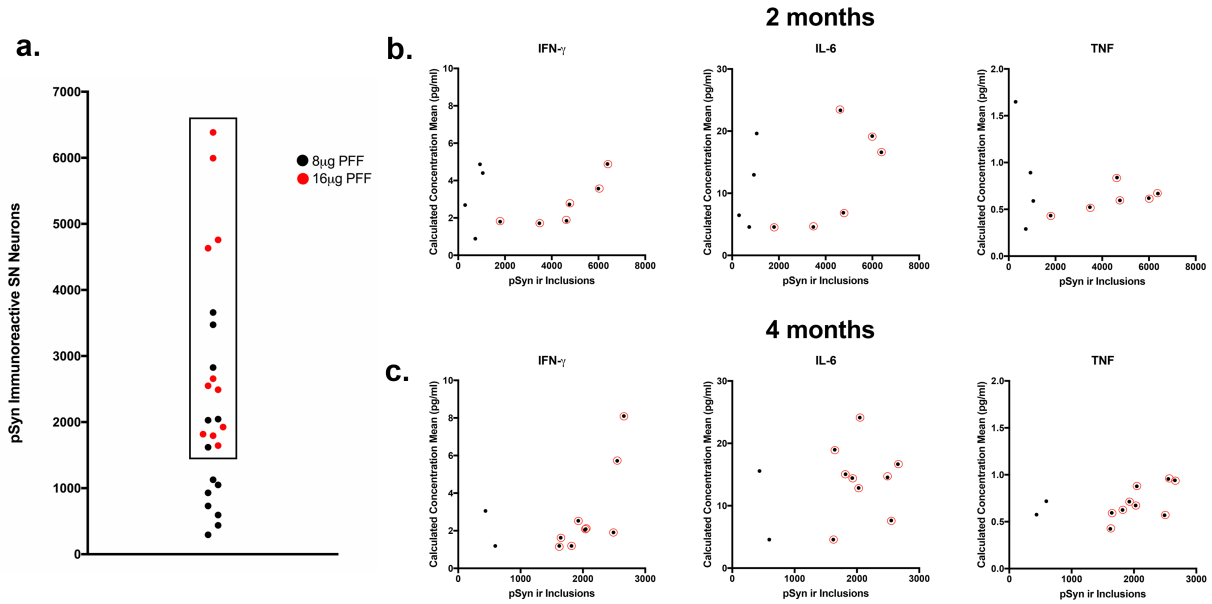

Figure 4.6: Distribution of pSyn aggregate number in PFF injected animals used for analyses

(a) Distribution of 2 and 4 month 8 μg and 16 μg PFF injected rats. Samples within the box were used for all comparisons and correlations. (B-C) Animals possessing <1600 pSyn inclusions fail to show a relationship to cytokines levels. Those animals possessing >1600 aggregates (red open circles) show a positive relationship between pSyn inclusion number and cytokines.

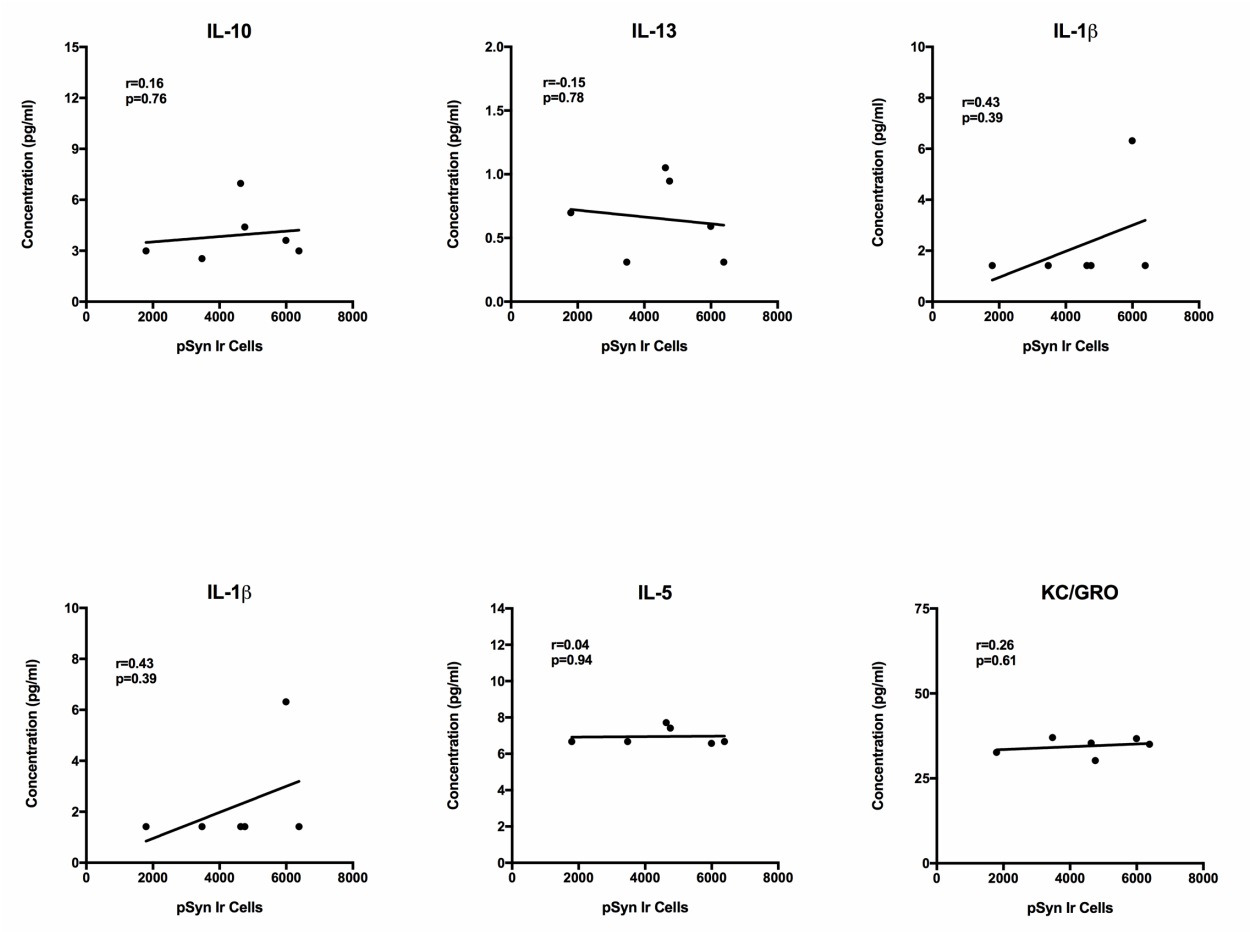

Figure 4.7: CSF IL-10, IL-13, IL-1β, IL-4, IL-5 and KC/GRO are not significantly correlated to SN pSyn-ir cells at 2 months.

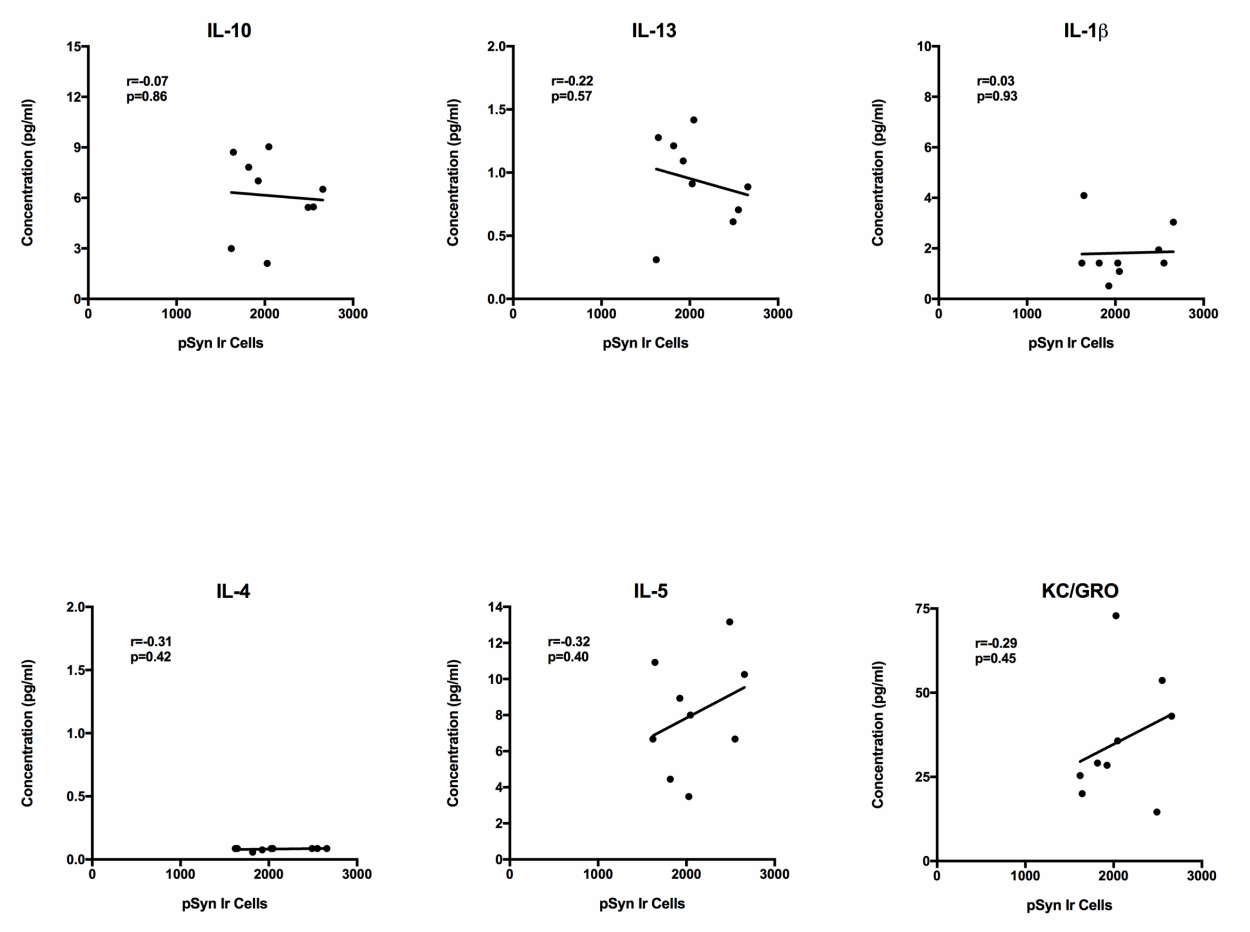

Figure 4.8: CSF IL-10, IL-13, IL-1β, IL-4, IL-5 and KC/GRO are not significantly correlated to SN pSyn-ir cells at 4 months.

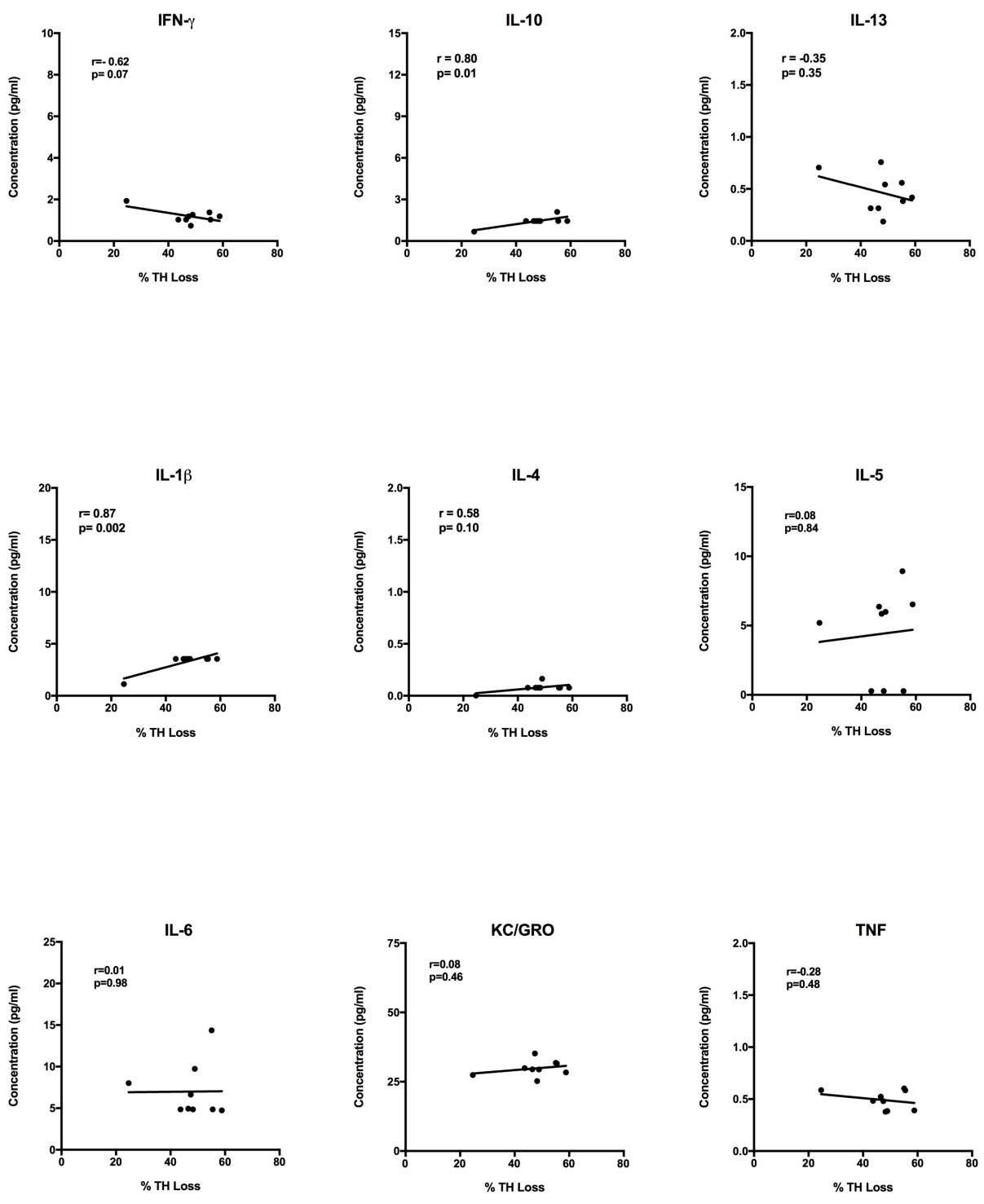

Figure 4.9: No CSF cytokines correlated significantly with magnitude of nigral degeneration.

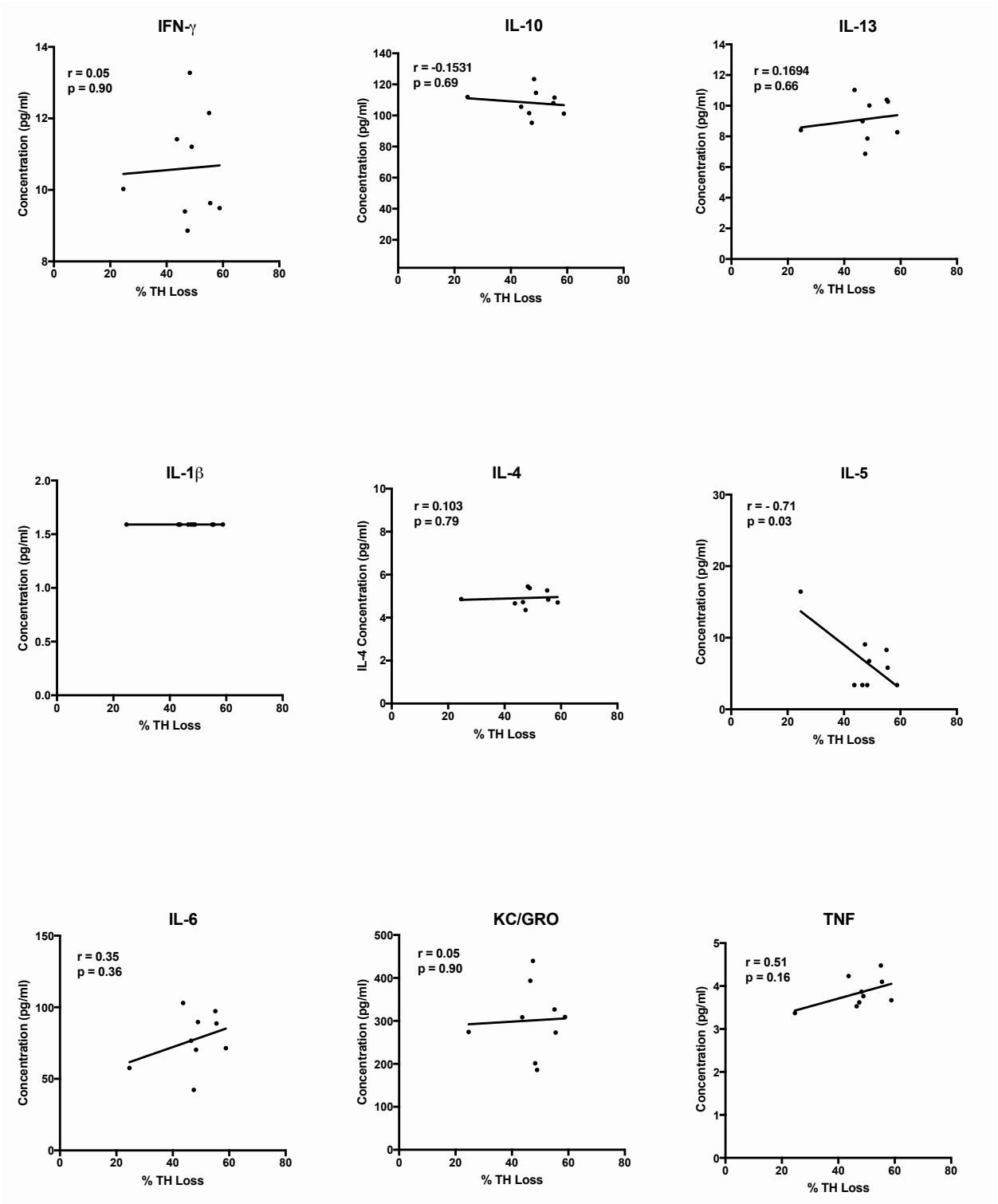

Figure 4.10: No plasma cytokines correlated significantly with magnitude of nigral degeneration.

REFERENCES

REFERENCES

1. Rocha, N.P., A.S. de Miranda, and A.L. Teixeira, *Insights into Neuroinflammation in Parkinson's Disease: From Biomarkers to Anti-Inflammatory Based Therapies.* Biomed Res Int, 2015. **2015**: p. 628192.

2. Blum-Degen, D., et al., *Interleukin-1 beta and interleukin-6 are elevated in the cerebrospinal fluid of Alzheimer's and de novo Parkinson's disease patients.* (0304-3940 (Print)).

3. Lindqvist, D., et al., *Cerebrospinal fluid inflammatory markers in Parkinson's disease – Associations with depression, fatigue, and cognitive impairment.* Brain, Behavior, and Immunity, 2013. **33**: p. 183-189.

4. Mogi, M., et al., *Interleukin (IL)-1 beta, IL-2, IL-4, IL-6 and transforming growth factor-alpha levels are elevated in ventricular cerebrospinal fluid in juvenile parkinsonism and Parkinson's disease.* Neurosci Lett, 1996. **211**(1): p. 13-6.

5. Reale, M., et al., *Peripheral cytokines profile in Parkinson's disease.* Brain, Behavior, and Immunity, 2009. **23**(1): p. 55-63.

6. Rocha, N.P., et al., *Reduced Activated T Lymphocytes (CD4+CD25+) and Plasma Levels of Cytokines in Parkinson's Disease.* Mol Neurobiol, 2018. **55**(2): p. 1488-1497.

7. Eidson, L.N., et al., *Candidate inflammatory biomarkers display unique relationships with alpha-synuclein and correlate with measures of disease severity in subjects with Parkinson's disease.* (1742-2094 (Electronic)).

8. Mogi, M., et al., *p53 protein, interferon-gamma, and NF-kappaB levels are elevated in the parkinsonian brain.* Neurosci Lett, 2007. **414**(1): p. 94-7.

9. Dilger, R.N. and R.W. Johnson, *Aging, microglial cell priming, and the discordant central inflammatory response to signals from the peripheral immune system.* J Leukoc Biol, 2008. **84**(4): p. 932-9.

10. Conde, J.R. and W.J. Streit, *Microglia in the aging brain.* J Neuropathol Exp Neurol, 2006. **65**(3): p. 199-203.

11. Rozovsky, I., C.E. Finch, and T.E. Morgan, *Age-related activation of microglia and astrocytes: in vitro studies show persistent phenotypes of aging, increased proliferation, and resistance to down-regulation.* Neurobiol Aging, 1998. **19**(1): p. 97-103.

12. Boisvert, M.M., et al., *The Aging Astrocyte Transcriptome from Multiple Regions of the Mouse Brain.* Cell reports, 2018. **22**(1): p. 269-285.

13. Clarke, L.E., et al., *Normal aging induces A1-like astrocyte reactivity.* Proceedings of the National Academy of Sciences of the United States of America, 2018. **115**(8): p. E1896-E1905.

14. Wong, D., K. Dorovini-Zis, and S.R. Vincent, *Cytokines, nitric oxide, and cGMP modulate the permeability of an in vitro model of the human blood-brain barrier.* Exp Neurol, 2004. **190**(2): p. 446-55.

15. Jaczewska, J., et al., *TNF-α and IFN-γ promote lymphocyte adhesion to endothelial junctional regions facilitating transendothelial migration.* Journal of Leukocyte Biology, 2014. **95**(2): p. 265-274.

16. Varatharaj, A. and I. Galea, *The blood-brain barrier in systemic inflammation.* Brain, Behavior, and Immunity, 2017. **60**: p. 1-12.

17. Popescu, B.O., et al., *Blood-brain barrier alterations in ageing and dementia.* J Neurol Sci, 2009. **283**(1-2): p. 99-106.

18. Marques, F., et al., *Blood–brain-barriers in aging and in Alzheimer's disease.* Molecular Neurodegeneration, 2013. **8**: p. 38-38.

19. Gray, M.T. and J.M. Woulfe, *Striatal blood-brain barrier permeability in Parkinson's disease.* J Cereb Blood Flow Metab, 2015. **35**(5): p. 747-50.

20. Daneman, R., *The blood-brain barrier in health and disease.* Ann Neurol, 2012. **72**(5): p. 648-72.

21. Dobbs, R.J., et al., *Association of circulating TNF-alpha and IL-6 with ageing and parkinsonism.* Acta Neurol Scand, 1999. **100**(1): p. 34-41.

22. Kim, H.O., et al., *Serum cytokine profiles in healthy young and elderly population assessed using multiplexed bead-based immunoassays.* Journal of Translational Medicine, 2011. **9**(1): p. 113.

23. Kortekaas, R., et al., *Blood-brain barrier dysfunction in parkinsonian midbrain in vivo.* Ann Neurol, 2005. **57**(2): p. 176-9.

24. Zhao, B. and J.P. Schwartz, *Involvement of cytokines in normal CNS development and neurological diseases: recent progress and perspectives.* J Neurosci Res, 1998. **52**(1): p. 7-16.

25. Kordower, J.H., et al., *Disease duration and the integrity of the nigrostriatal system in Parkinson's disease.* Brain, 2013. **136**(Pt 8): p. 2419-31.

26. Duffy, M.F., et al., *Lewy body-like alpha-synuclein inclusions trigger reactive microgliosis prior to nigral degeneration.* J Neuroinflammation, 2018. **15**(1): p. 129.

27. Paumier, K.L., et al., *Intrastriatal injection of pre-formed mouse alpha-synuclein fibrils into rats triggers alpha-synuclein pathology and bilateral nigrostriatal degeneration.* Neurobiol Dis, 2015. **82**: p. 185-99.

28. Murphy Kenneth, T.P., Walport Mark, Janeway Charles, *Janeway's Immunobiology*. 8 ed. 2012: Garland Science.

29. Collier, T.J., C.E. Sortwell, and B.F. Daley, *Diminished viability, growth, and behavioral efficacy of fetal dopamine neuron grafts in aging rats with long-term dopamine depletion: an argument for neurotrophic supplementation.* J Neurosci, 1999. **19**(13): p. 5563-73.

30. Gao, J., et al., *Influence of aging on the dopaminergic neurons in the substantia nigra pars compacta of rats.* Curr Aging Sci, 2011. **4**(1): p. 19-24.

31. Polinski, N.K., et al., *Recombinant adeno-associated virus 2/5-mediated gene transfer is reduced in the aged rat midbrain.* Neurobiology of aging, 2015. **36**(2): p. 1110-1120.

32. Luk, K.C., et al., *Intracerebral inoculation of pathological α-synuclein initiates a rapidly progressive neurodegenerative α-synucleinopathy in mice.* The Journal of Experimental Medicine, 2012. **209**(5): p. 975-986.

33. Volpicelli-Daley, L.A., K.C. Luk, and V.M. Lee, *Addition of exogenous alpha-synuclein preformed fibrils to primary neuronal cultures to seed recruitment of endogenous alpha-synuclein to Lewy body and Lewy neurite-like aggregates.* Nat Protoc, 2014. **9**(9): p. 2135-46.

34. Volpicelli-Daley, L.A., et al., *Exogenous alpha-synuclein fibrils induce Lewy body pathology leading to synaptic dysfunction and neuron death.* Neuron, 2011. **72**(1): p. 57-71.

35. Zarghami, A., et al., *A modified method for cerebrospinal fluid collection in anesthetized rat and evaluation of the efficacy.* Int J Mol Cell Med, 2013. **2**(2): p. 97-8.

36. Patterson JR, D.M., Kemp CJ, Collier TJ, Howe JW, Miller K, Stoll AC, Luk KC, Allen A, Kanaan NM, Paumier KL, Vaikath NN, Majbour NK, El-Agnaf OMA, Sortwell CE., *Optimization of the α-synuclein preformed fibril model of synucleinopathy in rats.* 2018.

37. Leys, C., et al., *Detecting outliers: Do not use standard deviation around the mean, use absolute deviation around the median.* Journal of Experimental Social Psychology, 2013. **49**(4): p. 764-766.

38. Harry, G.J., *Microglia during development and aging.* Pharmacol Ther, 2013. **139**(3): p. 313-26.

39. Kohman, R.A., *Aging microglia: relevance to cognition and neural plasticity.* Methods Mol Biol, 2012. **934**: p. 193-218.

40. Fiala, M., et al., *TNF-alpha opens a paracellular route for HIV-1 invasion across the blood-brain barrier.* Molecular Medicine, 1997. **3**(8): p. 553-564.

41. Sharief, M.K., et al., *Increased levels of circulating ICAM-1 in serum and cerebrospinal fluid of patients with active multiple sclerosis. Correlation with TNF-α and blood-brain barrier damage.* Journal of Neuroimmunology, 1993. **43**(1): p. 15-21.

42. Mogi, M., et al., *Tumor necrosis factor-alpha (TNF-alpha) increases both in the brain and in the cerebrospinal fluid from parkinsonian patients.* Neurosci Lett, 1994. **165**(1-2): p. 208-10.

43. Banks, W.A., A. Moinuddin, and J.E. Morley, *Regional transport of TNF-alpha across the blood-brain barrier in young ICR and young and aged SAMP8 mice.* Neurobiol Aging, 2001. **22**(4): p. 671-6.

44. Lv, S., et al., *Tumour necrosis factor-alpha affects blood-brain barrier permeability and tight junction-associated occludin in acute liver failure.* Liver Int, 2010. **30**(8): p. 1198-210.

45. Monteiro, S., et al., *Brain interference: Revisiting the role of IFNgamma in the central nervous system.* Prog Neurobiol, 2017. **156**: p. 149-163.

46. Mount, M.P., et al., *Involvement of interferon-gamma in microglial-mediated loss of dopaminergic neurons.* J Neurosci, 2007. **27**(12): p. 3328-37.

47. Mangano, E.N., et al., *Interferon-gamma plays a role in paraquat-induced neurodegeneration involving oxidative and proinflammatory pathways.* Neurobiol Aging, 2012. **33**(7): p. 1411-26.

48. Hashioka, S., et al., *Interferon-gamma-dependent cytotoxic activation of human astrocytes and astrocytoma cells.* Neurobiol Aging, 2009. **30**(12): p. 1924-35.

49. Wahner, A.D., et al., *Inflammatory cytokine gene polymorphisms and increased risk of Parkinson disease.* Arch Neurol, 2007. **64**(6): p. 836-40.

50. Nishimura, M., et al., *Influence of interleukin-1beta gene polymorphisms on age-at-onset of sporadic Parkinson's disease.* Neurosci Lett, 2000. **284**(1-2): p. 73-6.

51. McGeer, P.L., K. Yasojima, and E.G. McGeer, *Association of interleukin-1 beta polymorphisms with idiopathic Parkinson's disease.* Neurosci Lett, 2002. **326**(1): p. 67-9.

52. Delgado-Alvarado, M., et al., *Tau/α-synuclein ratio and inflammatory proteins in Parkinson's disease: An exploratory study.* Movement Disorders, 2017. **32**(7): p. 1066-1073.

Chapter 5: General Discussion and Future Directions

General Discussion

While the concept that neuroinflammation occurs in PD is not novel, the ability to investigate the question of whether inflammation may act as a contributor or is a mere consequence of nigrostriatal degeneration in PD has remained elusive. The development and characterization of the α-syn PFF model has afforded us the ability to examine the temporal sequence of these events in a manner previously unattainable.

Aim 1 investigated the time course of inflammation in relation to accumulation of Lewy body-like inclusions and nigrostriatal degeneration within the parenchyma in the SN and other areas affected in PD using immunohistological methodology. Interestingly, microglia in the SNr exhibit reactive morphology at the time point of peak pSyn inclusion burden in the adjacent SNc. Moreover, the number of microglia expressing MHC-II peaks concurrently with peak pSyn inclusions. Both of these observations occurred months prior to degeneration and were not observed during the interval of cell death in the SN. Furthermore, we observe a higher magnitude of degeneration on the ipsilateral side containing pSyn inclusions and MHC-II immunoreactive microglia. In contrast, the contralateral side exhibits less degeneration in the absence of pSyn and MHC-II. These results suggest that inflammation is related to early synucleinopathy pathology, to a much greater extent than merely being a consequence of degeneration and has the potential to contribute to disease progression.

While the experiments in Aim 1 establish a relationship between abnormal α-syn accumulation and increases in MHC-II-expressing microglia similar to observations in

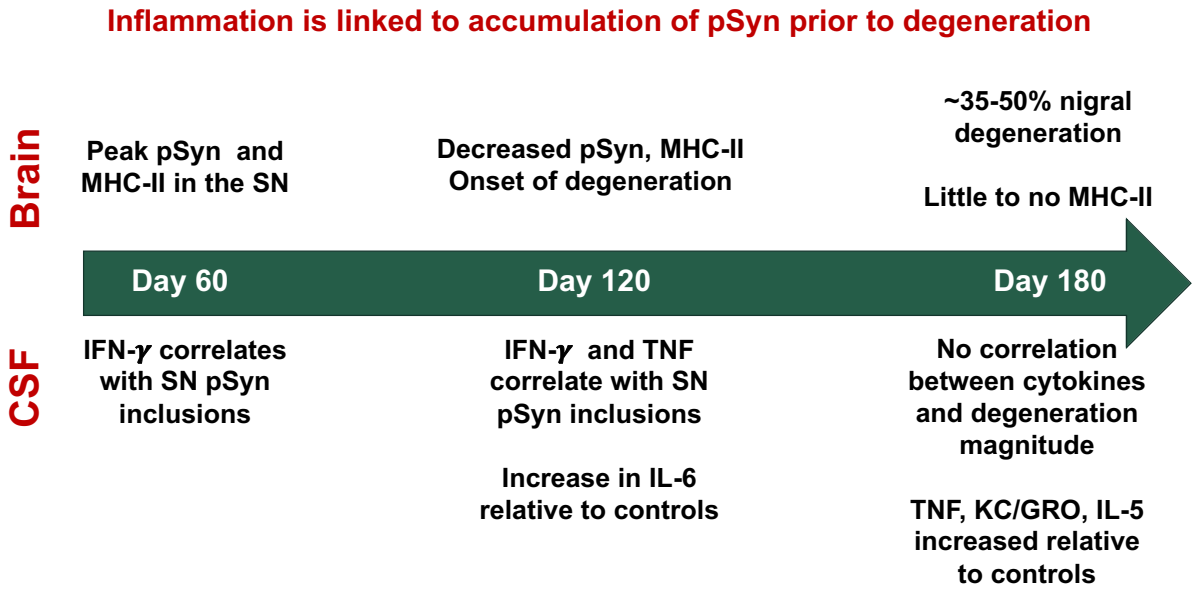

Figure 5.1: Summary of findings
Results from Aim 1 demonstrate an increase in microglia displaying an activated morphology and an increase in number of microglia expressing MHC-II, which correlates with pSyn burden in the SN months prior to degeneration. Decreases in MHC-II expressing microglia and absence of differentially increased microglial soma size were observed during the interval of degeneration, suggesting that inflammatory mechanisms, specifically antigen presentation, may be involved in the early stages of synucleinopathy. Aim 2 results demonstrate associations between CSF IFN-γ and TNF with pSyn inclusion load in the SN prior to degeneration, with overt group differences in inflammatory cytokines not observed until the onset of and during the interval of degeneration.

human tissue, several topics require further investigation [1]. First, while MHC-II is often concurrently expressed with proinflammatory cytokines, it is not clear whether the microglia expressing MHC-II in the PFF model display other proinflammatory markers such as IL-6 and TNF which are neurotoxic [2]. Identifying the pro- or anti-inflammatory status of these microglia will lend (or not) support to the notion that MHC-II immunoreactive microglia early in disease can contribute to disease progression.

While it's postulated that increased MHC-II expression leads to increased degeneration, there is little evidence supporting a direct contributory mechanism for MHC-II immunoreactive microglia in degeneration. A recent study by Jimenez-Ferrer et al. [3] demonstrated that contrary to expectations, rats with lower *Mhc2ta* and MHC-II gene expression have increased proportions of MHC-IIir microglia, exacerbated α-syn pathology and increased nigral degeneration compared to controls with higher Mhc2ta and MHC-II gene expression levels. The authors conclude that exacerbated neurotoxicity in this model may be due to inadequate antigen presentation ability to T-regulatory (Treg; anti-inflammatory) cells and thus represent a loss of function that may contribute to toxicity. As discussed in Chapter 2, it is likely that α-syn overexpression may not represent the most appropriate model for studying inflammatory mechanisms involved in PD. Future studies in which MHC-II expression is either increased or knocked down in the PFF model may provide more *directly* relevant insight into whether MHC-II expressing microglia observed at 2 months p.i. are true neurotoxic contributors to nigral degeneration.

Second, the stimulus inducing MHC-II expression in this model is still unknown. MHC-II expression may be classically induced by endocytosis of extracellular proteins which are broken down into small peptides and presented on the cell surface for recognition by CD4+ T cells and subsequent secretion of cytokines. It is possible that extracellular α-syn that is either released from cells or present in vesicles may be taken up by microglia, degraded into small peptides, and presented on the cell surface. Indeed, a recent paper by Sulzer et al. demonstrated that T-cells isolated from PD patients recognize α-syn-derived peptides of 9-10 amino acids from two regions: the Y39 region (near sites commonly associated with genetic forms of PD) and the S129 region (most common epitope found in Lewy bodies) [4]. Collectively, their results demonstrate an immune response initiated by CD4+ T-cells secreting IL-5 and IFN-γ as well as CD8+ T-cells secreting IFN-γ, suggesting that PD may be partially an autoimmune disease. However, it should be noted that the sample size for this study (N=67) was small and the results warrant replication. Additionally, a recent study by Kustrimovic et al. demonstrate an increased proportion of CD4+ T lymphocytes to the proinflammatory, Th1 subset, which secrete IFN-γ and TNF, and decreases in anti-inflammatory CD4+ Th2 lymphocytes in both drug naïve and medicated PD patients, further lending support that adaptive immunity is involved in the pathogenesis of PD[5].

In the context of the PFF model, we investigated the presence of CD4+ T-cells in the SN at 2 months p.i. when pSyn inclusion number and MHC-II expressing microglia numbers are highest. We failed to observe CD4+ T-cells within the SN using immunohistochemistry and RT-PCR failed to demonstrate a significant difference in

CD4 gene expression from control animals, although the study was underpowered. Lack of CD4 in the parenchyma in the PFF model may stem from several variables. The proportion of nigral neurons possessing pSyn aggregates is ~30% at its peak and the similar percentage that degenerate over 6 months may not meet the threshold of MHC-II expression levels and/or nigral degeneration required to initiate a full immune response. Second, the *gradual* temporal nature of the model may similarly not properly activate the immune system to its full potential. In contrast, T-cells have been observed in the parenchyma of other PD animal models induced by neurotoxicant [6, 7] or AAV-mediated overexpression [8, 9] of α-syn, models in which inflammation is likely artificial and degeneration reaches a magnitude of >50% over a very short period (2-8 weeks). Alternatively, MHC-II expression may be induced by IFN-γ. Indeed, experiments in Aim 2 demonstrate a positive correlation between IFN-γ in CSF and pSyn inclusion load in the SN. It is possible that IFN-γ secreted from T-cells in the CSF may gain entry into the parenchyma if the BBB is dysfunctional, however BBB permeability in the PFF model at this time point is unknown. Should IFN-γ act as the inducer of MHC-II expression, it is possible that MHC-II expression without concurrent peptide presentation renders microglia neutral, acting as bystanders, neither as contributors to- or protectors against degeneration as the peptide required to initiate a T-cell response is not present. Clarifying the direct role of MHC-II and the adaptive immune response, if any, as contributors to degeneration is warranted and may be investigated by direct manipulation of MHC-II levels by viral-vector-mediated silencing or germline transgenic manipulation.

Aim 2 investigated the inflammatory cytokine profile in CSF first during the course of normal aging and in distinct stages of synucleinopathy and degeneration (defined by Aim 1). Significant increases in TNF and KC/GRO were observed in CSF and plasma from naïve rats at 20 months of age, but not young adult and middle aged rats. Follow-up experiments investigating 1) the permeability of the BBB in naïve rats during normal aging and 2) cellular sources of TNF and KC/GRO will provide insight into the origin of these cytokines. These findings are particularly relevant to the concept that age is a major risk factor for many neurodegenerative diseases, and increased permeability of the blood brain barrier due to inflammatory cytokine secretion may play a role in disease initiation.

In animals injected with α-syn PFFs, we observe no overall group differences in cytokines between PBS and PFF injected animals at 2 months p.i., however, this is likely due to variability of pSyn inclusion burden, regardless of total amount of protein injected. We demonstrate significant correlations between number of pSyn inclusions and levels of IFN-**γ** and TNF months prior to degeneration, and significantly increased proinflammatory cytokine IL-6 prior to degeneration. At 6 months p.i., IL-5, TNF, and KC/GRO were significantly elevated in PFF-injected animals compared to PBS-injected controls, suggesting that the duration or magnitude of pathology, or both, may be important in inducing expression of cytokines that are detectable in biofluids. In plasma, only IL-6 was significantly increased at 6 months p.i., which is unsurprising given that plasma is farther removed from changes happening within the CNS. However, the cell-specific origin of cytokine increases observed remains unclear: One hypothesis is that

cytokines we observe at early time points (TNF, IFN-γ) are originating from CD4+ Th1 cells within the CSF. It is also possible that these cytokines originate from glia within the CNS and are leaking into the CSF due to decreased BBB integrity. Therefore, identifying the cell types responsible for secreting proinflammatory cytokines may represent a therapeutic target.

Collectively, these results suggest that while specific inflammatory cytokines may be associated with synucleinopathy early in disease, a certain threshold must be met for these associations to be detected. From a translational perspective, measurement of α-syn and/or pSyn concurrently with cytokines is crucial to observing disease-relevant aberrations in early disease stages, as variability will likely mask overt group differences.

Current State of Neuroinflammation in Human PD: A long way to go, but heading in the right direction.

Currently, 13 clinical trials are ongoing which have the primary goal to develop diagnostic tools to detect a Parkinson's specific inflammatory signature via imaging, biofluids, and breath collection [10]. While initially discouraging that no trials exist investigating specific inflammatory response component therapeutics, the critical groundwork to establish a time course of inflammation in human PD must be conducted first. These studies are limited in that PD subjects constitute those who have received clinical diagnosis, and thus have already undergone significant degeneration of the SNc and possessed Lewy pathology for many years. However, until a true biomarker which

allows for earlier disease detection is developed, the inclusion of patients with low Hoehn and Yahr and UPDRS scores is critical for true determination of early-stage related inflammation. Our results suggest that inflammation occurs early, prior to degeneration, and thus the best chance of disease modification by anti-inflammatory therapeutics lies in earlier treatment, necessitating earlier diagnosis. For now, laying the groundwork to determine the true time course of inflammation in the human disease is the most crucial step in understanding, and eventually [successfully] targeting inflammation in human PD.

Future Directions

Role of astrocytes in PFF-induced synucleinopathy, inflammation, and nigral degeneration

While microglia represent the main immune effector cells of the CNS, they do not act alone, rather, microglia act in concert with astrocytes and neurons to maintain homeostasis. Although much less studied than their microglial counterparts, markers of reactive astrocytes and observations of astrocytes containing α-syn have been documented in human PD tissue [11, 12], specifically in parallel with development of cortical Lewy pathology. Recent studies have implicated that microglia producing proinflammatory cytokines including TNF, interleukin-1 alpha (IL-1α) and complement 1 q-subcomponent (C1q) induce astrocytes to lose their phagocytic and synapse-maintaining function (A1 phenotype) [13]. Conditioned media from A1 astrocytes induced by proinflammatory microglia has been demonstrated to induce apoptosis of non-myelinating oligodendrocytes and specific subpopulations of neurons, including dopaminergic neurons through secretion of soluble factors. Interestingly, absence of

microglia precluded induction of A1 astrocytes *in vivo* following injection of LPS, suggesting that microglia are required for astrocytes to become toxic [13]. Furthermore, blocking of the A1 phenotype was shown to be neuroprotective in PFF and transgenic mouse models of PD [14].

A limitation of these dissertation experiments is that we did not characterize astrocyte phenotype during early synucleinopathy. Recent studies have demonstrated a 1:1 ratio of microglia to astrocytes in the SNr, home to one of the densest populations of glia within the brain [15]. Given our observations of reactive microglial morphology and increased MHC-II immunoreactivity at 2 months following PFF injection, it would be expected that reactive astrocytes also would be prevalent. Future studies examining transcriptomic profiles of both microglia and astrocytes would provide insight into microglia-astrocyte phenotypes within synucleinopathy and nigral degeneration.

Do microglia accelerate degeneration?

Given the descriptive nature of these dissertation aims, future studies identifying specific inflammatory mechanisms as contributors to degeneration are warranted. While these studies have demonstrated morphological changes and increased expression of MHC-II on microglia suggesting a pro-inflammatory phenotype prior to degeneration, the question of “Do microglia facilitate degeneration” still remains unanswered. While PFF-seeded pSyn inclusions can induce cell death in absence of microglia *in vitro*, this does not rule out the possibility that microglia in a chronic proinflammatory state may accelerate or exacerbate cell death. Indeed, previous

models demonstrate that inflammation can accelerate degeneration in α-syn overexpression models over α-syn or inflammation alone, suggesting a synergistic relationship.

To directly answer this question, future studies employing colony stimulating factor 1-receptor (CSF1R) inhibitors could be used. Microglia express colony-stimulating factor receptor-1 (CSF1R). Activation of CSF1R regulates microglial survival, differentiation and proliferation [16, 17]. Recent studies using CSF1R inhibitors (Plexxikon, Inc.) revealed that microglia can be eliminated from the mouse brain (~99%) in 3 weeks without any detectable adverse side effects in brain volume or cognitive function [16]. In addition, CSF1R inhibition resulted in decreased inflammatory gene expression following injection of the lipopolysaccharide (LPS) [16]. Moreover, CSF1R inhibitors have recently been used in mouse models of Alzheimer's disease, reducing cognitive deficits [18]. CSF1R inhibitors provide a novel pharmacological tool with which to directly test the role of microglia in accumulation of α-syn aggregates and resulting nigrostriatal degeneration. Recently, PLX3397 has been shown to cross the rat BBB [19]. Ideally, studies investigating microglial depletion in the context of synucleinopathy should be conducted in rat, given that the systematic time course of pSyn accumulation, microgliosis, and degeneration have already been conducted.

To definitively determine the role of microglia in synucleinopathy induced degeneration, depletion of ~99-100% is necessary beginning after injection of PFFs. It is possible that microglial depletion will impart neuroprotection but also highly likely that complete

depletion may accelerate and augment degeneration, as microglia are necessary in phagocytosing debris and maintaining homeostasis. Regardless of the result, it is unlikely that CSF1R inhibitors constitute a valid therapeutic for PD, as few studies have examined the long-term effects of microglial depletion, especially in an aged environment. Nonetheless, complete microglial depletion will provide definitive evidence as to whether microglia act as a contributor to degeneration.

What is the inflammatory signature of glial subsets in the SNc and SNr and does the ratio of pro- to anti-inflammatory shift over disease course?

Inflammation is consistently proposed as a factor contributing to the selective vulnerability of SNc neurons, as microglia and astrocyte densities in the adjacent SNr are particularly high compared to other brain regions. Given the regional specificity and positive correlation of MHC-II immunoreactive microglia to SNc pSyn inclusions, clarification of whether this subpopulation of microglia are pro- or anti-inflammatory is warranted. This may be accomplished via laser-capture microdissection, as the population of MHC-II expressing microglia is relatively small, and whole tissue punches of the SNc are likely to dilute the signal given the number of cell types and total number of cells present in that region.

Furthermore, given the dense population of astrocytes and microglia in the adjacent SNr, transcriptomic profiles of these populations also are worthy of future investigation, especially considering that the role of astrogliosis in PD is much less studied. As astrocytes and microglia can express and secrete many of the same cytokines, separate analysis of genes by cell-type is warranted, and may be accomplished via

fluorescence activated cell sorting (FACS) and RNA-sequencing. As both cell populations may have helpful and harmful roles depending on disease stage, assessment of the cell-type specific genetic inflammatory signature at different disease stages would provide a wealth of specific inflammatory contributors to disease and targets to therapeutically inhibit or upregulate.

Impact

This work has demonstrated that components of an immune response, specifically antigen presentation in the parenchyma and pro-inflammatory cytokines in CSF are increased prior to degeneration and are significantly associated with pSyn inclusion burden in the SN, months prior to degeneration. Importantly, these experiments have provided a foundation for investigating early neuroinflammation as a contributor to degeneration in distinct disease stages in the context of normal endogenous α-syn, more analogous to human sporadic PD.

REFERENCES

REFERENCES

1. Croisier, E., et al., *Microglial inflammation in the parkinsonian substantia nigra: relationship to alpha-synuclein deposition.* J Neuroinflammation, 2005. **2**: p. 14.

2. Spiller, K.L., et al., *The role of macrophage phenotype in vascularization of tissue engineering scaffolds.* Biomaterials, 2014. **35**(15): p. 4477-88.

3. Jimenez-Ferrer, I., et al., *Allelic difference in Mhc2ta confers altered microglial activation and susceptibility to α-synuclein-induced dopaminergic neurodegeneration.* Neurobiology of Disease, 2017. **106**: p. 279-290.

4. Sulzer, D., et al., *T cells from patients with Parkinson's disease recognize alpha-synuclein peptides.* Nature, 2017. **546**(7660): p. 656-661.

5. Kustrimovic, N., et al., *Parkinson's disease patients have a complex phenotypic and functional Th1 bias: cross-sectional studies of CD4+ Th1/Th2/T17 and Treg in drug-naïve and drug-treated patients.* Journal of Neuroinflammation, 2018. **15**: p. 205.

6. González, H., et al., *Dopamine Receptor D3 Expressed on CD4⁺ T Cells Favors Neurodegeneration of Dopaminergic Neurons during Parkinson's Disease.* The Journal of Immunology, 2013. **190**(10): p. 5048.

7. Martin, H.L., et al., *Evidence for a role of adaptive immune response in the disease pathogenesis of the MPTP mouse model of Parkinson's disease.* Glia, 2016. **64**(3): p. 386-395.

8. Thakur, P., et al., *Modeling Parkinson's disease pathology by combination of fibril seeds and α-synuclein overexpression in the rat brain.* Proceedings of the National Academy of Sciences, 2017. **114**: p. E8284-E8293.

9. Sanchez-Guajardo, V., et al., *Microglia acquire distinct activation profiles depending on the degree of alpha-synuclein neuropathology in a rAAV based model of Parkinson's disease.* PLoS One, 2010. **5**(1): p. e8784.

10. ClinicalTrials.gov. *Parkinson's disease and Inflammation*. 2018 [cited 2018 June 27]; Available from: https://clinicaltrials.gov/ct2/results?term=inflammation&cond=parkinson%27s&Search=Apply&recrs=b&recrs=a&recrs=f&recrs=d&recrs=e&age_v=&gndr=&type=&rslt=.

11. Halliday, G.M. and C.H. Stevens, *Glia: initiators and progressors of pathology in Parkinson's disease.* Mov Disord, 2011. **26**(1): p. 6-17.

12. Braak, H., M. Sastre, and K. Del Tredici, *Development of alpha-synuclein immunoreactive astrocytes in the forebrain parallels stages of intraneuronal*

pathology in sporadic Parkinson's disease. Acta Neuropathol, 2007. **114**(3): p. 231-41.

13. Liddelow, S.A., et al., *Neurotoxic reactive astrocytes are induced by activated microglia.* Nature, 2017. **541**(7638): p. 481-487.

14. Yun, S.P., et al., *Block of A1 astrocyte conversion by microglia is neuroprotective in models of Parkinson's disease.* Nat Med, 2018. **24**(7): p. 931-938.

15. De Biase, L.M., et al., *Local Cues Establish and Maintain Region-Specific Phenotypes of Basal Ganglia Microglia.* Neuron, 2017. **95**(2): p. 341-356.e6.

16. Elmore, M.R., et al., *Colony-stimulating factor 1 receptor signaling is necessary for microglia viability, unmasking a microglia progenitor cell in the adult brain.* Neuron, 2014. **82**(2): p. 380-97.

17. Hamilton, J.A. and A. Achuthan, *Colony stimulating factors and myeloid cell biology in health and disease.* Trends Immunol, 2013. **34**(2): p. 81-9.

18. Dagher, N.N., et al., *Colony-stimulating factor 1 receptor inhibition prevents microglial plaque association and improves cognition in 3xTg-AD mice.* J Neuroinflammation, 2015. **12**: p. 139.

19. Butowski, N., et al., *Orally administered colony stimulating factor 1 receptor inhibitor PLX3397 in recurrent glioblastoma: an Ivy Foundation Early Phase Clinical Trials Consortium phase II study.* Neuro-Oncology, 2016. **18**(4): p. 557-564.